PB95-191250
EPA No. 530-R-95-012

University of Nevada

Reno

Geochemical Modeling of Mine Pit Water: An Overview and Application of Computer Codes

A thesis submitted in partial fulfillment of the requirements for the degree of Master of Science in Hydrogeology

by

David A. Bird

Professor W. Berry Lyons, Thesis Advisor

December 1993

ACKNOWLEDGEMENTS

This thesis is the second of a two part study funded by the United States Environmental Protection Agency. Part one was completed by Margaret Saunders Macdonald, who graduated from UNR in 1992 with a Master's Degree in Hydrogeology. Much of the information in this thesis was taken from Meg's report, including many of the citations pertaining to the physical and chemical characteristics of pit lakes.

Thanks are in order for many people who contributed to the completion of this thesis. If I have forgotten anybody, I apologize, as the list is quite long:

* The members of my committee, Professors W. Berry Lyons, Glenn C. Miller, and Stephen W. Wheatcraft for their invaluable assistance, support, and encouragement toward the completion of this thesis.
* My office mates, Ann Carey, Georgia Doyle, Kevin Johannesson, Bill Ludwick, Phil Murphree, Bwire Ojiambo, Eric Swanson, and Jim Thomas for support and enlightening geochemical/hydrological discussions.
* Kathy Sertic, Dave Jones, and Doug Zimmerman at the Nevada Division of Environmental Protection, for their assistance, and for allowing access to files.
* Bill Upton of Placer Dome for granting permission to visit the Cortez Mine site and sample the pit water. Mark List and Eric Vokt of Cortez Gold Mines for their sincere efforts in providing data, and Eric Vokt for helping sample the Cortez Pit lake.
* Rab Bustos, Eric Seedorf, and Ron Zuck of Magma Mining Co. for providing data and tours, and allowing sampling of the Ruth District.
* Chuck Zimmerman of Newmont for allowing access to the Universal Gas Pit site, and Pam Gilbert for conducting the tour.
* Georgia Doyle for assistance in sample collection, organization, and geochemical insight. Thanks also for playing office traffic cop during rush hour.
* Anne Marie Harris for critical review of selected sections.
* Carl Palmer of Oregon Graduate Institute, and Andy Davis of PTI Environmental Services for helpful discussions regarding pit water modeling.
* Steve Wesnousky and the gang in Neotectonics for allowing access to computers.
* Professor Gary Vinyard of the UNR Biology Department, for the use of lake sampling equipment.

I would like to thank my advisor, Berry Lyons, for his motivation and leadership, for encouraging me to tackle this project, for his patience during my endless barrage of questions regarding elementary aqueous geochemistry, and for having more faith in me than I did.

A special note of thanks is reserved for Rhonda for her support, guidance, and unbelievable patience through 2 years of graduate school. I probably could not have done it without her.

This thesis is dedicated to my mother, whose courage, strength, and sense of humor in the face of personal tragedy was a source of inspiration, and reminded me of the importance of making use of the short time we have.

ABSTRACT

The impacts of mining on water quality in the western United States have become the focus of increased environmental concern and regulatory effort in recent years. An assessment of potential mining impacts on local water quality is necessary because of possible adverse effects including acid mine drainage, elevated trace metal concentrations, and high dissolved solids such as sulfate. In Nevada alone, at least 26 open pit mining operations now, or will in the future, require dewatering to allow excavation below the water table. Open pits now requiring dewatering will likely see the eventual development of pit lakes after mine closure. The water quality that evolves in pit lakes will be a function of many variables including, but not limited to: host lithology and buffering capacity; structure (fractures, faults); type, mass, and morphology (stratiform, massive, disseminated, structurally controlled) of ore, alteration, and gangue; groundwater temperature, flow rate and aquifer morphology (isotropy, homogeneity); pit geometry and size; biological activity; and climate (precipitation, evaporation, wind velocity).

Although a wide variety of geochemical modeling software packages are available, none are designed specifically for the purpose of modeling pit lake geochemistry, and no regulatory framework or standard exists for such modeling efforts. This study was designed to evaluate hydrogeochemical modeling software that might be applicable to modeling post-mining, pit water geochemistry. Data from the Cortez Mine, a carbonate-hosted, open pit, precious metal mine in Nevada, are used in an inverse model to determine geochemical mass transfer that has occurred between the mine wallrock and the pit lake. These results guide the development of a forward reaction path model that may be used for future mine sites.

For inverse modeling, the geochemical mass transfer code BALANCE (USGS) was used because of its ability to incorporate trace metal phases. The reaction path (forward) model, combining MINTEQA2 (EPA) and PHREEQE (USGS), used the inverse model results to perform the dissolution, precipitation, and adsorption modeling. For this study, PHREEQE was expanded to include over 200 aqueous species and minerals of arsenic, cadmium, copper, lead, mercury, silver, thallium, and zinc. PHREEQE handled the pit wall dissolution, while MINTEQA2 was used to constrain and calibrate solubility controls and model trace metal adsorption onto amorphous ferric hydroxide.

The study demonstrates that pit lake chemical evolution can be modeled with available software packages, using existing mine environments to guide model development. The incorporation of site-specific kinetic data will allow application of this model to the prediction of geochemical evolution in future pit lakes.

TABLE OF CONTENTS

LIST OF FIGURES

LIST OF TABLES

1. INTRODUCTION

In the past two decades, the number of open pit precious-metal mines in the western United States has increased significantly. The economics and technology of today's mining industry allow the extraction of ore from great depths by open pit methods, which has raised concerns about potential impacts on local and regional groundwater systems. Mines excavating below the level of the local water table require removal of groundwater through dewatering in order to keep the mine area dry. Mine dewatering will affect the local hydrologic system by creating a cone of depression in the piezometric surface, and steepening the hydraulic gradient in the immediate area. The deeper the mine, the more dewatering required, and the deeper and broader will be the cone of depression. On its proposed completion in 2001, the Gold Quarry pit in Eureka County, Nevada is projected to be 460 meters deep, 270 meters below the level of the regional water table (PTI, 1992). The cone of depression is projected to be 64 kilometers in diameter at its maximum width (HCI, 1992).

When a mine is decommissioned and dewatering ceases, the cone of depression will start to recover, and the pit may begin to fill with water. Several decades may elapse before the regional groundwater table returns to pre-mine conditions and the pit fills to its steady state depth. If allowed to fill at an undisturbed rate, the Berkeley pit in Butte, Montana, would require 27 years to reach maximum depth at the level of the ambient water table (Davis and Ashenberg, 1989). The Gold Quarry pit is predicted to reach 95% of the final level approximately 20 years after cessation of dewatering (HCI, 1992).

In Nevada alone, at least 26 open pit mine sites are currently water-filled, or have active and/or proposed dewatering operations (MacDonald, 1992). Figure 1-1 shows the locations of these mines. Although most pits that will ultimately contain standing water are still

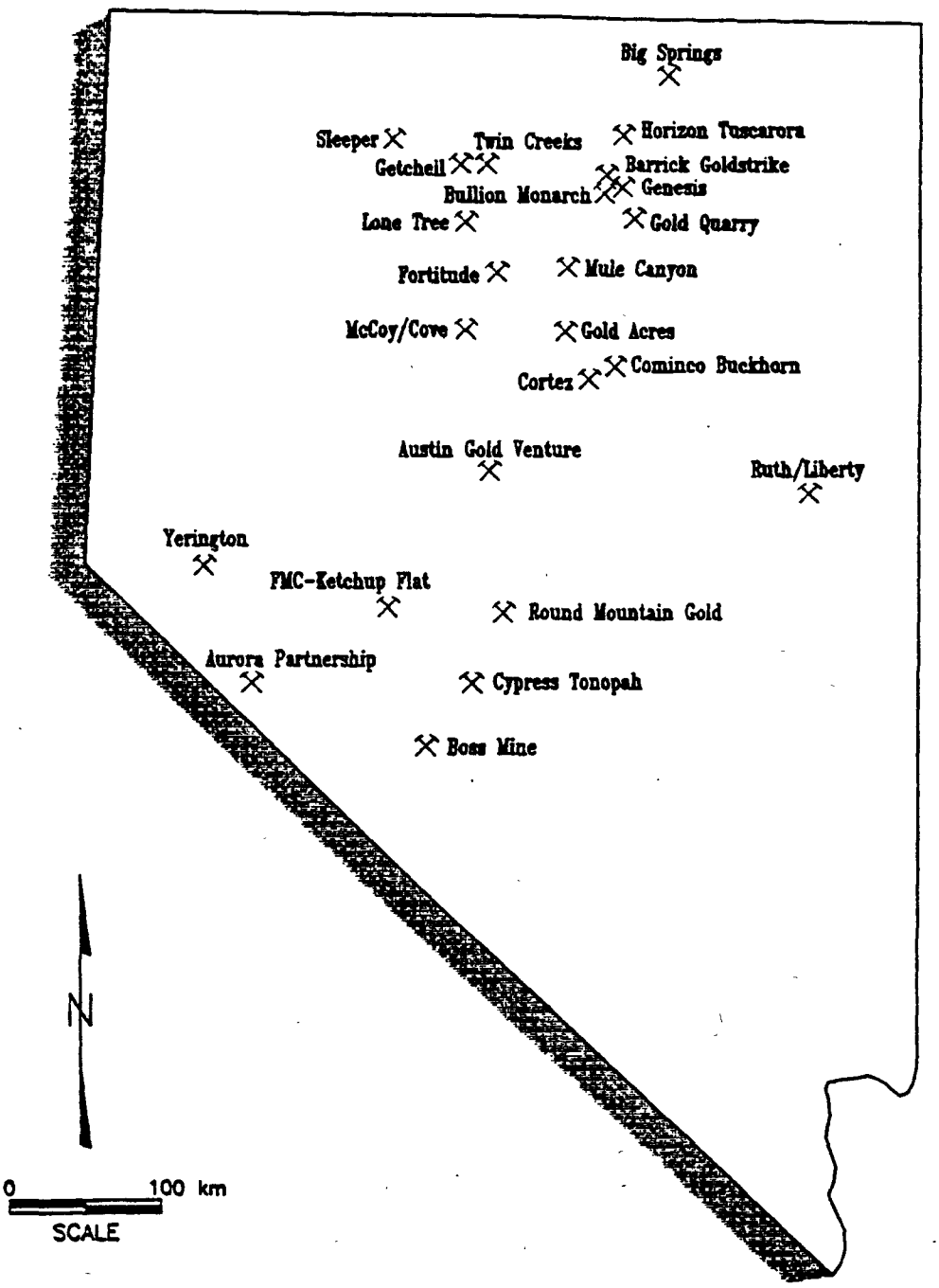

Figure 1-1: Location map for Nevada open pit mines requiring dewatering (from Macdonald, 1992).

being mined, seven pit lakes are known in Nevada (Macdonald, 1992):

Name	County	Type of mine
Boss	Nye	Precious Metal
Cortez	Lander	Precious Metal
Liberty	White Pine	Porphyry Copper
Ruth	White Pine	Porphyry Copper
Tuscarora	Elko	Precious Metal
Universal Gas	Eureka	Precious Metal
Yerington	Lyon	Porphyry Copper

Large volumes of water are being pumped in dewatering processes, with staggering projections. The Gold Quarry mine is expected to require a pumping rate of over 50 million gallons per day (over 58,000 acre feet per year) in the year 2001 (HCI, 1992).

In recent years, the mining industry has become the target of environmental concerns pertaining to water quality, including the water chemistry that will evolve in the pit lake as a result of rock-water interaction between the inflowing groundwater and the pit wall minerals. As recently as 10 years ago, the only extent to which mining companies were required to address the issue of post-mining pit water quality was to include the following statement in the permit (Harris, 1992):

Upon closure, the open pit will infill and become a permanent lake.

Until the enforcement of water quality regulations in the last four years, mining companies were only required to monitor the effects of their operations on local water quality after the inception of mining. This has resulted in some serious environmental consequences, such as acid mine drainage and contaminated pit lakes.

The most serious pit water problem known exists at the Berkeley pit, a current Superfund site (see Davis and Ashenberg, 1989; Baum and Knox, 1992). Similar scenarios, but of smaller scale, exist at the Ruth and Liberty pits, located in the Ruth District in eastern Nevada. The water chemistry of the Berkeley and Liberty pits is shown in Table 1-1.

Sites such as these, with very low pH and high trace metal concentrations, have stimulated reevaluation of the regulatory framework surrounding the permitting of new mining operations.

TABLE 1-1: Water chemistry, Berkeley and Liberty pits (mg/l).

	Berkeley * (100m depth)	Liberty ** (surface)	
Alkalinity, bicarbonate	0.0	0.0	
Chloride	20	40.1	
Fluoride	NA	0.16	
TDS	NA	NA	
Sulfate	7060	3780	
Aluminum	206	90	
Arsenic	0.7	< 0.002	
Barium	NA	0.0	
Cadmium	1.9	0.036	***
Calcium	506	522	
Chromium	NA	NA	
Copper	218	51	***
Iron	1040	59	
Mercury	NA	NA	
Potassium	25	5.08	
Magnesium	272	351	
Manganese	162	146	***
Sodium	73	53.3	
Lead	NA	0.0	
Silica	NA	48	
Zinc	496	67	***
pH	3.0	3.02	

Source: * Davis and Ashenberg, 1989
** UNR sampling (1993)
*** NDEP files
NA = Not available

Regulatory agencies now expect greater detail in studies predicting the impacts of surface mining activities on surface and groundwater resources. Companies with proposed mining operations are being asked to assess these impacts during the permitting process before mining can proceed. Such assessments now must also be provided during permitting for expansions of existing operations. Many assessments incorporate detailed geochemical models to predict the long term chemistry of pit lakes.

Geochemists rely on a variety of modeling methods to predict the impacts of mining on local and regional hydrologic systems. Hydrogeochemical equilibrium and reaction path models are used in conjunction with limnological, and in some cases numerical flow modeling computer codes, to predict the geochemistry that will result in the pit lakes.

Purpose of Study

The primary objective of this work is to evaluate the suitability of the hydrogeochemical computer modeling codes BALANCE, MINTEQA2, PHREEQE, WATEQF, and WATEQ4F to the task of modeling post-mining pit water geochemistry. The advantages and disadvantages of these codes are discussed, and considered in regard to their utility for pit water modeling. Detailed descriptions pertaining to the operation of each software code are given in chapter 4. These are directed towards readers with limited experience using the codes, and are intended to summarize the important features of each. Chapter 2 contains a detailed discussion of introductory aqueous geochemistry, and how the concepts are integrated into chemical models. This chapter is intended for readers with limited aqueous geochemistry background.

The underlying questions that the thesis addresses are: Can post-mine pit water be predicted using the hydrogeochemical codes listed above, how many of the variables can be integrated into the model, and what level of accuracy and validity can be expected in the results? The study attempts to demonstrate that pit water chemical modeling, with an understanding of the variables, can be accomplished with these software packages.

Scope of Study

As the focus of the study was on computer modeling, minimal field work was performed. All computer programs used in the study are available from the respective author and/or federal agency where they were developed. Most aqueous geochemical, lithochemical, and mineralogical data were either provided by site personnel, or obtained from the literature or public files. Samples were collected from the Cortez and Liberty pits for the purpose of providing more detail in existing geochemical sample suites.

The initial purpose of the study was to learn how to use the computer codes, BALANCE, MINTEQA2, and PHREEQE, and evaluate their suitability to pit water chemical modeling. WATEQF and WATEQ4F were subsequently added to the evaluation. In the process of evaluation, occasional references and comparisons are made to other codes, such as EQ3/6 (Wolery, 1992), HYDROGEOCHEM (Yeh, 1989), PHREEQM (Nienhus et al, 1991), and PHRQPITZ (Plummer et al, 1988). The hydrochemical computer codes considered in the study are listed in Table 1-2. All of the codes evaluated are DOS based and PC-compatible.

TABLE 1-2: Computer codes evaluated.

Software Code	Author	Source
BALANCE	Parkhurst, et al. (1980)	USGS
MINTEQA2	Allison, et al (1991)	EPA
NETPATH	Plummer, et al (1991)	USGS
PHREEQE	Parkhurst, et al (1980)	USGS
WATEQF	Plummer, et al (1984)	USGS
WATEQ4F	Ball and Nordstrom (1991)	USGS

EPA: United States Environmental Protection Agency
USGS: United States Geological Survey

No attempt was made to examine any programs other than the hydrogeochemical codes listed above. Limnological software (e.g. CE-QUAL-R1; U.S. Army, 1986) and numerical flow modeling programs (e.g. MINEDW, HCI, 1992a; MODFLOW, McDonald and Harbaugh, 1984) have also been used in pit water modeling, but were not evaluated in this study. A consideration of groundwater flow modeling is beyond the scope of the study, as the emphasis is on water quality.

The Cortez pit of Lander County in east-central Nevada, and the Universal Gas pit in Eureka County, were chosen as example sites for modeling simulations. Chemical analytical data from the Cortez pit was used as input in the computer code BALANCE (Parkhurst et al, 1982) to determine chemical mass transfer. The results from BALANCE were used as

input for PHREEQE and MINTEQA2 to attempt to duplicate the actual Cortez pit water chemistry.

Speciation simulation codes used were WATEQF, WATEQ4F, MINTEQA2, and a version of PHREEQE expanded to include trace metals believed by the author to be important in mine water quality. Speciation simulations, utilizing one or more of the aforementioned codes, were performed on the Cortez, Universal Gas, Liberty, and Berkeley pits to gain an understanding of the chemical speciation and saturation states of the pit lakes. The simulations of the Cortez pit water were used to guide interpretations of the pit water evolution predicted by subsequent "inverse" models (i.e. BALANCE) and "forward" models (i.e. PHREEQE, and MINTEQA2).

The water in the Cortez and Universal Gas pits might be representative of many that will evolve in sediment-hosted disseminated precious metal deposits. However, they are not likely representative of some of the high sulfide systems in Nevada, such as Rabbit Creek, which has a 25 foot thick stratibound zone containing up to 75% total sulfide (Bloomstein et al, 1991).

Previous Work

Little is known about pit water quality, because few open pits exist that contain standing water. Open pit mining techniques have only seen widespread application to precious metal deposits in the last 10 to 20 years, and most pits excavated below the water table are still being actively mined (Macdonald, 1992).

Numerous studies have been done on water quality in mining environments (Caruccio et al, 1976; Chapman et al, 1983; Davis and Ashenberg, 1989; Davis and Runnells, 1987; Filipek et al, 1987; Herlihy et al, 1988; Huang and Tahija, 1990; Karlsson et al, 1988; Macdonald, 1992; Nordstrom and colleagues, 1977, 1979b, 1982, 1985 (2), 1990;

Potter and Nordstrom, 1977; Rampe and Runnells, 1989; Steffen Robertson and Kirsten, 1989; Wicks et al, 1991; Wicks and Groves, 1993). Most of these works studied acid mine drainage environments.

Glynn et al (1992) define forward chemical modeling as the application of an assumed reaction model to an initial condition to predict chemical composition of water and rock as a function of reaction progress, and inverse chemical modeling as the use of observed chemical, isotopic, petrographic, and hydrologic information at initial and final points to define reaction models that are consistent with the data. Studies by Plummer et al (1983), Plummer (1984), and Plummer et al (1990) lay the groundwork for development of forward models through application of inverse modeling results. Chemical models were developed in these studies and applied to the Madison Aquifer in the northern U.S., and to the Florida Aquifer. Helgeson and colleagues (1968, 1969) were the first to apply computer techniques to mass transfer in geochemistry (Nordstrom et al, 1979a).

Pit water geochemical modeling is a new discipline in the mining industry, done primarily by hydrologic and geochemical consultants. Few modeling studies have been submitted for regulatory review (Gold Quarry Mine, PTI Environmental Services and Hydrologic Consultants, Inc.; Lone Tree Mine, Hydro-Search, Inc.; Betze Mine, ENSR Consulting and Engineering and Dr. James I. Drever).

Comparative studies have been performed for hydrogeochemical codes (Nordstrom et al, 1979a; INTERA, 1983), but nothing has been performed on the scale of this study specifically for pit lake geochemical modeling.

General Modeling Background

A model is a simplification of reality. A hydrogeochemical model is an attempt to represent, through mathematical equations describing

thermodynamic relationships and species/mineral stabilities, a system of chemical components or reactions in an aqueous environment. The model may be constructed to represent a variety of size and time scales. The environment could be a lake, a stream, groundwater, or, in the cases considered in this study, a pit lake and the adjacent groundwater.

The origins of aqueous geochemical modeling can be traced to Back's papers (1961, 1966) on hydrochemical facies (Figure 1-2). The Garrels and Thompson (1962) seawater speciation model is often cited as the work that launched the quantitative aspect of chemical modeling, and established the framework for many of the computer codes used today.

Figure 1-3 shows the evolution of the more popular hydrogeochemical computer programs in the last 30 years. The Garrels and Thompson seawater speciation model was the first milestone, and two subsequent events, the 1979 and 1989 ACS Chemical Modeling Symposia, inspired the outgrowth of new or revised codes. Those codes surviving the last 14 years of evolution have seen significant revision. The trend in the late 1970's toward many different codes gave way in the 1980's to refinement and improvement of existing codes. No single code has been developed capable of treating the wide range of environmental problems to which equilibrium calculations have been applied, nor would such a code be practical (Plummer, 1984).

Geochemical Modeling Applied to Mine Water Quality

An attempt to produce a comprehensive model that can be applied to many mining scenarios will probably meet with unsatisfactory results. The variation in geologic, hydrologic, physical, and chemical parameters that determine pit water geochemistry can produce different water qualities even among geologically similar deposits. Examples are illustrated by the pit water chemistry for the Yerington pit (Table 1-3) versus the Liberty and Berkeley pits (Table 1-1), all of which are

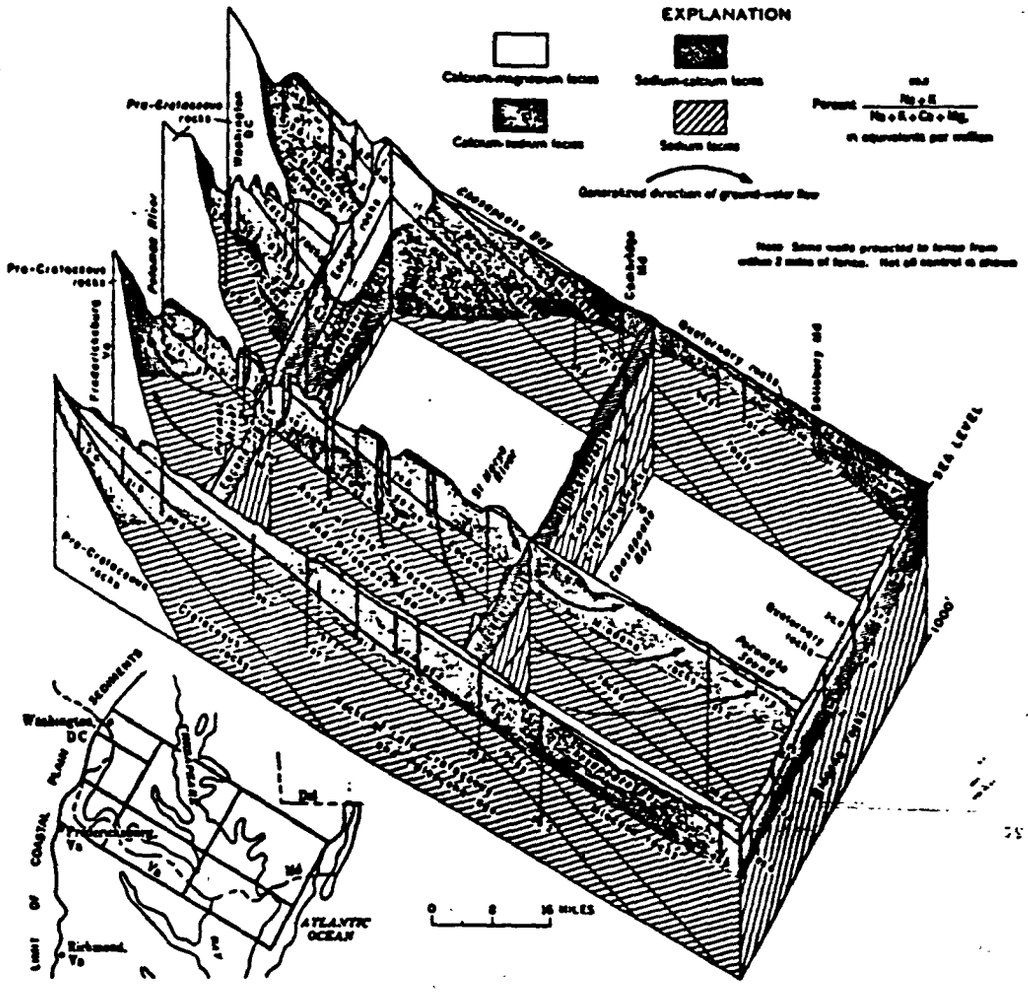

Figure 1-2: Fence diagram of part of the Atlantic Coastal Plain showing hydrochemical facies (from Back, 1961).

porphyry copper deposits. The Liberty and Ruth pits have experienced anthropogenic disturbance (treatment and addition of tailings), but are still similar to the Berkeley pit.

The Yerington pit water quality is much better than either of the other porphyry copper systems. Clearly, a comprehensive model for porphyry copper terrains must consider the variables that could

potentially control these differences.

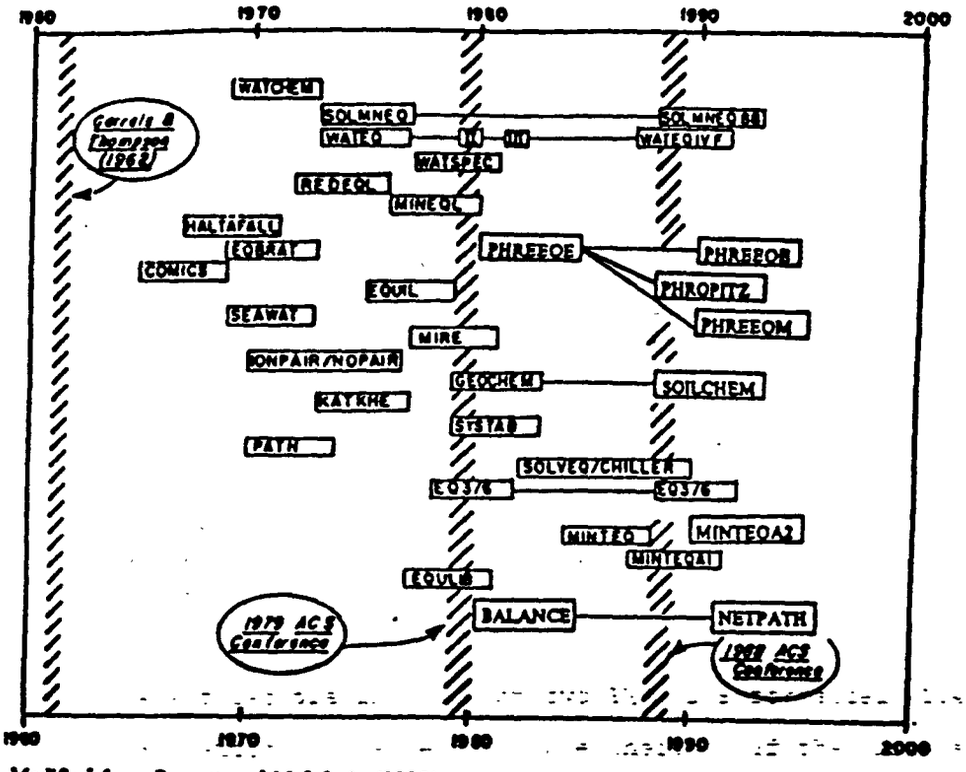

Modified from Bassett and Melchoir (1990)

Figure 1-3: Evolution of hydrogeochemical codes (from Glynn et al, 1992).

The Cortez pit and the Universal Gas pit waters show slight variations in water chemistries (Table 1-4), even though both are derived from carbonate aquifers with a minor siliceous component. The variation in ore, gangue, and alteration mineralogy, which help determine the elements released to solution, is sufficient to introduce notable differences in the respective water chemistries.

As these two examples demonstrate, modelers of mine pit water are presented with a wide variety of parameters, even among genetically

similar deposits, that must be considered in describing the inputs to the models.

TABLE 1-3: Water chemistry, Yerington pit.
Source: NDEP files.

	(ppm)
Alkalinity, bicarbonate	134.0
Chloride	40.0
Fluoride	1.77
TDS	628
Sulfate	242
Arsenic	0.014
Barium	0.034
Cadmium	0.008
Calcium	230
Chromium	0.004
Copper	0.232
Iron	0.581
Mercury	< 0.001
Potassium	6.9
Magnesium	22.3
Manganese	0.076
Sodium	74.0
Lead	0.012
Silica	NA
Zinc	0.081
pH	8.21

Data Disk

All of the output files generated in the computer modeling exercises are included on two 3½", DOS formatted (1.4 MB), floppy diskettes, contained with the thesis. If the disks are missing or unreadable, printouts of the files can be examined in the main library archives at the University of Nevada, Reno.

TABLE 1-4: Water chemistry, Cortez and Universal Gas pits. (values in ppm).

	Cortez *	Universal Gas **
Alkalinity, bicarbonate	282.3	77.5
Chloride	24.4	342
Conductivity, in µmhos/cm.	NA	903
Fluoride	2.4	0.394
Ammonia	NA	0.13 ***
Nitrate Nitrogen	0.207	1.3 ***
Nitrate	NA	5.7
Solids, Dissolved (TDS)	432.3	691
Sulfate	90.2	30.7
Aluminum	< 0.02	0.174
Arsenic	0.0383	< 0.180
Barium	0.0603	0.12
Cadmium	NA	< 0.007
Calcium	45.4	145
Cobalt	NA	0.02
Chromium	< 0.01	< 0.01
Copper	< 0.007	< 0.007
Iron	0.134	0.134
Mercury	0.00046	< 0.5
Potassium	11.7	3.74
Magnesium	18.1	38
Manganese	0.0017	0.071
Sodium	68.63	50
Nickel	NA	< 0.015
Lead	0.0043	< 0.05
Selenium	NA	< 0.13
Silica	34.43	19.49
Strontium	NA	0.514
Thallium	NA	< 0.15
Tungsten	NA	0.051
Vanadium	NA	< 0.007
Zinc	0.002	< 0.005
pH	8.067	8.67

Source: * Cortez Gold Mines (1992) or UNR/Cortez Gold Mines joint sampling (1993).
** Geraghty & Miller, Inc.
*** Nestmont Gold.
NA = Not available.

2. GEOCHEMICAL OVERVIEW

Most geochemical modeling codes incorporate the fundamental mathematical relationships of aqueous geochemistry, including ionic strength, activity, equilibrium, speciation, and solubility. In solutions containing numerous ions and chemical species, the calculations of ionic strength, activity coefficients, and chemical speciation become too cumbersome to be attempted manually, and are best handled by computer.

A general knowledge of the basic physical principles of aqueous geochemistry is important in understanding how the programs solve problems. These principles are at the root of geochemical computer modeling, since the necessity of rapid computational ability in solving these problems was the driving force that inspired the development of computer modeling software.

Ionic Strength

Ionic strength considers the higher degree of electrostatic effectiveness of polyvalent ions in solution, which would be neglected in simple consideration of total molal concentration (Drever, 1988). Ionic strength (Equation 1) is a required parameter for calculation of activity coefficients, using molal concentrations from the input data:

$$I = \tfrac{1}{2} \sum m_i z_i^2 \qquad (1)$$

The variable m_i is the molal concentration of the ith ion, and z_i is the charge on the ith ion. Equation (1) illustrates the greater weight given polyvalent ions in the calculation of ionic strength, i.e. charge is raised to the power of two. If the component is an uncharged species, such as H_4SiO_4, then $z_i^2 = 0$, causing the term for that species to fall out of the equation. Uncharged species, therefore, do not contribute to the calculation of solution ionic strength.

An example of the relative significance of ionic strength is seen by comparing the Sierra Nevada ephemeral spring water of Garrels and Mackenzie (1967), which had an ionic strength of 0.000485 molal, or $10^{-3.3}$ (calculated by author in WATEQF), to seawater, which has an ionic strength of around 0.6799 molal, or $10^{-0.17}$ (Parkhurst et al, 1980), more than 3 orders of magnitude higher.

Activity Coefficients

Nearly all geochemical computer models are based on the ion association theory, which describes the behavior of ions in solution in terms of *activity*. The activity of an ion in solution can be defined as its "effective concentration" (Drever, 1988), and incorporates the assumption that charged ions exert a different influence over adjacent ions depending on the ion's size, charge, and the solution ionic strength. The ratio of a species' activity to its molal concentration is called its *activity coefficient*. The equation that adjusts molal concentration (m_i) by the activity coefficient (γ_i) to obtain activity (a_i) is:

$$a_i = \gamma_i \cdot m_i$$

A consideration of activity is essential because only in ideal solutions does the molal concentration of an ion or species equal its activity (Drever, 1988), but the condition of ideality does not exist in natural waters. Electrostatic interactions between charged species, and between ions and solution, impart non-ideal behavior to the system. Under such conditions, the concentration of an ion is best described by its activity.

Morel and Hering (1993) define an ideal system as "one in which the free energy of a species is independent of the nature and concentration of other species," and state that this occurs in either of the two following cases:

1. The system is very dilute, and all individual solute molecules are far apart and effectively "ignorant" of each other (i.e., they have no energetic interactions and their individual free energies are unaffected by each other's presence). This is the "infinite dilution" reference state.

2. The major solutes (those accounting for the bulk of the dissolved species) are considered to be at a fixed concentration and whatever effects they have on the free energy of another species are accounted for in the standard value (μ_i) of the chemical free energy of that species. This is the "fixed composition" reference state.

Since neither of these cases is encountered in natural waters, activity coefficients are needed to describe interactions among ions and species in natural waters.

Several theories have evolved to explain the activities of species in solution, and calculate activity coefficients. The appropriate formulas for calculating activity coefficients differ depending on the solution ionic strength.

Debye-Hückel Equation: In relatively dilute solutions ($I \leq 10^{-3}$), deviations from ideal behavior are primarily caused by long-range electrostatic interactions (Stumm and Morgan, 1981). At these ionic strengths, a simple, single-ion activity coefficient formula, the Debye-Hückel equation, is assumed to give an adequate description of ion interactions for the purpose of calculating activity coefficients. The Debye-Hückel equation assumes that ions are point charges, the interactions are entirely electrostatic, and arrangement of ions about one another conforms to a Boltzmann distribution (Drever, 1988). The Debye-Hückel equation assumes that ions behave "as charged particles of finite sizes in an electrostatic field of uniform intensity" (Hem, 1985). Therefore, the Debye-Hückel equation contains no term to account for size or hydration effects of the ion.

The simplest form of determining the activity coefficients (γ_i) is also the simplest form of the Debye-Hückel equation:

$$\log \gamma_i = -Az_i^2\sqrt{I} \qquad (2)$$

where z is the charge on the *i*th ion, and I is the ionic strength of the solution. Equation 2 is valid to ionic strengths of about 10^{-3} molal. The constant A is expressed as (Truesdell and Jones, 1974):

$$A = \frac{(1.82483 \times 10^6)(d^{½})}{(\epsilon T)^{3/2}} \text{ (moles}^{-0.5}) \text{ } (10^3 \text{ g } H_2O)^{½}$$

where d is the density of water, T is the absolute temperature, and ϵ is the dielectric constant of water.

At higher ionic strengths, the Debye-Hückel equation becomes inaccurate, because the formula predicts impossibly high concentrations of ions in close proximity to one another (Drever, 1988), and tends to underestimate the degree of ion association (Truesdell and Jones, 1969).

Extended Debye-Hückel Equation: For ionic strengths up to 10^{-1} molal, the extended Debye-Hückel formula, which incorporates two additional constants to account for ionic interactions, provides a better approximation:

$$\log \gamma_i = \frac{-Az_i^2\sqrt{I}}{1 + Bå\sqrt{I}} \qquad (3)$$

The constant å represents the hydrated radius of the particular ion, and B is expressed as (Truesdell and Jones, 1974):

$$B = \frac{(50.2916 \times 10^8)(d^{½})}{(\epsilon T)^{½}} \text{ (cm}^{-1}) \text{ (moles}^{-0.5}) \text{ } (10^3 \text{ g } H_2O)^{½}$$

The constant å is commonly referred to as the "Debye-Hückel å constant," or simple DHA.

Robinson-Stokes Debye-Hückel Equation: A modified version of the extended Debye-Hückel equation, for use at higher ionic strengths,

incorporates a second term with another adjustable parameter, b (Truesdell and Jones, 1974; Robinson and Stokes, 1955):

$$\log \gamma_i = \frac{-Az_i^2\sqrt{I}}{1 + B\mathring{a}\sqrt{I}} + bI \qquad (4)$$

The b parameter is constant for a given ion, and accounts for the decrease in concentration of solvent that occurs at higher ionic strengths. The bI term causes an increase in the activity coefficient with increased ionic strength (Drever, 1988). Ball, et al (1979) considered this equation to be more reliable than either the extended Debye-Hückel or the Davies equation, and thus incorporated it into the WATEQ2 code. Several USGS codes refer to Equation (4) as the "WATEQ Debye-Hückel equation."

The A and B constants, and the Debye-Hückel å and b parameters (shown in Appendix A) are tabulated in many aqueous geochemistry texts, and are incorporated into computer speciation codes. The A and B constants are calculated from the dielectric constant, density, and temperature (Hamer, 1968). For deviations from 25°C, they require temperature and pressure correction before being applied to calculation of activity coefficients, a task which all computer codes perform.

Davies Equation: The Davies equation (Equation 5) incorporates semi-empirical data to account for ion interactions. It is generally accurate at ionic strengths up to about $10^{-0.3}$ (0.5 molal). Davies eliminated the parameters å and b, the constant B, and added the empirically derived linear term (cI), where c lies between 0.2 and 0.3. Davies' original derivation of the equation set c at 0.2, which he later changed to 0.3 believing it provided a better fit to experimental data (Davies, 1962). The Davies equation is used in many cases by computer codes because the å parameter required for the Debye-Hückel equations

frequently cannot be estimated (Ball and Nordstrom, 1991).

$$\log \gamma_i = -Az_i \left[\frac{\sqrt{I}}{1 + \sqrt{I}} \right] - cI \qquad (5)$$

The principal advantage of the Davies equation is to provide, a "quasi-constant value of the activity coefficients in the range I = 0.3 to 0.7 M" (Morel and Hering, 1993). The ionic strength of natural waters rarely exceeds 0.7 M, and the inaccuracies shown by the Davies equation in the 0.3 to 0.7 M range are usually less than errors introduced from other sources (Morel and Hering, 1993). Different computer codes use different values for c in the Davies equation. In PHREEQE, WATEQF and WATEQ4F, c = 0.3, whereas in MINTEQA2, c = 0.24.

A comparison of activity coefficients for different ions using three of the aforementioned equations (Debye-Hückel, extended Debye-Hückel, and Davies) is shown in Figure 2-1. Pankow (1991) observed that the term -0.2I in the Davies equation causes a minimum near log $\sqrt{I}$ = 0 in the plot of γ_i vs. log $\sqrt{I}$. As the plot shows, γ_i does not decrease steadily as I increases, but rather increases for large ionic strength. This occurs because the amount of solvent available for solvation of ions decreases as the ionic strength increases (Bockris and Reddy, 1970).

Figure 2-1 also illustrates that activity coefficients approach 1.0 in very dilute solutions, causing activity to approach molal concentration. At higher ionic strengths, activity coefficients generally decrease, with the noted exception of those calculated by the Davies equation, which begin increasing again after log $\sqrt{I}$ = 0. Similar behavior is shown in Figure 2-2, which plots γCa^{2+} calculated from the three Debye-Hückel equations, vs. ionic strength.

Table 2-1 summarizes the four previously discussed formulas, and

their range of applicability.

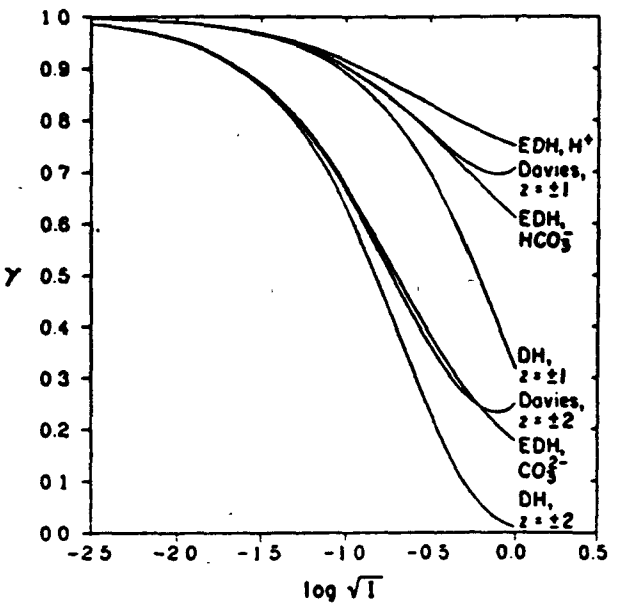

Figure 2-1: Activity coefficients vs. log √I. The Debye-Hückel equation deviates as ionic strength increases, producing lower activity coefficients than the Davies or extended Debye-Hückel equations (from Pankow, 1991).

Ion interaction models: Beyond ionic strengths of 0.5, ion interactions become so great that deviations from the ideal solution behavior are attributed mostly to short-range interionic forces (Stumm and Morgan, 1981) which are more appropriately described by ion interaction models.

The Brønsted-Guggenheim model was one of the early models that met with success (Harvie and Weare, 1980), but the ion-interaction models of Pitzer (1973, 1979, 1980) are probably the most popular today.

Drever shows a simplified form of the Pitzer formula:

$$\frac{G_{ex}}{RT} = (D\text{-}H) + \sum_i \sum_j \lambda_{ij}\,(I) m_i m_j + \sum_i \sum_j \sum_k \mu_{ijk} m_i m_j m_k \qquad (6)$$

where G_{ex} is the excess Gibbs free energy per kilogram of water, D-H represents a Debye-Hückel term, λ_{ij} represents binary interactions, and μ_{ijk} represents ternary interactions, which are significant only at very high ionic strengths (Drever, 1988). Harvie and Weare (1980) have performed what many believe to be the most successful application of Pitzer models to brine solutions (Nordstrom and Ball, 1983). PHRQPITZ (Plummer et al, 1988), and SOLMINEQ.88 (Kharaka et al, 1988 utilize ion-interaction theories, and can be applied to modeling highly concentrated solutions. For purposes of modeling mine pit water,

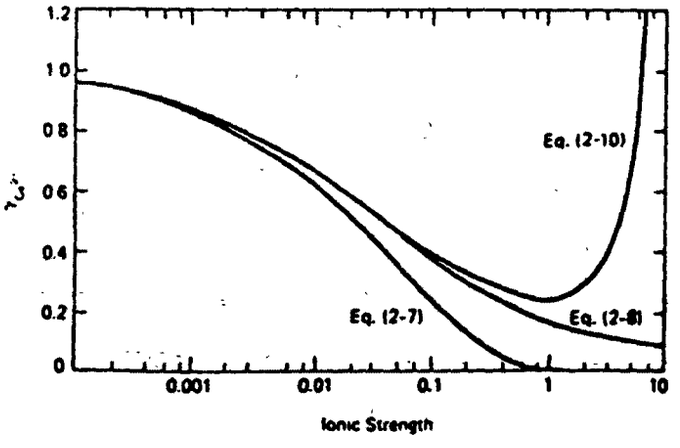

Figure 2-2: Variation of the activity coefficient for γCa^{2+} according to the three forms of the Debye-Hückel equation (from Drever, 1988; Eq. (2-7) = basic Debye-Hückel, Eq. (2-8) = Extended Debye-Hückel, Eq. (2-10) = Robinson-Stokes Debye-Hückel).

it is unlikely that ionic strengths will exist high enough to warrant use of the ion interaction models. Even the most concentrated pit water known, the Berkeley Pit, has an ionic strength of 0.3 molal (calculated by author in WATEQ4F, see datadisk file BPSP01W4.OUT), which does not approach the levels seen in brines and seawater.

TABLE 2-1: Equations for activity coefficient (γ_i), adapted from Pankow (1991). Applicable ionic strength range obtained from Stumm and Morgan (1981).

Equation Name	Formula	Applicable Ionic Strength Range
Debye-Hückel	$\log \gamma_i = -Az_i^2\sqrt{I}$	$I < 10^{-2.3}$
Extended Debye-Hückel	$\log \gamma_i = \frac{-Az_i^2\sqrt{I}}{1 + Ba\sqrt{I}}$	$I < 10^{-1.9}$
Robinson-Stokes Debye-Hückel	$\log \gamma_i = \frac{-Az_i^2\sqrt{I}}{1 + Ba\sqrt{I}} + bI$	$I < 10^{-1.8}$
Davies	$\log \gamma_i = -Az_i^2 \left[\frac{\sqrt{I}}{1 + \sqrt{I}} \right] - cI$	$I < 10^{-0.3}$

Ion Pairs: Above ionic strengths of 10^{-1}, departures from the behavior predicted by the Debye-Hückel theory are thought to be due to short-range interactions, such as those responsible for the formation of ion pairs (Garrels and Thompson, 1962).

The formation of ion pairs has two effects (Drever, 1988). First, charged ions come together to form uncharged species, thus decreasing ionic strength, and second, the concentrations of free ions such as Ca^{2+} and SO_4^{2-} decrease as they become associated in ion pairs. This can produce misleading results in calculations of ionic strength and activity coefficients. Codes that use equation (1) to calculate ionic strength, and contain uncharged ion pairs in the database, may generate suspiciously low ionic strength. The Pitzer models, which incorporate very few uncharged ion pair species, give a more realistic depiction of ionic strength. Table 2-2 shows a comparison of values calculated in both WATEQF and PHRQPITZ for various water samples.

MacInnes Convention: The MacInnes convention (MacInnes, 1919), or mean salt method, can be invoked in some codes at the user's request, to estimate activities of free ions. The convention assumes that the

Table 2-2: Comparison of activity coefficients modeled in PHREEQE vs. PHRQPITZ (top line of each pair of simulations is from PHREEQE, bottom line is from PHRQPITZ; from Glynn et al, 1992).

Name	aH_2O	Ionic Strength	Log PCO_2	Saturation Index[b]			
				Calcite	Dolomite	Gypsum	Halite
	0.999	0.0081	-1.67	0.12	0.09	-2.61	-10.89
Jones Sp., SD	0.999	0.0084	-1.71	0.12	0.21	-2.78	-10.88
	0.997	0.102	-1.16	-0.41	-1.27	-0.42	- 4.25
Keg Coulee, MT	0.998	0.114	-1.23	-0.33	-0.97	-0.42	- 4.23
	0.981	0.68	-3.49	0.82	2.55	-0.59	- 2.50
Seawater	0.981	0.72	-3.58	0.85	2.73	-0.64	- 2.49
	0.922	2.53	-1.52	0.34	0.53	-0.87	- 1.21
Harris Co., TX	0.919	2.54	-1.25	0.26	0.45	-1.03	- 1.20
	0.802	6.14	—	—	—	0.13	- 0.13
Red Sea	0.763	6.17	—	—	—	-0.04	- 0.07
	0.900	3.41	-3.17	1.66	3.99	-4.93	- 1.48
Sweetwater, WY	0.899	6.57	-3.76	1.04	2.72	-5.94	- 1.51
	0.806	9.38	-2.63	-0.05	1.12	-0.38	- 0.30
Dead Sea	0.687	9.40	-1.03	-0.29	0.71	0.02	- 0.07
	0.806	10.96	-0.73	-1.30	-2.76	0.33	- 0.81
Angora-Lena	0.661	10.98	-0.01	-2.82	-5.61	0.45	- 0.57
	0.881	4.73	-0.29	-1.28	0.48	0.09	- 1.54
Eddy Co., NM	0.836	13.34	-0.01	-1.87	-0.26	-0.22	- 1.25

single-ion activity coefficients of K^+ and Cl^- are equal to each other and to the mean activity coefficient of KCl at all ionic strengths. By definition:

$$\gamma_+ = \gamma_- = \gamma^2_{\pm}$$

If

$$\gamma_{\pm}KCl = \gamma K^+ = \gamma Cl^-$$

then

$$\gamma Na^+ = \frac{\gamma^2_{\pm}NaCl}{\gamma_{\pm}KCl}$$

and

$$\gamma Ca^{2+} = \frac{\gamma^3_{\pm}CaCl_2}{\gamma^2_{\pm}KCl}$$

and

$$\gamma Br^- = \frac{\gamma^2_{\pm}KBr}{\gamma_{\pm}KCl}$$

and so forth.

This method gives reasonable estimates for the activity coefficients of

free ions since K^+ and Cl^- salts do not normally form strong ion pairs (Millero and Schreiber, 1982).

Truesdell and Jones' (1969) comparison of the Debye-Hückel equation, Davies equation, and the MacInnes Assumption are shown in Table 2-3.

TABLE 2-3: Comparison of the Debye-Hückel equation, Davies equation, and the MacInnes Assumption (modified from Truesdell and Jones, 1969).

Method	Advantage	Limits
(A) Debye-Hückel Equation: $\log \gamma_i = \frac{-Az_i^2\sqrt{I}}{1 + Ba\sqrt{I}}$	Justified from theoretical studies. Can be used at all temperatures.	å must be estimated from experimental data. Ionic strength must be less than 0.1 for most monovalent ions, less than 0.05 for most divalent ions. If å is carefully chosen, equation may be accurate at greater concentrations.
(B) Davies Equation: $\log \gamma_i = \frac{-Az_i^2\sqrt{I}}{1 + \sqrt{I}} - cI$	No adjustable parameters. No experimental data needed.	As above, without an adjustable parameter, its use at higher ionic strengths is suspect.
(C) MacInnes Assumption: $\gamma K^+ = \gamma Cl^- = \gamma \pm KCl$	Can be applied to concentrated solutions.	Experimental values of $\gamma \pm$ needed. Limited by solubility of KCl to $I \leq 4.5$. Inaccurate for complexed ions such as CO_3^{2-} unless corrected for ion association.

Neutral species: Although neutral species are excluded from calculations of ionic strength, they are not immune from the influence of activity coefficients. Activity coefficients (γ_i) of uncharged species can be approximated by the following formula (Helgeson, 1969):

$$\gamma_i = 10^{0.1I}$$

where I is the ionic strength of the solution. This approach is used in

the USGS codes and MINTEQA2 for all neutral species except H_2O.

According to this formula, as ionic strength approaches zero (dilute solutions), the activity coefficients of uncharged species approach one. With increasing ionic strength, the activity coefficient rises slightly above one. The probable reason for this behavior is that much of the water in concentrated solutions forms the hydration shells of ions, making less water available to solvate uncharged species (Drever, 1988).

Limitations: A model is only as good as the assumptions on which it is based. Nordstrom et al (1979a) express reservations about ion association theories and the non-thermodynamic assumptions from which they were derived. The activity coefficients used to describe the non-ideal behavior of ions represent semi-empirical equations with inherent uncertainty. The assumption of ion association may actually be a naive representation of the true interactions of "ions" in aqueous solution (Nordstrom et al, 1979a).

The inconsistency of the equations and thermodynamic data used in different codes may produce discrepancies. Nordstrom et al (1979a) demonstrated this by running the same input through 14 different codes, and comparing calculated results for molality, activity coefficient, and saturation index. In some cases, the discrepancies between codes exceeded several orders of magnitude.

A significant source of uncertainty could be the activity of uncharged species. Reasons for this are the lack of reliable information on the activity of neutral ion pairs, and the fact that they often comprise the dominant species in aqueous systems (Nordstrom et al, 1979a).

Ionic Balance

Ionic balance refers simply to the balance between cations and

anions in solution. To determine ionic balance, concentrations of individual anions and cations must be converted to equivalents. Since equivalents are generally too large for application to natural waters, the convention of milliequivalents per liter (meq/l) is commonly used. To convert from concentration in mg/l or ppm to meq/l, the following formula is used (adapted from Mazor, 1991):

$$\text{meq/l} = \frac{\text{mg/l}}{\text{gfw}} \times \text{charge}$$

By summing the positive meq/l values and comparing with the negative meq/l values, the accuracy of the ionic balance for the particular water analysis is revealed.

A comprehensive analysis for the major elements in a water sample should reflect the ionic balance with minimal error, i.e. < 10% (Lyons, personal communication). Plummer (1984) recommends that analyses with more than 5% charge imbalance should be checked carefully. All natural waters are charged balanced (Plummer et al, 1983), so a balance discrepancy indicates an error or omission somewhere, either in sample collection, analysis, transport, or data input. Prior to conducting any detailed study of a water chemical analysis, such as a modeling effort, the chemist should verify the validity of the chemical analysis by checking its ionic balance.

For waters with high trace metal and H^+ concentrations (as in some mine-related waters), omission of ions normally regarded as "trace metals" and H^+ in the analyses may result in a significant imbalance. An example is the Berkeley pit, in which Al, Fe, Cu, Zn exist at higher concentrations than some of the major ions (see Table 1-1). Therefore, sampling and analyses must be conducted in the context of the aqueous and geologic environment studied, i.e. knowledge of minerals present and that may contribute to solution chemistry.

All computer programs have some provision for determining the ionic balance, and display a printout of the results. Some codes shut down if the ionic balance of the input analysis exceeds some error tolerance, such as 30% difference between cations and anions. Others may only provide an error message. If the program runs, but reports a significant charge imbalance, the results should be interpreted with caution.

Some computer codes, including WATEQ4F, report the ionic balance in terms of equivalents per million (EPM). PHREEQE reports the ionic balance as the difference between cations and anions in molality.

Mass Balance

Mass balance is an ambiguous term in the literature that may refer to one of the following two concepts:

1. Change in mass of a particular element, compound, or chemical species during dissolution or precipitation along a reaction path. Mass balance can be considered as a "budget" of sources from which the dissolved constituents in a water originate. A simplified equation can be written (Plummer et al, 1983; Plummer, 1984):

   Initial solution composition + Reactant phases ---> Final solution composition + Product phases

Plummer (1984) and Plummer et al (1983) provide good discussions of this aspect of mass balance, and how it affects the progression of calculations in subsequent geochemical processes. This process is also referred to as "mass transfer" if the mass balance reaction involves the shifting of chemical constituents from the solid to the aqueous phase and vice versa (dissolution/precipitation), or from the aqueous to the gaseous phase (degassing/ingassing).

The concept of mass balance also applies to conservation of electrons if the problem involves redox, such as sulfate reduction, pyrite oxidation, or other transfer of electrons from one species to another. Hydrated electrons do not exist in effective concentrations in

solution (Thorstenson, 1984) so that if electron transfer does occur through a redox reaction, the electrons transferred are conserved among the dissolved species (Plummer, 1984). Mass balance equations for hydrogen and oxygen are often not included in chemical models, because of the impracticality of analytically determining the total masses of these elements in solution (Plummer et al, 1983).

The most difficult aspect of mass balance modeling is the non-unique nature of modeled results that usually occurs (Plummer, 1984).

2. Conservation of mass in the calculation of chemical speciation, sometimes referred to as mole balance. When partitioning the total mass of a particular ion among its various species, the computed sum of the free and derived (complexes) species must be equal to the given total concentration (Nordstrom et al, 1979a), for example:

$$\text{Total[Ca]} = CaCO_3 + CaOH + CaHCO_3 + CaSO_4$$

Garrels and Thompson (1962) provide an example of mass balance on total sodium for some possible species:

$$m_{Na^+\ TOTAL} = m_{Na^+ uncomplexed} + m_{NaHCO_3^0} + m_{NaCO_3^-} + m_{NaSO_4^-}$$

Mass balance is closely tied to chemical speciation, since the mass of the element distributed over the aqueous species must equal the mass of the total element. As the above equation illustrates, a mass balance equation is only as valid as the accuracy and completeness of the chemical model. If modeling is done using computer codes, the speciation will only be as complete as the thermodynamic database allows. Furthermore, if analytical data is inaccurate, the error will be propagated into the speciation calculations.

Mass Transfer: Mass transfer refers to the change in state and/or transport that minerals, elements, or aqueous species undergo during chemical reactions or other processes such as adsorption and dispersion. An example would be the dissolution by water of 1 mmol/kg of calcite to

release 1 mmol/l of Ca^{2+} ion and 1 mmol/l of HCO_3^-. The mass transfer that occurred is the transfer of 1 mmol/kg of solid calcite into solution as dissolved Ca^{2+} and HCO_3^-.

Incorporation of mass transfer calculations into a model is usually a necessity for any forward reaction path simulation. Mass transfer occurs during reversible equilibration reactions between minerals and solution, and the subsequent speciation, as in the dissolution of calcite described above. Mass transfer also occurs in irreversible reactions such as dissolution of pyrite from pit wall rocks. Mass transfer calculations require some extent of user manipulation regarding which minerals to include, and in the case of irreversible reactions, the quantities of minerals involved.

Equilibrium Thermodynamics

As presented by Drever (1988), for a hypothetical reaction in which *a* moles of A ion reacts with *b* moles of B ion to form *c* moles of C and *d* moles of D:

$$aA + bB = cC + dD \qquad (7)$$

at equilibrium the following equality will hold true:

$$\frac{a_C^c \cdot a_D^d}{a_A^a \cdot a_B^b} = K_{eq} \qquad (8)$$

where a is the activity of the particular ion, and K_{eq} is the equilibrium constant for the reaction (also referred to as K_{sp} for solubility product constant, or K_T). The standard means of expressing the relationship depicted in equation (7) is to place the reactants on the left side, and the products on the right, which would correspond to dissolved ions on the left and solid mineral on the right. As an example, the equation may correspond to the reaction between ferric iron and hydroxide to form ferric hydroxide and water:

$$Fe^{3+} + 3OH^- = FeO(OH) + H_2O \qquad (9)$$

If the activities of water and pure solids are assumed to be unity, as is customarily done, then an equilibrium equation can be written as follows:

$$a[Fe^{3+}] \cdot a[OH^-]^3 = K_{eq} \qquad (10)$$

Equilibrium constants can also be derived from basic thermodynamic data (such as the free energy of formation ΔG_f^0) as presented by Drever (1988).

Saturation Index: The product $a[Fe^{3+}] \cdot a[OH^-]^3$ is called the *ion activity product* (IAP), and at equilibrium, IAP = K_{eq}. The quantity IAP/K_{eq} is called the *saturation index* (SI), and at equilibrium will be 1.0 (or log SI = 0). The saturation index is most commonly expressed in logarithmic form, since the values may span many orders of magnitude:

$$\log SI = \log_{10} \frac{IAP}{K_{eq}} \qquad (11)$$

If the system is not at equilibrium, then the IAP will not equal the K_{eq}, and reaction (7) will tend to proceed in one direction or the other. If SI < 1 (log SI < 0), the system will be undersaturated with respect to the particular mineral, and the mineral will tend to dissolve into the solution. In equation (7), if the mineral and water are represented by the components cC and dD respectively, then the reaction will tend to proceed from right to left. If SI > 1 (log SI > 0), the system will be supersaturated (also referred to as oversaturated) with respect to the mineral, the reaction will tend to proceed from left to right, and the mineral will tend to precipitate from solution.

The thermodynamic data in a computer code's database may come from several different sources. One potential discrepancy that may be

encountered in tabled thermodynamic data is that results of one experiment (values for ΔG_f or K_{sp}) may not match the results for the same species from another researcher's experiment. The determination of thermodynamic data has been a subject of active research among chemists, and the data are continuously being revised and expanded. New thermodynamic data periodically find their way into the computer codes, so the user should be aware of the sources of the data, and the potential differences in modeling results that may occur.

Errors in thermodynamic and analytical data will cause a range of uncertainty for the SI that must be considered when interpreting the output. This uncertainty will vary according to the complexity of the mineral stoichiometry and input data errors (Ball and Nordstrom, 1991). Nordstrom et al (1979b) chose an "equilibrium zone" around the saturation index equal to the estimated uncertainty of the solubility product constant. Within these limits, the solution is considered to be in equilibrium with respect to the mineral phase, and only outside the limits is the mineral considered over or under saturated.

Examination of saturation indices for natural waters will often reveal many mineral phases that are oversaturated by several orders of magnitude. These phases may not necessarily be precipitating in the system, even though thermodynamics say they should. Minerals must often overcome a level of energy known as the "activation energy" before precipitation can occur. As reactants go to products, they must pass through an intermediate stage of higher energy than the reactants that ultimately will form (Drever, 1988). Precipitation may also be hindered by a lack of available nucleation and growth sites (Davison and House, 1988).

Modelers must also be aware of cases of "partial equilibrium" (Plummer et al, 1983). Although a mineral may actually be dissolving or precipitating in a groundwater system, the SI calculation may indicate

equilibrium with respect to the mineral. Partial equilibrium occurs when one or more slow mineral-water reactions, or changes in pressure or temperature, drive a larger set of faster reactions, the latter of which may continually shift to maintain equilibrium (Helgeson, 1968).

Plummer (1984) concluded that a mineral was in equilibrium along flow path if it was both saturated and had zero mass transfer. The mineral was in apparent equilibrium if speciation calculations showed saturation in the system, but had non-zero mass transfer along the flow path. If the mineral has non-zero mass transfer along the flow path, but is not saturated, it is reacting irreversibly. Minerals that are not saturated in the system and have zero mass transfer are either not present along the flow path or, for kinetic reasons may be considered inert on the time scale of the flow system (Plummer, 1984).

Reversible vs irreversible reactions: Modelers use the term reversible to describe a reaction involving a mineral that may reach equilibrium in solution. The mineral may dissolve or precipitate along reaction path as thermodynamics demand to maintain a state of equilibrium in the system. An irreversible reaction is one in which the mineral is not expected to reach equilibrium in the system, or is unable to because of thermodynamic conditions. Irreversible reactions generally involve slow dissolution of one or more minerals that do not reach equilibrium (Plummer et al, 1983).

Incongruent dissolution: Many aluminosilicate minerals dissolve incongruently, leaving a residual clay mineral, such as K-feldspar weathering to kaolinite (Drever, 1988):

$$2KAlSi_3O_8 + 2H^+ + 9H_2O = Al_2Si_2O_5(OH)_4 + 2K^+ + 4H_4SiO_4$$

This behavior presents problems in chemical modeling, since the mineral

may not demonstrate reversible, equilibrium solubility behavior (Nordstrom et al, 1990). Although a modeling simulation may show a solution to be supersaturated with respect to a certain silicate mineral phase, one should not expect to see the mineral precipitating in the field. This may be a common problem in chemical modeling, since many simulations will involve silicate assemblages. Therefore, equilibrium constants for many silicates should be used with caution. The problem applies to feldspars, smectites, illites, chlorites, amphiboles, micas, pyroxenes, and pyrophyllites (Ball and Nordstrom, 1991).

Solubility vs. K_{sp}: Values for K_{sp} do not necessarily correlate with mineral solubility, and cannot be used to predict relative solubilities of minerals because of complications introduced to the K_{sp} equation by polyvalent ions. Sawyer and McCarty (1978) provide a good illustration of this point, using barium sulfate and calcium fluoride as examples. At 20°C, the solubility of these compounds is:

$$BaSO_4 = 1.1 \times 10^{-5}\ M$$
$$CaF_2 = 2.05 \times 10^{-4}\ M$$

which shows that CaF_2 is about 20 times more soluble than barium sulfate. Substituting these values into the solubility product equation gives:

$$[Ba^{2+}][SO_4^{2-}] = [1.1 \times 10^{-5}][1.1 \times 10^{-5}] = 1.2 \times 10^{-10}$$
$$[Ca^{2+}][F^-]^2 = [2.05 \times 10^{-4}][4.1 \times 10^{-4}]^2 = 3.4 \times 10^{-11}$$

which demonstrates that the most soluble mineral, CaF_2 has the smallest solubility product constant, because fluoride concentration is raised to the second power. Chemical modeling provides a fast means of comparing mineral solubilities with equilibrium constants.

Temperature/pressure dependency: Dissociation/equilibrium constants are thermodynamic constants, and are independent of the solution ionic strength, but not independent of temperature and pressure (Garrels and Thompson, 1962). The derivation from first principles shows the relationship between the equilibrium constant and the standard free energy of reaction, which also illustrates the dependency on temperature and pressure (Drever, 1988):

$$K_{eq} = \frac{a_C^c \cdot a_D^d}{a_A^a \cdot a_B^b} = \exp\left[\frac{-\Delta G^\circ}{RT}\right]$$

Values for ΔG° and K_{eq} are experimentally derived, generally at 25°C and 1 atmosphere pressure (standard temperature and pressure, STP). Deviations from STP will change the value of ΔG° and K_{eq}, and hence change the thermodynamic behavior of the particular mineral or aqueous species. Most minerals exhibit higher solubility with higher temperature, resulting in higher concentrations of dissolved species. Calcite is the notable exception, which becomes less soluble with higher temperature. Gases also show higher solubility in colder solutions.

Computer codes use one of two formulas to correct constants for temperature deviations from 25°C. The preferred formula is (Allison et al, 1991; Ball and Nordstrom, 1991; Parkhurst et al, 1980; Plummer et al, 1984):

$$\log K_T = A + BT + C/T + D\text{Log}(T) + ET^2 + F/T^2 + GT^4 \quad (12)$$

Unfortunately, the constants (A through G) are only available for a limited number of chemical species and minerals. Only 38 species in WATEQ4F have the constants available (Ball and Nordstrom, 1991), 34 in PHREEQE (Parkhurst et al, 1980), and only 25 of the more than 1000 species in the MINTEQA2 database have the constants (Allison et al, 1991). For species without the constants, the Van't Hoff equation is

used:

$$\log K_T = \log K_{Tr} - (\Delta H_r^0/2.303R) \times (1/T - t/T^r) \qquad (13)$$

For temperatures far from 25°C, the variation of ΔH_r^0 with temperature should be recalculated from heat capacity data (Drever, 1988)

Chemical Speciation

A species is defined as a chemical entity such as an ion, molecule, solid phase, etc., that is present in solution (Drever, 1988). Species are generally grouped on the basis of the major cation. Chemical analyses typically express the concentration of a particular ion in terms of the "total" Na, K, Ca, Mg, etc., and the sum of the molal concentrations of the ion in each species will equal the "total" ionic concentration.

An illustration of speciation is seen in the Garrels and Thompson model (1962), in which they express their hypothesized speciation distribution of the major cations in seawater:

$$Na^+ \text{ TOTAL} = Na^+ + NaHCO_3^\circ + NaCO_3^- + NaSO_4^-$$
$$K^+ \text{ TOTAL} = K^+ + KSO_4^-$$
$$Ca^{2+} \text{ TOTAL} = Ca^{2+} + CaHCO_3^+ + CaCO_3^\circ + CaSO_4^\circ$$
$$Mg^{2+} \text{ TOTAL} = Mg^{2+} + MgHCO_3^+ + MgCO_3^\circ + MgSO_4^\circ$$

Using sodium, they show that a mass balance relation can be written for each analyzed constituent:

$$m_{Na^+ \text{ TOTAL}} = m_{Na^+ \text{uncomplexed}} + m_{NaHCO_3^\circ} + m_{NaCO_3^-} + m_{NaSO_4^-} \qquad (14)$$

where $m_{Na^+ \text{ TOTAL}}$ is the molal concentration of total sodium.

Species can also be grouped on the basis of a particular system. For example, in the system $CaCO_3$-H_2O-CO_2, possible species may include Ca^{2+}, CO_2, $CO_{2(aq)}$, H_2CO_3, HCO_3^-, CO_3^{2-}, H^+, OH^-, $H_2O_{(l)}$, $H_2O_{(g)}$, $CaCO_{3(s)}$, plus various complexes (Drever, 1988). The MINTEQA2 code includes the following ten "soluble" species in a $CaCO_3$ solution at equilibrium:

Ca^{2+}, $CaOH^{+}$, $CaCO_3^{\circ}$, $CaHCO_3^{+}$, H_2CO_3, HCO_3^{-}, CO_3^{2-}, H^{+}, OH^{-}, H_2O

The determination of aqueous species distribution is accomplished by means of a chemical model similar to that developed by Garrels and Thompson (1962), which was the first application of the method of successive approximation. Although their model only considered 17 species, Garrels and Thompson stated, "the manipulations involved in solving these (equations) simultaneously are tedious," which is why such calculations today are left to computers.

Geochemical speciation codes write solute reactions as association (formation) reactions, whereas the solid reactions are written as dissociation (dissolution) reactions (Ball et al, 1979). The association and dissociation equations are sets of nonlinear mass action and mass balance equations that are based on the equilibrium relationships discussed in the previous section. Codes used in this study (MINTEQA2, PHREEQE, WATEQF, WATEQ4F) determine speciation by solving these equations through the mathematical approach known as the continued fraction method (Wigley, 1977).

An example of a speciation calculation, as it is performed by the WATEQ codes, is demonstrated by Truesdell and Jones (1974). Anionic weak acid species, such as silicic acid, are computed first. By combining mass action and mass balance equations, the speciation distribution can be determined from the total analytical concentration, pH, the equilibrium constant, and the activity coefficient. The WATEQ example demonstrates silica speciation ($H_3SiO_4^{-}$ and H_4SiO_4) beginning with the mass action equations:

$$H_4SiO_4 = H^{+} + H_3SiO_4^{-}$$

and

$$H_3SiO_4^{-} = H^{+} + H_2SiO_4^{-2} \qquad (15)$$

rearranging these equations gives:

$$K_1 = \frac{^{m}(H_3SiO_4^-)\,(\gamma H_3SiO_4^-)\,(10^{-pH})}{^{m}(H_4SiO_4)\,(\gamma H_4SiO_4)} \qquad (16)$$

and

$$K_2 = \frac{^{m}(H_2SiO_4^{-2})\,(\gamma H_2SiO_4^{-2})\,(10^{-pH})}{^{m}(H_3SiO_4^-)\,(\gamma H_4SiO_4)}$$

The mass balance (or mole balance) equation for total silica (silicic acid and silicate ions) is:

$$^{m}Si_{total} = {}^{m}H_4SiO_4 + {}^{m}H_3SiO_4^- + {}^{m}H_2SiO_4^{-2} \qquad (17)$$

The mass action equations can be combined with the mass balance equations to solve for $^{m}H_4SiO_4$, as shown by:

$$^{m}H_4SiO_4 = \frac{^{m}Si_{total}}{1 + \gamma H_4SiO_4 \left[\frac{K_1 10^{pH}}{\gamma H_3SiO_4^-} + \frac{K_1 K_2 10^{2pH}}{\gamma H_2SiO_4^{-2}} \right]} \qquad (18)$$

The quantity $^{m}H_4SiO_4$ is then substituted back into the mass action equations (15) to solve for $^{m}H_3SiO_4^-$ and $^{m}H_2SiO_4^{-2}$. A similar procedure is used for speciation of other components, such as phosphate, borate, and sulfide. Carbonate-bicarbonate distribution also includes pH and alkalinity after correction for other weak acid radicals (Truesdell and Jones, 1974).

Garrels and Thompson (1962) derived a total of 17 species from the major ions in seawater, requiring 17 independent equations. They admit that their model is a first approximation, through their assumption that interactions among the major ions result only in the formation of ion pairs. Despite the shortcomings, the eight major ions analyzed, and their associated species, constitute over 99 percent of the dissolved solids of sea water. Subsequent studies have expanded the number of known species in seawater to at least 60 (Parkhurst, et al 1980).

Limitations: The results of speciation calculations, such as those performed by computer, are only as good as the input data. The use of unreliable equilibrium constants or activity coefficients can completely change the predominant form of a complexed species, and therefore the interpretation of the water chemistry (Millero, 1975, 1977; Nordstrom and Ball, 1983). This can have impacts on subsequent modeling for points further along a reaction path, and will propagate any error introduced.

The number of species that can be modeled depends on the availability of data for the chemical model. For computer simulations, this will be a function of the size of the database. Addition of desired species or minerals to the code's thermodynamic database may be necessary before modeling is attempted. For example, it would be futile to attempt to model the chemistry of a silicate aquifer if the only silica-bearing minerals contained in the code's thermodynamic database were quartz and amorphous silica. Furthermore, a particular model that has a larger database of aqueous species for a particular element will predict lower concentration of free ion (Nordstrom et al, 1979a). The model predicting higher concentration of free ion may be invalid.

Species that are rare or absent in natural waters may be important in anthropogenically influenced systems, but thermodynamic data may not yet exist. An example was suggested by Nordstrom et al (1979b) who noted that data for ion triplets such as $Fe(SO_4)_2^-$ are not accurately known and possible complexes such as $FeHSO_4^{2+}$ and $Fe(HSO_4)_2^0$ have not been properly identified.

A model is "saturation sufficient" if the code database is suitably comprehensive to define saturation indices for a given set of plausible phases in the system (Plummer et al, 1983). An incomplete database may predict an erroneous saturation index for a mineral, which could be propagated through the modeling effort. They cite the two most

common examples of saturation insufficient data as the absence of analyses for dissolved iron and aluminum.

Recent studies show that organic matter may be responsible for complexation of up to 100% of some metals in natural waters (Morel and Hering, 1993). Since geochemical code databases are mostly limited to inorganic species, abundant organic complexation may render a computer simulation highly inaccurate. The user should be aware of the amount of TDC (total dissolved carbon) in the system, and potential inaccuracies that may arise through the exclusion of organic complexation.

To add species to a computer code's thermodynamic database, the user generally must provide values for ΔH_f^0 and K_{eq}. Prior sections demonstrated how these data are used to calculate speciation and saturation indices. The ΔH_f^0 and K_{sp} data can be obtained from published sources.

Oxidation/Reduction (Redox)

A redox species is defined as a species of any element which can exist in more than one oxidation state in natural aqueous environments (Parkhurst et al, 1982). Examples are ferrous (Fe^{2+}) vs. ferric iron (Fe^{3+}), arsenite (AsO_3^{3-}) vs. arsenate (AsO_4^{3-}), and nitrate (NO_3^-) vs. ammonia (NH_4^+). Other elements with redox chemistry include Cu, Hg, Mn, S, and Tl. Redox reactions usually are kinetically controlled and many are microbially mediated (Ball and Nordstrom, 1991).

Applying a field Eh to rigorous geochemical problems involving redox can be risky, since redox couples do not tend to reach equilibrium with each other in natural waters (Lindberg and Runnells, 1984). Redox potentials measured in natural waters usually represent mixed potentials. Most system are likely in internal disequilibrium and determining which couple is most responsible for the measured value will be difficult without separate analyses for each component (Lindberg and

Runnells, 1984). As and Se, and probably all oxyanions, do not give reversible potentials at a platinum electrode (Runnells and Lindberg, 1990; Runnells and Skoda, 1990). Only dissolved iron, dissolved sulfide, and possibly dissolved uranium and vanadium are likely to give reversible potential measurements for a platinum electrode, and then only when the concentrations are high enough (Ball and Nordstrom, 1991). The HS^-/SO_4^{2-} can be discounted as redox controls because sulfate is not involved in reversible redox reactions at low temperatures (Lindberg and Runnells, 1984).

Geology

Under normal circumstances, the chemical composition of a terrestrial water is directly controlled by rock/water interaction in the watershed or aquifer. Exceptions might include anthropogenic contamination, such as spills or agricultural runoff. The "major ions" will generally indicate from which type of lithology/mineralogy a water has evolved, such as carbonate or silicate. The major ions most commonly seen in solution from weathering of carbonate and silicate rocks are: Ca^{2+}, Mg^{2+}, Na^+, K^+, Cl^-, HCO_3^-, and SO_4^{2-}. Concentrations of these ions in natural waters typically range from 10^{-5} to 10^{-2} molal.

Understanding the local geology will be vital in successfully interpreting any model, even simple speciation models. Forward modeling, in which future water chemistry is predicted after interactions with minerals, will obviously require detailed knowledge of the minerals. The same is true for inverse modeling, which requires detailed knowledge of mineral mass transfer as a water body evolves along a flow path.

The solubility and thermodynamic behavior of common minerals will aid an understanding of water chemistry. The modeler must recognize implausible minerals or reactions in simulation results. A familiarity

with the behavior of minerals and aqueous species will allow more accurate interpretations of modeling results. Examples are seen in the thermodynamic behavior of carbonates, sulfates, silicates, and sulfides.

Carbonates dissolve congruently and exhibit reversible dissolution/precipitation behavior. They are fairly soluble, and have relatively rapid kinetics. Carbonates are generally responsible for the bulk of calcium, magnesium, and bicarbonate in solution.

Sulfates, such as gypsum and anhydrite, are also very soluble, reversible, and can contribute high concentrations of calcium and sulfate to solution.

Silicates are more difficult to model, since they dissolve incongruently, have a wide range of solubilities, and do not exhibit reversible dissolution/precipitation behavior. As an example, Garrels and Mackenzie (1967) discovered in the Sierra Nevada spring study that plagioclase weathers disproportionately higher than other silicates and contributes the bulk of ions to solution. Quartz and K-feldspar remain as solid residues, eventually removed by mechanical weathering. The results of this study suggest that dissolved SiO_2 in the Sierra spring water, and likely most natural waters, comes from silicate weathering, not quartz dissolution.

Sulfides are fairly soluble and weather rapidly, but may form an oxidation product such as iron hydroxide, or dissociate during oxidation and form free ferric iron, sulfate, and hydrogen ion. Unlike most carbonates and silicates, however, the stability of iron species is redox dependent.

There are probably no groundwater systems that are in overall chemical equilibrium with their host mineralogy (Plummer, 1984). This likely applies to rivers and lakes as well. Although more soluble minerals like carbonates and sulfates may reach equilibrium, most mineral phases probably will not. Therefore, the Saturation Index of

most minerals will be some distance from 1.0, indicating a tendency for either dissolution or precipitation. Most waters are generally undersaturated with respect to the minerals of the local lithologies, favoring continued mineral dissolution.

3. MODEL DEVELOPMENT AND APPLICATION

The objectives of chemical modeling may include any or all of the following: to determine 1) what chemical reactions have occurred, 2) the extent to which reactions have proceeded 3) the conditions under which the reactions occurred (open vs. closed, equilibrium vs. disequilibrium, constant vs. variable temperature), and 4) how the water quality and mineralogy will change in response to natural processes and perturbations to the system (Plummer, et al, 1983).

The process of developing and applying a chemical model is accomplished in a series of steps, similar to the development of groundwater flow numerical models. Development of the conceptual model is followed by development and testing of the numerical model, calibration, and validation. Once these steps have been successfully completed, the model is ready for application.

Conceptualization

The information desired about a hydrogeochemical system will guide the development of a conceptual model on which to base the numerical model. Conceptual model development starts by first determining the information desired from the model, and the input required to run the model.

Information desired: Chemical modeling simulations generally fit into one of three categories - speciation, inverse, and forward. The complexity of the model will be proportional to the quantity and quality of information desired.

A speciation model is basically a "snapshot" of a water sample at a point in time, and is the simplest type model to learn and apply. A speciation model will be sufficient if the only desired information is the distribution of chemical species, ionic balance, saturation indices,

or determination of possible mineral phases in contact with the water. No reactions or mass transfer are modeled, and no predictions are made of future water chemistry.

If information is desired regarding chemical mass balance of minerals and dissolved species between two points along a hydrologic flow path (i.e. mineral dissolution/precipitation between two wells), then an inverse model is required (Plummer et al, 1983). Inverse modeling demands more complete and precise input data, as well as more geologic and geochemical insight. An example of a scenario requiring inverse modeling techniques is shown in Figure 3-1. The desired information is mass transfer between the two wells, which is determined from the water chemistry of each and a set of hypothetical, user-specified mineral phases. The mass transfer between well #2 and the lake in Figure 3-1 could also be considered an inverse modeling problem.

Included under mass transfer are all calculations for which there is a recomputation of the distribution of species in response to changes

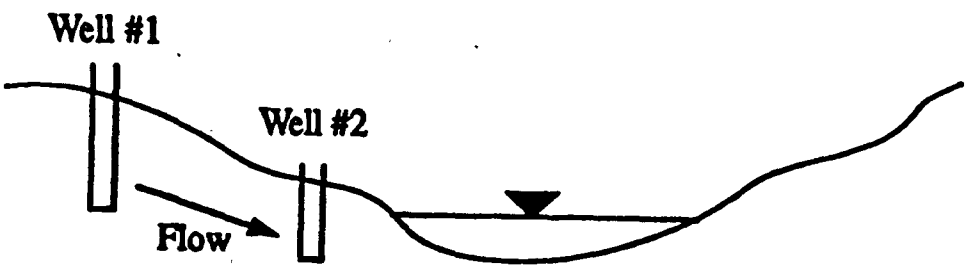

Figure 3-1: Scenario requiring inverse modeling methods (from Glynn et al, 1992).

in the composition, temperature and/or pressure of the fluid (Plummer, 1984). This includes mineral solubility, dissolution, precipitation, irreversible reactions in partial equilibrium systems, adsorption,

mixing of water, etc. The mass transfer calculations predict the amounts of minerals transferred among aqueous, gaseous and solid phases as a function of irreversible reactions and/or thermodynamic constraints.

Inverse modeling may require little more real data input than the speciation models, but the mental input required is substantial. Since inverse modeling involves the determination of mass balance/mass transfer, the user needs both comprehensive chemical analyses of the waters, and thorough knowledge of the mineralogy of the system. However, the determination of these mineral phases requires a level of common sense regarding geologic processes and mineral stabilities. As stated in the NETPATH manual: "The validity of the mass-balance models depends significantly on the geochemical insight of the modeler in selecting appropriate phases in the model."

Inverse modeling is not constrained by thermodynamics, and may imply reactions that are thermodynamically impossible (Parkhurst et al, 1982). It may therefore be necessary to verify the mass balance calculations by speciation modeling. Inverse model results can be used as input for forward models, provided thermodynamic constraints are not violated. Plummer and colleagues have applied inverse and forward modeling techniques to the Florida and Madison Aquifers (1983, 1984, 1990).

Inverse models may also carry errors through the simulation unchecked. For example, if the ionic balance input to inverse models carries a significant error, it may be carried into the mass transfer calculations, resulting in faulty molal transfers and erroneous interpretations regarding the chemical evolution of the water.

The results of an inverse model will be valid only if the two data sets are from the same hydrologic flow path (i.e. along a groundwater stream line, or two points on a river). Attempts to model changes in

water chemistry between two unrelated waters will be meaningless (Plummer, 1984).

Forward modeling is required if the desired information includes predictions about water chemistry that might arise through chemical reactions, biological activity, ion exchange, adsorption, or other process contributing to the chemical evolution of a water body (Plummer, 1984). Forward models generally have less data available than inverse models, hence forward methods may be required in situations where an inverse model should be utilized, if only one analysis is available along flow path. This scenario is illustrated in figure 3-2. The setting is identical to the inverse model, but no second well exists. The desired information might be the groundwater chemistry at the location of Well #2 from the previous example.

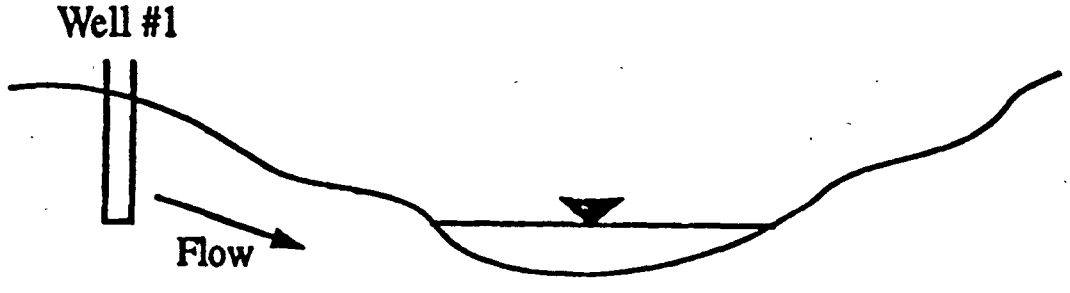

Figure 3-2: Scenario requiring forward modeling methods (from Glynn et al, 1992).

The most complex application of a forward model is the reaction path simulation. Reaction path modeling is designed to determine the chemical composition of an aqueous solution, and the masses of minerals dissolved and precipitated based on a set of hypothetical reactions and thermodynamic constraints imposed by the user. Reaction path models

require a thermodynamic model, an initial water composition, and an assumed set of irreversible reactions and/or mineral-water equilibrium constraints. Using these, the model predicts the evolution of water and rock as a function of reaction progress (Plummer et al, 1983). Reaction progress is measured in terms of a progress variable, such as pH, temperature, or the moles of a reactant dissolved into solution. If kinetic data are available, time may be chosen as the progress variable (Plummer et al, 1983). A valid reaction path model, therefore, requires detailed knowledge of mineral suites in the system, pH and redox states, biological processes, and gas exchange.

Most modeling exercises, both forward and inverse, will usually generate multiple results. To eliminate implausible results and isolate the best model, the researcher must then draw upon geological and geochemical knowledge, or in some cases geologic "common sense" if no data are available. Even then, only an approximation of the actual system may be obtained. As stated by Plummer et al (1983): "Rarely, if ever, will the unique reaction which corresponds with reality be isolated."

Input required: A speciation model requires a chemical analysis for the water, and physical parameters such as pH, Eh and temperature. Thermodynamic constants are required for each dissolved species and mineral of interest, but are built into the databases of all speciation codes considered in this study. However, the thermodynamic database of each code is different, and the researcher must be aware of the differences and be prepared to modify thermodynamic data if necessary and if the code allows. An example of a small discrepancy in thermodynamic data between codes is seen in the solubility constant for quartz in PHREEQE (log K_{sp} = -4.0477) vs. WATEQF (log K_{sp} = -4.075). Although this difference is minor and probably will not introduce significant error in calculations involving quartz, the example

illustrates the potential differences that may be encountered in thermodynamic data.

Program output will include chemical species distribution, ionic balance, and saturation states of all plausible mineral phases contained in the software database. Speciation modeling is often an integral component of subsequent interpretation of inverse or forward simulations (Plummer et al, 1983). The inverse program NETPATH runs WATEQF speciation models for each water sample before performing any mass balance/mass transfer simulations.

The inverse model requires two additional bits of information beyond the speciation model: Water chemistry from a second water sample along the same evolutionary flow path as the first, plus a set of plausible mineral and gas phases in contact with both waters along flow path. The specified mineral and gas phases will interact with the first water to produce the second while satisfying mass balance among all components.

Sulfur and carbon isotopic information can also be incorporated to help define mass transfer along flow path in groundwater (Plummer, 1984; Plummer et al, 1983, 1990). Although mass transfer calculations can be accomplished without isotopic data, they provide an additional constraint that helps eliminate implausible results. The inverse model assumes the effects of hydrodynamic dispersion are negligible (Plummer et al, 1983).

The output from an inverse model is a set of scenarios indicating the possible mass transfer that occurred among the selected mineral phases to generate the second water from the first. Thermodynamic constraints are not an explicit part of the mass balance methodology, so it is usually necessary to check each model for thermodynamic violations (Plummer et al, 1983). This can be accomplished by speciation calculations at the endpoints of the flow path. For example, an inverse

model may predict dissolution of a mineral along flow path, but speciation models at each endpoint show the mineral as oversaturated. Either the inverse model has generated invalid results, or the mineral is undersaturated somewhere between the endpoints. Examples of inverse model application are provided by Plummer (1984) and Plummer et al (1983, 1990).

The most difficult aspects of inverse modeling are selection of hypothetical phases, and calibration of the model through elimination of implausible modeling results. The selection of plausible mineral phases requires detailed information on the mineralogy of the system, combined with geologic "common sense." The value of the mass balance calculations is directly proportional to the amount of analytical data available (Plummer et al, 1983). The modeler may be unable to identify all mineral phases present and reacting in the system (due to inadequate data), which will adversely affect the mass balance calculations, and hence, the validity of the model.

The forward model is the most demanding and involves the highest degree of uncertainty, because less information is usually available than for the inverse model. Forward modeling requires educated guesses regarding reversible and irreversible chemical reactions that determine the chemical evolution of the water. The forward model also requires definition of initial conditions (i.e. a starting water sample), but the final conditions can vary depending on the location along flow path at which the simulation terminates. The model of the forward problem is complete when all appropriate equilibrium or apparent equilibrium mineral-water reactions are included (Plummer, 1984).

Plummer (1984) discusses the importance of adjusting initial water input concentrations to attain electrical neutrality. This step can be ignored if the modeler chooses to maintain the analytical integrity of the initial solution. The modeler must decide when it is better to

leave the analytical data unadjusted, in which case the charge imbalance will be distributed among the computed mass transfer coefficients. For this study, analytical data was left intact and charge imbalance was carried into subsequent simulations.

The output of a forward model is a prediction of water chemistry, and perhaps an estimate of mineral mass transfer and mass distribution generated as reactions occurred along flow path. Unlike inverse model results, forward model results will not contain violations of thermodynamic constraints. The selection of plausible results will be based on information such as final dissolved concentrations, mass distribution or transfer, or parameters such as pH or Eh.

Inverse modeling is the method of choice when the necessary information is available. Forward modeling is regarded as a method of last resort when information is unavailable. Inverse modeling can also be thought of as determining what *has* happened, whereas forward modeling predicts what *will* happen.

The ideal scenario for development of a forward model is when information is available to allow calibration with an inverse model, a procedure that has been applied in this study. If a reaction is found through forward modeling that satisfies the net mass transfer constraints defined by the inverse model, then the calculated path is thermodynamically valid (Plummer et al, 1983).

The Numerical Model

Development: The development of the numerical model involves gathering and compiling data, and incorporation of these and other parameters into the conceptual model to give the simulation unique characteristics representative of the field situation. This information represents input to the computer modeling codes.

What constitutes input "data" may not be explicitly definable, and

may be subject to considerable user discretion. Examples include the selection of plausible mineral phases, estimates of irreversible reaction stoichiometries, ratios, and/or masses, or selection of ion sources and sinks. Input data therefore will be a combination of actual field data, and a set of user-defined variables or parameters that will act upon, or be acted upon by, the actual data.

Field data can include water chemistry, aquifer or wallrock mineralogy, mineral percentages, precipitation/evaporation rates, and perhaps groundwater flow rates. The user-defined parameters might include mixing ratios of different water parcels, irreversible mineral dissolution masses, kinetic data, time frames, or minerals involved in reversible equilibrium reactions.

Both inverse and forward hydrogeochemical models will require initial and boundary conditions, not unlike numerical groundwater flow models. The boundaries, i.e. the beginning and end of the flow path, depend on the information desired and the availability of data (Plummer, 1984). The boundaries of an inverse model are strictly defined as the initial and final points along the modeled flow path.

The boundaries of a forward model may be less rigorously defined, hence subject to higher uncertainty. The initial condition is generally the chemical analysis for the initial water. The final condition depends on the objectives of the study, and may be varied through sensitivity analyses. For example, the initial condition in pit water modeling is the chemistry of groundwater immediately upgradient of the pit. The final condition may be the pit water after a specific time period, at a specified water level, or after a series of reactions have occurred, or it might be groundwater at some point hydraulically downgradient from the pit.

During model development, many specific questions must be answered which will influence the selection of modeling parameters and software.

Plummer (1984) posed the following questions in defining the inverse model of the Madison Aquifer in the northern U.S. These questions will likely be applicable to development of any inverse or forward model:

* What minerals are present and what are their abundances?
* How does mineral abundance, including trace mineralogy, vary spatially in the system?
* What is the actual composition (elemental substitution, exchangeable ions, etc.) of each mineral and how does this vary spatially?
* What is the isotopic composition of the minerals and how does this vary spatially?
* Are there any regional trends in mineralogy or composition that can be related to direction of flow?
* From thin section or SEM examination, which minerals appear to be secondary and which are being replaced?
* Is there evidence of coatings or zoned crystals? And, if so, how does the composition of the coating vary in the crystal:
* Is the mineralogy of more permeable rocks in the system different from that in less permeable zones?

A crucial step in forward model development is the recognition of potential irreversible reactions (Plummer, 1984), such as:

* Oxidation of organic matter, as during sulfate reduction.
* Dissolution of minerals that rarely reach equilibrium in the ground water environment, e.g. primary silicates like pyroxenes, feldspars or trace minerals.
* Gain or loss of gases in the system, such as methane, oxygen or carbon dioxide.

Recognition of reversible reactions will be a key component of either model. Identification of mineral phases with which the water is, or could be, in equilibrium will help constrain the model and isolate implausible results.

Additional questions that may need answering to help define the system during model development include:

* Is the system open to gases such as CO_2, O_2, CH_4, in a reversible reaction?

* What is the scale, both temporal and spatial, of the simulation (i.e. is the pit lake being modeled at incremental depths or at ultimate depth; what distance from the pit do we want to model)?
* Do we need to incorporate reaction kinetics?
* Do we need to model trace elements?

Researchers must be careful not to overconstrain the model. This can be done by violating the phase rule, or by specifying too many fixed components or too few variables. An example is provided by Peterson et al (1987) for carbonate equilibria. The variables are alkalinity, pH, and pCO_2. If all of these are fixed, then a forward simulation that predicts changes to the system is not possible. The execution may terminate and indicate that a phase rule violation has occurred, or may simply remove one of the variables.

When all questions have been answered regarding model conceptualization, the level of sophistication required from the software can be determined. Since each program is designed for a different purpose, each modeler should use a program based on the research objectives. The software are discussed in the next chapter.

Execution: The execution of the actual numerical model proceeds in a series of steps. Model calibration may require an iterative process based on the results of sensitivity analyses, as illustrated below:

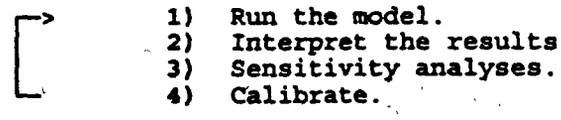

Running the model is self-explanatory in the context of this study, since only "canned" computer software packages are considered. The only constraints are the availability of computer memory and mathematical processing capability, provided the data have been entered correctly into the model.

Interpretation and Sensitivity Analyses: Interpretation of modeling results will be site-specific, and is not a skill that can be acquired by reading a manual. The user must draw on a wide spectrum of geochemical, geologic, and modeling expertise to separate the plausible results from the implausible or invalid. The reader is again referred to Plummer et al (1983) for examples of model calibration.

The selection of the most plausible result might be best achieved through sensitivity analyses that provide a range of possibilities. Sensitivity analyses will provide the combined benefit of bracketing the results within the window of uncertainty, as well as seeing the effect of varying input parameters on modeling output as results move from implausible to plausible within simulations.

The problem of excess plausible phases can be complicated by the existence of mineral phases of variable composition, solid solution or impurities that can change the mineral stoichiometry from that assumed by ideality. This exemplifies the utility of field examination or petrographic data for the geologic system being modeled.

Plummer et al (1983) discuss the difference between possible reaction paths and the net reaction path, which is illustrated in Figure 3-3. The net reaction path is depicted by path 2 in each figure, whereas possible reaction paths are depicted in paths 1, 1a, and 3. In each case, PC (Polk City) is the initial water and W (Wauchula) is the final water. Relative rates of dissolution/precipitation may cause curved paths, but the net reaction path generally is a straight line. The actual reaction path may be definable through small incremental steps in reaction simulation. This type of reasoning may be required in many modeling exercise to eliminate implausible results.

There are several ways of eliminating implausible reaction models from further consideration. First the computed mass transfer should be consistent with the saturation indices (Plummer 1984). Petrographic or

SEM data, plus isotopic data can help eliminate implausible models.

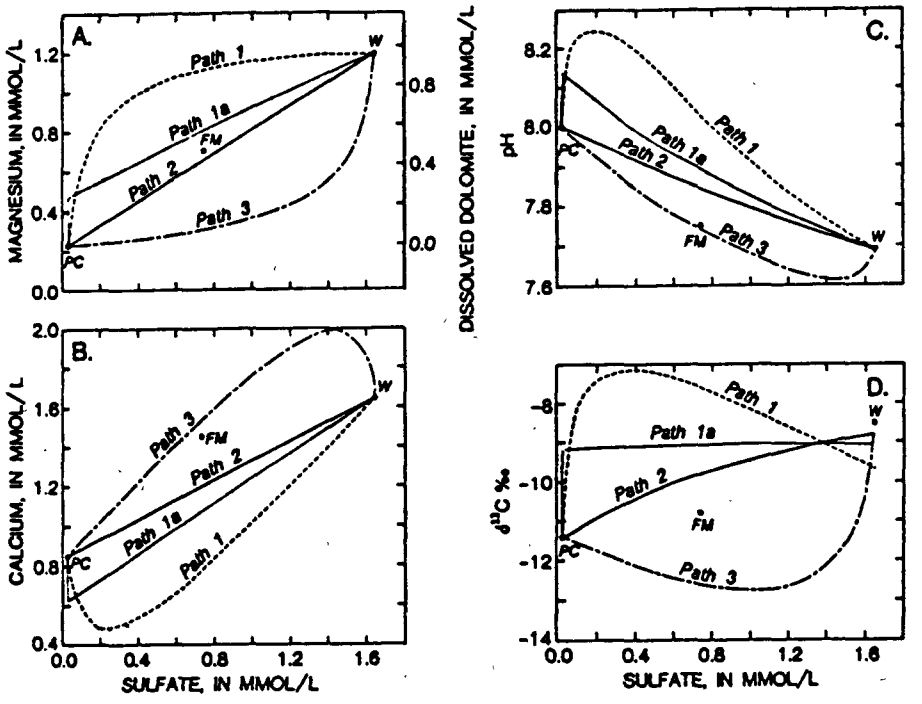

Figure 3-3: Actual vs. net reaction path. Predicted variation of magnesium, calcium, pH, and $\delta^{13}C$ in ground water between Polk City (PC) and Wauchula (W) (from Plummer et al, 1983).

Conditions that may limit the success of chemical modeling are (Plummer, 1984):

* Fracture flow, causing different residences times at different locations in the aquifer.
* Vertical mixing from either leakage or recharge,
* Chemically stratified flow systems (changes in chemistry with depth),
* Groundwater systems that have been altered hydrochemically such as through injection.

Calibration: Calibration is the process of adjusting specific input parameters, such as initial or boundary conditions, and rerunning

the model in an attempt to converge on the desired result. Calibration may be an iterative process requiring several loops through steps 1 to 4 to attain convergence. Calibrating an inverse model can be more difficult than a forward model, because in the inverse model, the final condition is known, and any model which produces different results is obviously invalid. If model calibration is not possible due to faulty input data, then more data collection and compilation may be necessary.

In the forward situation, the modeler generally has a less definitive idea of what to expect in the final condition. Calibration may not be so much an attempt to obtain a final result, but to refine the output to bracket more believable geochemical values.

The success of calibration depends on the availability of real world examples with which the model can be compared. Not all forward models will have the luxury of an example location, in which case the best educated guess may be the only reference with which the model may be compared. Pit water modeling is a case in which a limited number of real world examples exist for comparison.

When a model is calibrated, the input of a certain combination of parameters and boundary conditions will reproduce field measured data as output (Wang and Anderson, 1982). However, the results may not be unique, and multiple models may remain after all tests have been exhausted. In this case, the problem is non-unique and will remain so until appropriate new data are introduced (Plummer, 1984).

Verification/Validation: The final test of a model is to determine whether it successfully simulates field observations. When a numerical groundwater flow model meets these criteria, it is said to be calibrated and verified (Wang and Anderson, 1982). The goal of numerical model verification is to demonstrate that the model can simulate some historical hydrologic event for which field data are available.

The process of verification and validation applies to chemical models as well. Peterson et al (1987) refer to validation as "the coherence, to some acceptable accuracy, of laboratory and field data," and to verification as meaning that "the coding and mathematical algorithms in the computer code were certified to be correct." Models may be verified by comparing the results obtained from the code with results from other codes, or the computations could be checked by hand (Peterson et al, 1987).

Once the model has been calibrated and verified/validated, it is ready for application.

4. SOFTWARE

This chapter discusses the software codes that were used in this study for application of the pit water models (BALANCE, MINTEQA2, PHREEQE, WATEQF, and WATEQ4F). Each code is designed for a different purpose, and therefore each has different input requirements, capabilities, and limitations. The output files generated by each code vary in complexity and length, both of which increase with the number of functions the program is asked to perform.

Speciation modeling codes are discussed first, followed by the inverse, then the forward modeling codes. The order presented also parallels the difficulty of use, and the variety of functions each code can perform. The user friendliness of a code is generally inversely proportional to its capabilities.

Basic input: All simulations require as input the concentrations of dissolved ions obtained from chemical analyses. Most codes require temperature and pH, although PHREEQE can calculate pH depending on the concentrations of other components (alkalinity, pCO_2). If no temperature is provided, codes will generally default to 25°C. If the problem involves redox, either dissolved oxygen or Eh/pe must be specified, or the concentrations of separate redox couples must be provided from which the code can calculate the Eh.

If analytical data for a particular ion are not available, no speciation or saturation calculations will be performed for any species or minerals of which the ion is a component, and that data will be missing from the output. This is a critical concept. Missing analytical data for particular ions will introduce deficiencies in the modeling of speciation and mineral saturation indices.

Database Limitations: The size of each program's thermodynamic database will limit its effectiveness in assigning a valid and complete suite of aqueous species and minerals to the modeled system. This may

be the most significant limiting factor among the various codes. Figure 4-1 shows a comparison of the different databases for several codes. WATEQF has a much smaller database than WATEQ4F. The EQ3/6 and MINTEQA2 databases exceed all others, containing a large collection of trace metal thermodynamic data appropriate for mine-related modeling applications.

===

	PHREEQE	PHRQPITZ	SOLMINEQ88	SOLVEQ CHILLER	REACT	WATEQF	WATEQ4F	WATEQX	EQ3/6	MINTEQA2
Elements	19	14	27	32	19	19	33	19+	47	39
Minerals	43	22	220	203	90	101	322	101+	716 + 16 ss.	456
Gases	3	3	4	11	10	3	3	3+	11	16
Org. Ligands	0	0	3	33	1	0	2	7	0?	8
Hard-coded?	N	N	Y	N	N	Y	Y	N	N	N
Temperature	0-100 C	0-100 C	0-350 C	25-300 C	any T	0-100 C	0-100 C	0-100 C	0-300 C	0-100 C
Pressure	1 atm.	1 atm.	1-1000 bars	limits of thermo. data, (steam line for SOLVEQ)	any P	1 atm.	1 atm.	1 atm.	steam line (max 500 bars)	1 atm.
Aqueous Activity Coefficients	EDH[1] B-dot Davies	Pitzer	Pitzer B-dot	Helgeson's B-dot (ext.	Helgeson's B-dot (ext.	B-dot Davies	B-dot Davies	B-dot davies Mean salt	B-dot Davies Pitzer	B-dot Davies
Redox?	Y	N	Y	No EH input	Y	Y	Y	Y	Y	Y
Redox Couples or pO_2?	Y	N	Y	Y	Y	Y	Y	Y	Y	Y
Mass Transfer?	Y	Y	Y	SOLVEQ N CHILLER Y	Y	N	N	N	Y	Y
Adsorption or Ion Exchange?	Ion exch. (const. comp. exchgr)	Ion exch. (const. comp. exchgr)	Ion exch. Adsorp.	N	N			N	Ion Exch. Adsorp.	Ion Exch. Adsorp.
Solid-Solutions?	N (not released)	N	N	manual	N	N	N	N	manual	N
Kinetics?	N	N	N	N	N	N	N	N	Y	N
Interactive?	Y	Y	Y	Y (in part)	N	Y	Y	Y	Y (partly)	Y
PC Version? (IBM series)	Y	Y	Y	Y	Y	N	Y	Y	N	Y
Version Reviewed	3/90	10/88	10/88	3/89	4/88	12/78	4/89	10/88	11/88	10/90

Figure 4-1: A comparison of databases for some geochemical speciation and mass transfer codes (from Glynn et al, 1992).

===

Speciation Modeling Codes

The speciation modeling codes are the simplest of the software packages to use, primarily because of their limited capabilities. They

are only designed to calculate activity coefficients, ionic balance, chemical speciation, and saturation states (including gas partial pressures) of a water analysis. The only input data required are field parameters (temperature, pH, and solution density) and concentrations of dissolved aqueous components (expressed as total calcium, sodium, sulfate, alkalinity, etc.). Optional field parameters include pe/Eh, dissolved oxygen, and conductivity.

WATEQF and WATEQ4F: The WATEQ codes of the USGS, for which WATEQF and WATEQ4F are the latest versions, are among the most widely used geochemical modeling programs. They have easily understood menu-driven input packages, and provide clear, concise output files. They can be applied to stand-alone speciation studies, or incorporated into more comprehensive studies to help interpret forward or inverse models.

The original WATEQ was written by Truesdell and Jones in 1973 (published by USGS in 1974, Journal of Research) in PL-1 (Programming Language/One). WATEQ contained a thermodynamic database consisting of 22 master species, 100 aqueous species, and 56 minerals. Plummer et al. (1976) translated the PL-1 version into FORTRAN IV (WATEQF, USGS Water-Resources Investigations 76-13), and made minor revisions including addition of manganese species and minerals. WATEQ2 (Ball et al, 1979) incorporated 10 additional trace elements and many additional complexes and minerals. USGS publication WRI 78-116 (Ball et al., 1980) introduced some revisions and corrections to WATEQ2, and WATEQ3 (Ball et al, 1981) added uranium species. The latest version, WATEQ4F (Ball and Nordstrom, 1991), contains a thermodynamic database with 32 master species and over 600 aqueous species and minerals.

The current version of WATEQF (Plummer et al, 1984) is called program WATEQF.PATH, which creates input files for the NETPATH program. WATEQF first calculates activity coefficients, speciation, ionic balance, and saturation indices of each water analysis. WATEQF include

provisions for entering isotopic analysis to be used in mass transfer calculations. The files are then available to be loaded into NETPATH for mass balance calculations in the inverse model. The greatest shortcoming of WATEQF in the context of mine water modeling is the absence of any trace metal data other than iron. WATEQF is therefore inadequate for application to speciation modeling of mine waters containing trace metals beyond iron. WATEQ4F has a larger thermodynamic database, with many trace elements applicable to mine water modeling, including arsenic, cadmium, copper, lead, nickel, silver, uranium, and zinc. Neither WATEQF or WATEQ4F contain thermodynamic data for mercury species.

WATEQ4F has greater flexibility in handling redox problems than WATEQF. WATEQ4F has 9 separate areas in which redox calculations are applied, and 14 means with which to calculate or input an Eh value (Ball and Nordstrom, 1991). A useful application of WATEQ4F is to verify field Eh measurements by calculating redox potential from the concentrations of each component in a redox couple (e.g. Fe^{2+}/Fe^{3+}, or NH_4^+/NO_3^-). WATEQ4F can calculate the system pe/Eh from any of several redox couples, then can redistribute the remaining redox couples bases on the calculated pe/Eh.

The WATEQ codes can calculate speciation in water samples ranging in temperature from 0° to 100° C. However, thermodynamic solubility constants are specified for 25°C, and adjustments to K_{sp} values via the Van't Hoff equation for departures from 25°C increase the uncertainty in the modeling results (Ball and Nordstrom, 1991).

WATEQF and WATEQ4F compute charge imbalance by the following formula:

$$\Delta\% = \frac{\text{(Sum of Cation Species - Sum of Anion Species)}}{\text{(Sum of Cation Species + Sum of Anion Species)/2}} * 100$$

WATEQF provides an error message if the ionic balance exceeds 30%, and asks if you wish to proceed anyway. As stated earlier, it would be unwise to proceed with an error of that magnitude, since it usually indicates an error or omission somewhere along the line from sample collection to data input. WATEQ4F terminates the run and provides an error message if charge imbalance exceeds 30%.

WATEQF uses the Robinson-Stokes Debye-Hückel equation to calculate activity coefficients for Ca^{2+}, Mg^{2+}, Na^{+}, K^{+}, Cl^{-}, SO_4^{2-}, CO_3^{2-}, and HCO_3^{-}. The user has the option of selecting either the Debye-Hückel equation, or the Davies equation (c = 0.3) for all other activity coefficients.

WATEQ4F does not allow the user to choose between methods for calculation of activity coefficients. The extended Debye-Hückel equation (equation 3) is used for polysulfide species, carbonates, H^{+}, and Sr species. The Robinson-Stokes Debye-Hückel equation (equation 4) is applied to those species for which the b parameter is available, and the Davies equation (c = 0.3) is used for calculation of all other activity coefficients.

The thermodynamic database of both WATEQF and WATEQ4F are hard-coded, meaning that they are part of the source code, and no additions or corrections can be made to the database without recompiling the source code.

Inverse Modeling Codes

Inverse modeling is the calculation of net geochemical mass transfer reactions between an initial and final water along a hydrologic flow path (Plummer et al, 1991). BALANCE and NETPATH are the only codes evaluated in the study with inverse modeling capability. These codes require chemical analyses from two different water samples along the same evolutionary path, plus plausible phases with which the water reacts to generate mass transfer dissolution or precipitation products.

These plausible phases generally are mineral solids, but may also include gases, ion exchangers, or (if a mixing problem is being modeled) other aqueous solutions (Parkhurst et al, 1982). The output produced by an inverse model will be the mass transfer that occurred, in terms of molality of components added to or removed from solution, between the initial water and the mineral phases to produce the final water composition.

BALANCE: BALANCE was developed in 1982, and was designed to help define and quantify chemical reactions between ground water and minerals (Parkhurst et al, 1982). The program calculates the amounts of phases entering or leaving the aqueous phase (mass transfer) to account for the changes in chemical composition between two solutions along the same hydrologic flow path. The purpose of the program is to derive balanced reactions of the form (Parkhurst et al, 1982):

Initial solution + Reactant phases --> Final solution + Product phases

BALANCE is designed specifically for mineral-water interactions, but can solve any set of linear equations formulated by the user (Parkhurst et al, 1982). This includes: 1) mass balance on elements, 2) mixing end-members waters, 3) oxidation-reduction reactions, and 4) simple isotope balance. Examples of each are provided in the BALANCE manual (Parkhurst et al, 1982).

The primary advantage of BALANCE lies in the ability of the user to manually add elements and minerals to the database. BALANCE is well suited for inverse modeling in mining environments, since the user can add trace metals such as arsenic, mercury, zinc, or others.

NETPATH: NETPATH is a revision of BALANCE, and offers improvements in the construction and management of input and output files. Isotopic fractionations can be incorporated more easily in NETPATH. The ability is retained to compute mixing proportion of two

initial waters and net geochemical reactions that can account for the observed composition of a final water. NETPATH also allows incorporation of evapoconcentration in the determination of mass transfer.

NETPATH has no provision for manually entering elements, such as trace metals, into the calculations. Only new minerals for which elements already exist in the database can be defined. Unfortunately, NETPATH contains no trace metal data beyond iron. This shortcoming renders NETPATH inadequate for mass balance calculations on mine waters containing any trace metals other than iron. NETPATH could become an important tool in determining mass transfer in pit wall dissolution if these capabilities were incorporated.

Forward Modeling Codes

Forward modeling can range from a simple equilibrium simulation to one in which chemical evolution is followed as a function of reactions with a suite of minerals. Forward modeling may also involve predicting the evolution of the water down a hypothetical flow path which encounters a number of different processes and environments. This type of modeling is known as reaction path modeling.

The variables that may be encountered along the flow path can become numerous and complex, making the modeling effort difficult and subject to multiple interpretations. Reaction kinetics, adsorption, gas exchange, biologic activity, and many other processes may influence the chemical evolution of a water body along flow path.

MINTEQA2: MINTEQA2 is an equilibrium speciation software package with the largest thermodynamic database of all codes considered in this study. The program can calculate ion speciation, solubility, adsorption, oxidation-reduction, gas phase equilibria, and precipitation/dissolution of solid phases (Peterson et al, 1987).

MINTEQA2 can accept a finite mass for any solid considered for dissolution. The code contains many trace metals of interest in mining, including arsenic, cadmium, cesium, chromium, copper, mercury, lead, selenium, silver, thallium, and zinc.

The original MINTEQ was developed at Batelle Pacific Northwest Laboratory by Felmy et al (1984). MINTEQ combined the thermodynamic database of WATEQ3 with the mathematical structure of MINEQL (Schecher and McAvoy, 1991). The latest edition of MINTEQA2, version 3.11 was published December 1991, and incorporates the input file generator PRODEFA2 version 3.11.

For the level of sophistication it provides, MINTEQA2 is the most user friendly of the forward codes. The interactive file generator, PRODEFA2, allows easy construction of input files for both forward and speciation models.

MINTEQA2 solves multi-component chemical equilibrium problems much the same way as other codes, by simultaneous solution of the nonlinear mass action expressions and linear mass balance relationships. MINTEQA2 uses the mass action expressions to modify the mass balance equations into the form necessary for the calculations. This procedure is illustrated by Peterson et al (1987). The user must be aware that MINTEQA2 uses formation constants rather than dissolution constants.

MINTEQA2 performs a computational loop of iterating to equilibrium, checking for precipitation or dissolution, and shifting mass between the aqueous and solid phases until equilibrium is achieved and there are no oversaturated "possible" solids and no undersaturated "existing" solids. The reader is referred to the manual for definitions applied to various types of variables (e.g. solids) in the code. MINTEQA2 uses the Newton-Raphson approximation method to refine estimates within each iterative loop. Figure 4-2 is a flowchart diagramming the procedural loop MINTEQA2 follows in solving a chemical

equilibrium problem.

MINTEQA2 provides two options for calculating activity coefficients. If the user selects the Robinson-Stokes Debye-Hückel

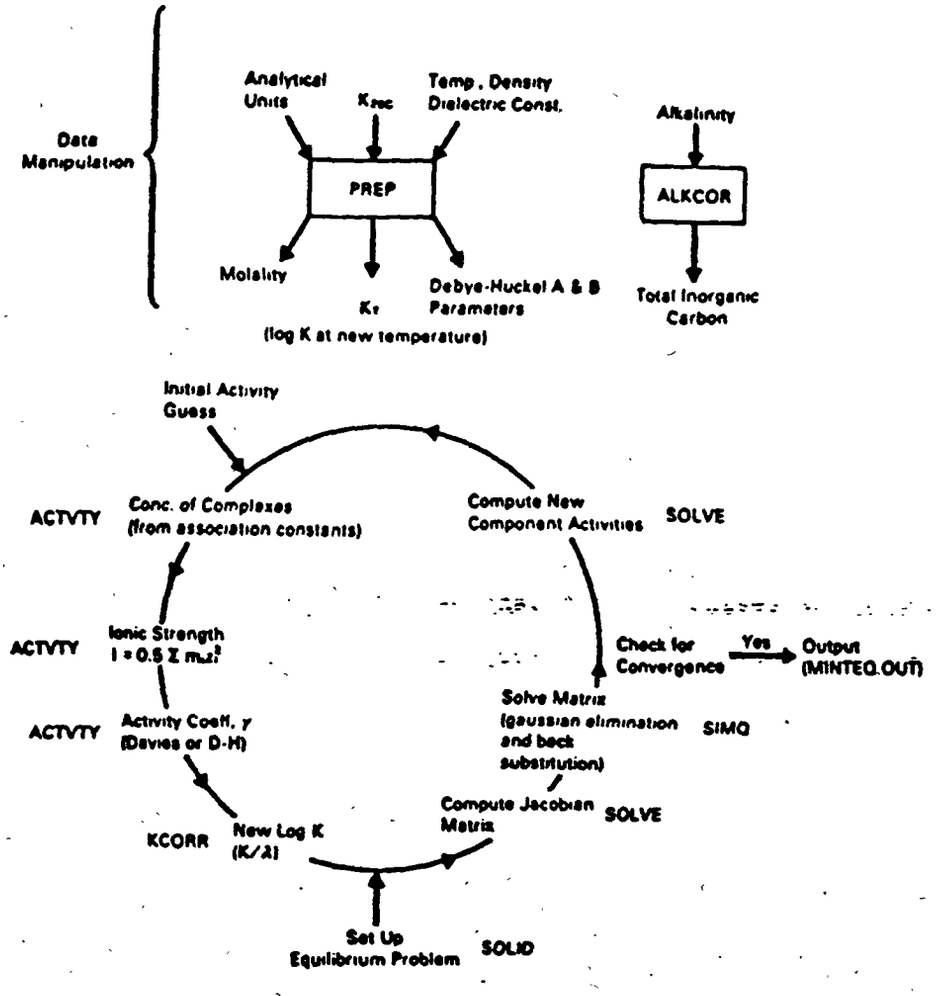

Figure 4-2: Path that MINTEQA2 uses in solving a chemical equilibrium problem (from Peterson et al, 1987).

equation, it is used for all species with the necessary ion size parameters, and the Davies equation is used for all others. If the user selects the Davies equation, it will be used throughout the simulation for all species. MINTEQA2 refers to the Robinson-Stokes Debye-Hückel

equation as the "modified Debye-Hückel equation." MINTEQA2 uses a slightly different version of the Davies equation, where the last term is 0.24I (Allison et al, 1991). MINTEQA2 starts the iterative process by estimating the activities if none is provided. The concentration of each component is divided by 10 to obtain an initial activity guess.

MINTEQA2 offers some flexibility in the data input requirements. A measured value of pH or pe may be specified as fixed, or MINTEQA2 can calculate equilibrium values. As with WATEQ4F, MINTEQA2 can calculate the system pe/Eh from a variety of redox couples, then can redistribute the remaining redox couples based on the calculated pe/Eh. Also, a mineral may be specified as presumed present at equilibrium, but subject to dissolution if equilibrium conditions warrant, or definitely present at equilibrium and not subject to complete dissolution (Allison et al, 1991). The ionic strength can also be fixed or computed. MINTEQA2 offers useful options in the manipulation and variation of pH, pe, and in controlling the influence of gases.

MINTEQA2 designates solid phases as either possible, finite, or infinite. The user specifies infinite phases and the amount present (moles). The solid may then dissolve if equilibrium conditions warrant, up to the total amount specified. Finite solids are also user defined, and are available for complete dissolution up to equilibrium, as solution thermodynamics dictate. Both solids are redesignated as possible solids if they dissolve completely, in which case they may reprecipitate if they become oversaturated. If dissolution is desired beyond the equilibrium concentration, the solid must be "hand dissolved" (Peterson et al, 1987), in which the components of the solid are entered as Type 1 components in PRODEFA2.

The modeler may allow mineral precipitation if oversaturation occurs, or they may be excluded from precipitation. MINTEQA2 contains a sweep option, in which a range of values or concentrations can be

entered to evaluate the effect on the system from the perturbation. This option is useful in sensitivity analyses.

Expansion or revision of the thermodynamic database is easier in MINTEQA2 than in any other code. The program is not hard-coded, and addition of components, species, and minerals is achieved interactively through PRODEFA2. These additions may be added to the permanent database, or simply included for the current problem being executed.

Adsorption Models: One of the most attractive features of MINTEQA2 is the incorporation of adsorption models, including a limited amount of surface complexation thermodynamic data. Seven adsorption models are available:

1) Activity K_d
2) Activity Langmuir
3) Activity Freundlich
4) Ion exchange
5) Constant capacitance
6) Triple-layer
7) Diffuse-layer

Only one adsorption model may be chosen per simulation, but within that up to five different surfaces (i.e. adsorbent mineral phases such as ferric hydroxide, or manganese hydroxide) may be defined for a single program execution, with up to two types of sites per surface. This capability is consistent with experimental data published on adsorption surfaces such as hydrous ferric oxide (Dzombak and Morel, 1990), which appears to possess two different sites with different surface energies and different adsorptive capacities.

The user must provide information regarding site density, specific surface area, adsorbent concentration, and surface potential. The definition of these variables distinguishes one adsorption model from another. There is no intrinsic difference within MINTEQA2 that distinguishes one surface from another, nor one site on a surface from another (Allison et al, 1991).

With the exception of one auxiliary input file for the diffuse layer model, the authors of MINTEQA2 have chosen to omit thermodynamic constants for adsorption reactions, and leave the selection of them to the discretion and problem-specific knowledge of the user. They chose this route because natural adsorbent phases often occur as mixtures of impure amorphous substances that vary widely in chemical behavior among sites (Allison et al, 1991).

The large database and adsorption capability make MINTEQA2 a very useful tool for mine water quality modeling. The primary shortcoming of MINTEQA2 is its limited ability to model reaction path geochemical processes. The program cannot dissolve ions into the pit water to concentrations beyond equilibrium. Once equilibrium is reached with respect to the most solubility mineral thermodynamically plausible, the dissolution process stops. If a higher concentration is desired, the user must "hand dissolve" the minerals.

PHREEQE: PHREEQE (PH-REdox-EQuilibrium Equations) is designed to model geochemical reactions, and can calculate pH, redox potential, and mass transfer as a function of reaction progress (Parkhurst et al, 1980). In addition to most capabilities of the speciation codes, the program can also determine the composition of a solution in equilibrium with multiple phases.

PHREEQE can simulate addition of reactants to a solution, mixing of two waters, and titration of one solution with another. In each of these cases, PHREEQE can simultaneously maintain the reacting solution at equilibrium with multiple phase boundaries (Parkhurst et al, 1980). The program can perform a sequence of simulations in a single computer run.

PHREEQE allows the entire reaction path to be modeled in one input data set. The building of this data set can be a long process if the user does not have a firm grasp of the desired reactions from the start.

Furthermore, a mistake in one of the early steps will be propagated and magnified through each remaining step until the simulation runs its course, likely rendering the entire simulation useless. During reaction simulations, the program calculates pH, pe, total dissolved concentrations of ions and species, the mass transfer of phases between the aqueous, solid, and gaseous phases, and saturation indices of all plausible minerals.

The main disadvantage of PHREEQE is that the database is significantly smaller than the MINTEQA2 or either WATEQ database. However, the advantage of PHREEQE is that the elements, species, and mineral phase databases are external to the computer code (not hard-coded), and are easily modified or expanded. The aqueous model is completely user-definable with respect to elements and species, and components are easily added or revised. For this study, 8 elements, 113 aqueous species, and 130 minerals were permanently added to the PHREEQE thermodynamic database.

PHREEQE's database can theoretically be expanded well beyond the size specified in the manual, to a level exceeding other codes with larger databases (Parkhurst, personal communication). This cannot be done with the assistance of the input file generator (PHRQINPT), and requires editing of the databases and source code, and recompilation.

PHREEQE draws from three equations to calculate activity coefficients: the extended Debye-Hückel equation (Equation 3), the WATEQ Debye-Hückel equation (Equation 4), or the Davies equation (Equation 5). The non-linear equations are solved using a combination of two techniques: (1) a continued fraction approach, as in Wigley (1977), is used for mass balance equations, and (2) a modified Newton-Raphson technique is used for all other equations. The reader is referred to the PHREEQE manual for thorough discussions of these methods (Parkhurst et al, 1980).

PHREEQE has the ability to dissolve masses of solids into solution well beyond system equilibrium. This represents an advantage over MINTEQA2, which cannot perform this function automatically. PHREEQE can compute the amount of irreversible reaction required for the solution composition to reach the intersection of an assigned phase boundary, with or without the inclusion of other mineral-water apparent equilibria (Plummer, 1984). PHREEQE can model mixing of two waters at any specified proportion, a potential advantage in pit water models requiring simulation of mixed conditions. A comparison of PHREEQE and MINTEQA2 is shown in figure 4-3.

The major distinction between the reaction path capability of PHREEQE, and true reaction path codes such as EQ3/6, is that PHREEQE solves for the solution composition and mass transfer only at requested points in reaction progress (Plummer, 1984). The disadvantage of increased user manipulation is countered by better computational efficiency. Plummer (1984) cites a comparison of PHREEQE and EQ3/6 performed by INTERA (1983) that gave identical results when using the same aqueous model and thermodynamic data.

To solve solution chemistry problems, PHREEQE uses equations representing the following:

* Total masses of each element in the system. The total concentrations of the elements must be known for PHREEQE to begin any calculation at a reaction increment. The total concentration must satisfy mass balance.
* Mass action equations for ion pairs. These are usually represented by formation constants, also referred to as equilibrium constants.
* Electrical neutrality. PHREEQE can adjust the pH of the system to bring the solution to electrical neutrality.
* Phase equilibria. An additional equation is required for each mineral added to the system, and is provided by the solubility product constant for the mineral.
* Conservation of electrons (for problems involving redox). PHREEQE keeps track of those species whose valence can change over the range of pe-pH conditions covered by the chemical stability of water.

	PHREEQE	MINTEQA2
Capability to irreversibly add or substract a net stoichiometric reaction, in specified or equal-increment steps?	Yes (extensive)	No (except dissolution to equilibrium of a fixed quantity of solid)
Capability to mix two waters or to titrate one with the other?	Yes	No
Capability to add a net stoichiometric reaction until a mineral phase boundary is reached?	Yes	No
Capability to change equilibration temperature in equal or specified increment steps?	Yes	No (separate problems must be run)
Automatic charge balancing with a specified cation/anion or with pH?	Yes	No
Adsorption, Surface complexation and Ion exchange?	No (PHREEQM does ion exchange)	Yes
Only precipitate solids *if* supersaturated?	No (PHREEQM does it)	Yes
Fix activities of given species (1 per component)?	No	Yes
Exclude given species/minerals? (excluded species will cause an inconsistent thermo. database)	Yes	Yes
Solid-solution Aqueous-solution equilibria?	No	No
Density correction?	Yes	No
Maximum number of components that can be entered in a given simulation?	30	35 (database has more, but code must be recompiled)
Multi-problem capability?	Yes	Yes
Capability to use the solution made in one problem as input for the next?	Yes	No
Input program?	Yes	Yes
Graphical output?	No	No
Spreadsheet output?	No	Yes

Figure 4-3: Comparison between MINTEQA2 (version 3.0) and PHREEQE (1990); from Glynn et al, 1992.

Limitations: PHREEQE cannot remove minerals from solution via precipitation and adjust the resulting solution concentration, unless the mineral is specified as a reversible reaction. This procedure could become tedious if PHREEQE were used alone to model such reactions, which is why MINTEQA2 was incorporated in this study for modeling precipitation reactions.

PHREEQE includes equations for charge balance and conservation of electrons, but mass balance constraints are not imposed on O and H (i.e. the model assumes a constant mass of water). This assumption can lead to errors in modeling reactions involving hydration and dehydration of minerals, and redox conditions near or beyond the stability of water (Plummer, 1984). The only constraint on H_2 and O_2 are equilibrium and electron balance constraints, so there are no limits on the amounts of H_2 or O_2 that can be made or destroyed in the computations performed to satisfy the reaction constraints of a simulation. If the masses of H_2 and O_2 involved in chemical reactions become significant relative to 1 kilogram of water, then the simulation may start to deviate from reality (Parkhurst et al, 1980). The assumption is valid as long as the mass of water involved in heterogeneous and homogeneous reactions is small relative to one kilogram of water (~55.5 moles; Plummer et al, 1983). The error introduced when modeling natural waters is usually negligible.

A more significant problem occurs if PHREEQE is used to model systems in which large amounts of water are involved in mineral precipitation or dissolution, such as might be encountered in brines. For example, precipitation of 1 mole of natron ($Na_2CO_3 \cdot 10H_2O$) from 1 liter of solution would remove 10 moles of H_2O from the aqueous phase, causing an increase in concentration of all remaining constituents in the solution. The increase in concentration would be about 20 percent, but would not be taken into account in PHREEQE's present computation system.

PHRQPITZ: PHRQPITZ is designed for modeling highly concentrated solutions such as brines. PHRQPITZ is basically identical to PHREEQE in the general format for input and output, with two major exceptions: 1) PHRQPITZ incorporates the Pitzer parameter ion-interaction formulas to calculate ionic activities, and 2) the database is restricted to species and minerals (e.g. trona, mirabilite, etc.) typically found in brines. To revise and expand PHRQPITZ to allow mine water modeling would be more painstaking than the effort required for PHREEQE, so the user would be better advised to revert to PHREEQE for such a project.

5. PIT WATER MODELING CONSIDERATIONS

There are many factors that can influence the chemical evolution of pit water, and which require varying degrees of attention when modeling the system. Some variables are obviously more important than others, and many are interrelated. A change in one variable can affect several others. These considerations guide the model conceptualization and must be factored into the numerical model development. The recognition and/or definition of these variables basically define the numerical model.

Figure 5-1 shows a cross section of a hypothetical pit lake, and illustrates some of the many factors and processes that will influence pit water chemical evolution. The factors can be categorized generally as either physical or chemical.

Chemical Factors

Classification of Deposit: The genetic classification of the mineral deposit will allow broad generalizations on the type of water quality expected at the mine site. Deposits are generally classified by type of ore, morphology of the ore, and type of mineralogy or lithology in which the ore was deposited (host rock or wall rock). Examples include carbonate hosted disseminated gold deposit, porphyry copper deposit, stratiform massive sulfide, and stratibound base metal deposit.

If the ore host is carbonates, acid mine drainage is unlikely, and if the ore is disseminated, high quantities of metal sulfides may be unlikely. However, if the ore is porphyry copper or massive sulfide, both high metals and acidic waters may result, as was seen in Table 1-1.

The most common type of mineral deposit in Nevada is sediment-hosted, disseminated gold deposit (Bonham, 1991). Deposits hosted in other lithologies, such as volcanic or metamorphic rocks, comprise a

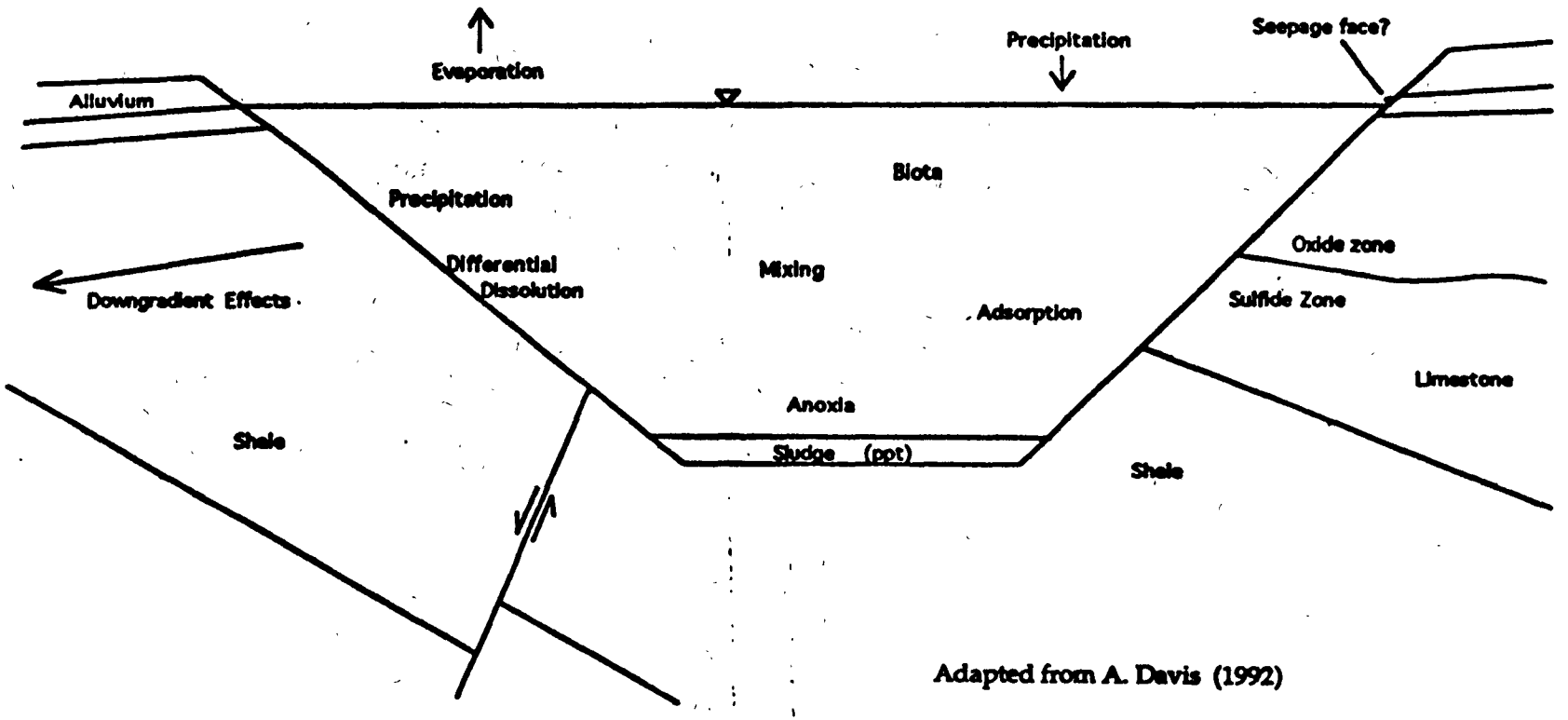

Figure 5-1: Cross section of hypothetical open pit.

smaller subset of disseminated precious metal deposits.

Ore may also be categorized depending on the extraction and processing techniques required, such as mill-grade, refractory, or leach-grade, which may refer to sulfidic, carbonaceous, oxide or siliceous ore.

Wallrock mineralogy: No single factor will have greater bearing on the bulk chemistry dissolved into the pit water than the composition of the rocks in the pit wall. Mineral deposits commonly consist of four major mineralogic/lithologic suites:

(1) Host rock or wall rock
(2) Gangue minerals
(3) Ore minerals
(4) Alteration minerals

Host rocks for most of the precious metal mines in the Great Basin are Paleozoic age (240-570 million years old) sedimentary rocks, such as limestone, dolomite, siltstone, and shale. Tertiary age (2-63 million years old) volcanic rocks comprise the second most abundant host rock. Of 107 bulk-mineable precious metal deposits in Nevada, 77 are hosted in sedimentary rocks, 27 in volcanics, and 3 in plutonics (Bonham, 1991). Porphyry copper deposits, by definition, appear in plutonic, porphyritic, igneous rocks. The Ruth and Yerington districts are examples of porphyry copper deposits in Nevada.

Gangue minerals are those that were deposited by ore-forming processes cogenetically with ore minerals, but have no economic value. The most common gangue minerals are silica, silicates, and carbonates, and to a lesser extent oxides, fluorides, and sulfates (Guilbert and Park, 1986). Gangue can also include sulfides of accessory trace metals deposited with the ore, such as pyrite (FeS_2), arsenopyrite (FeAsS), orpiment (As_2S_3), realgar (AsS), stibnite (Sb_2S_3), and others. A gangue mineral at one mine may be an ore mineral at a different mine.

Ore minerals are those which contain the elements of economic interest, such as gold, silver, copper, lead, or zinc. Examples of ore

minerals include electrum (Au-Ag mixture), gold-tellurides (Au + Te), argentite (Ag_2S), chalcocite (Cu_2S), sphalerite (ZnS), galena (PbS), and pyrite.

Alteration minerals are those that have undergone changes in composition as a result of physical or chemical means, especially by hydrothermal fluids (Guilbert and Park, 1986). Alteration minerals in hydrothermal deposits are generally clays, including kaolinite, illite, sericite, chlorite, and micas.

Depending on the site-specific characteristics of the deposit, dissolution of host rocks and gangue will likely contribute the majority of the major ions to solution, while trace metals could be contributed by both ore and gangue. Alteration minerals, being primarily insoluble aluminosilicate clays, will contribute a small mass of major ions, and possibly trace metals. They could also modify the pit water chemistry through ion exchange.

An illustration of the variety of water chemistries that can evolve from different host rocks is seen in the analytical data of Tables 1-1, 1-3, and 1-4. The pit waters derived from porphyry copper deposits, in general, show the highest concentrations of metals. The Berkeley Pit marks the worst case scenario of known porphyry copper pit waters, whereas the Yerington Pit represents the best case. Although Yerington is a porphyry copper deposit like Butte and Ruth, the water is less contaminated. Only two metals, Mn and Fe, exceed Federal standards, and the pH of the water is near neutral. The Yerington pit has better water quality for two reasons. First, the porphyry has a chrysocolla oxidation cap (copper silicate) rather than a sulfide cap, and the high pyrite zone was eroded off in the Tertiary, leaving little acid generating material in the mine area (Macdonald, 1992). Yerington, therefore, has significantly less trace metals and acid-generating sulfides, resulting in neutral pH and lower concentrations of dissolved

metals in the pit water.

Pit waters derived from carbonate host rocks tend to have lower TDS, neutral pH, and lower concentrations of metals (Tables 1-1, 1-3, 1-4). This is primarily due to the acid-neutralizing capability of the carbonate host rocks, which buffers the pH of the water to the neutral range. Dissolution of carbonate minerals produces bicarbonate and consumes hydrogen ions, making less acid available to dissolve metals from the host rock. The neutral pH, in turn, favors the formation and stability of hydroxides of Fe, Mn, and Al, which could remove up to 100% of many trace metals from solution via adsorption (Balistrieri and Murray, 1982).

Water derived from volcanic-hosted precious metal deposits could, potentially, be similar to waters in porphyry copper pits, since the host rocks are of similar chemical composition. Unfortunately, very few pit lakes exist in volcanic-hosted mines to confirm this hypothesis. Figure 5-2 shows that quartz monzonite consists of approximately 5-20% quartz, 35-65% plagioclase feldspar, and 35-65% alkali feldspar. Therefore, volcanic host rocks such as quartz latites will be closely related chemically to porphyry copper mines in quartz monzonite. The buffering capacity should be relatively low as in porphyry copper terrains, and the quantities of trace metals may be high. Alkaline or quartz rich volcanic rocks will have equally poor acid-neutralizing capacity. However, quantities of sulfides may be considerably less in volcanic hosted precious metal deposits.

An important factor that will complicate pit water chemical modeling is the possibility that several mineralogical and lithological suites might be present in one pit. As the pit fills, the water may encounter different mineralogic or lithologic suites, causing different rock/water interactions. A typical example exists at the Gold Quarry Pit (PTI, 1992), in which the rising groundwater will encounter first

limestone, then siltstone. The likely result is that the initial water levels will display neutral pH levels, due to buffering by the

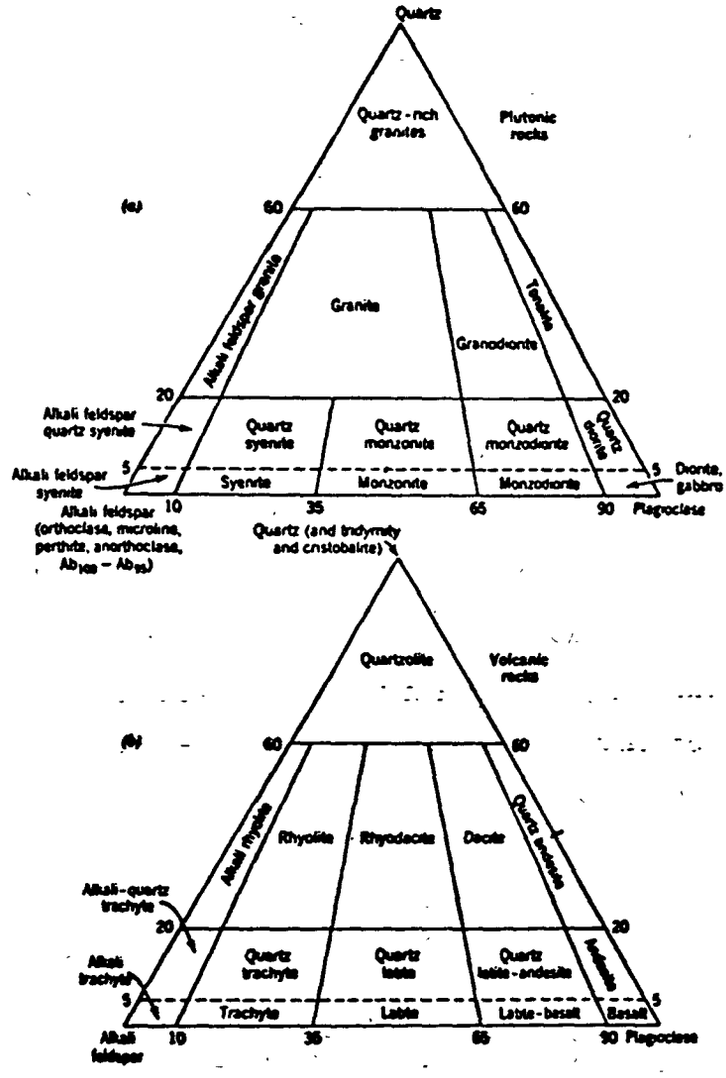

Figure 5-2: General classification and nomenclature of common plutonic and volcanic rock types. Classification bases on relative percentages of quartz, alkali feldspar, and plagioclase, measured in volume percent (From Hurlbut and Klein, 19th ed., 1977)

carbonate. As the water encounters siltstone, the pH may start to decline as the effect of the carbonate rock is offset by the absence

buffering capability in the siltstone. However, this scenario might only occur if the pit lake fails to turn over regularly. The fact that the pit water will always be in contact with a thick carbonate rock suite may allow sufficient buffering that the acid generating potential of the siltstone becomes negligible.

Typical precious metal deposits exhibit a zone of oxidized minerals overlying an unoxidized zone consisting of sulfidic and/or carbonaceous rocks. Alteration or gangue mineral suites are generally present, such as pervasive silicification, decalcification, or argillic (clay) alteration, which disturb or obscure the primary mineralogy. This type of alteration assemblage is common in sediment-hosted disseminated gold deposits (Percival et al, 1988). The host rock may grade from unaltered to altered zones, or from silicified to calcareous or carbonaceous, making masses of specific minerals difficult to quantify and model. As the incoming groundwater encounters the different mineralogical regimes, different reactions may occur before, during, and after the water enters the pit. Far from the pit, the system may approximate a closed system, becoming more open to atmospheric gases as the water approaches the pit wall. An oxidation rind may extend into the pit wall (PTI, 1992), in which case the approaching groundwater may encounter progressively decreasing quantities of unoxidized minerals (e.g. sulfides), and more oxides (e.g. goethite).

Acid Mine Drainage: Acid mine drainage (AMD) is probably the most widely studied aspect of mine-derived environmental contamination. One recent study says that AMD is the greatest problem caused by mining (U.C. Berkeley Mining Waste Study Team, 1988). The three key ingredients needed to produce acid mine drainage are a sulfide mineral, an oxidizing agent (e.g. atmospheric oxygen or ferric iron), and water

(Nordstrom, 1985). The most common sulfide mineral is pyrite (FeS_2), although sulfides of other minerals (Cu, Zn, As) oxidize rapidly and will also produce AMD. Acid mine waters most commonly form by the oxidation of pyrite under moist, oxygenated conditions typical of many active or inactive coal and sulfide ore deposits (Nordstrom, 1985).

The ability of a rock sample to generate net acidity is a function of the relative content of acid generating and acid consuming minerals (SRK, 1989). As mentioned above, typical sediment-hosted precious metal deposits in Nevada will contain both acid generating and acid consuming minerals. The balance between the two will determine the extent to which rock/water interaction produces acidic water.

Recorded pH values from AMD are as low as *less than* -1.0 (Iron Mountain, California; Nordstrom and Alpers, 1990). Dissolved metal concentrations have been recorded as high as 46,000 ppm Cu (Butte, MT; Nordstrom, 1985), 50,000 ppm Zn (Baldwin, Burma; Nordstrom, 1985), 43 mg/l Cd (Iron Mountain, CA; Nordstrom and Alpers, 1990), 56 mg/l As (Iron Mountain, CA; Nordstrom and Alpers, 1990), 55,600 ppm Fe (Iron Mountain, CA; Nordstrom and Alpers, 1990), 10,000 ppm Al (Comstock, NV; Nordstrom, 1985), and 420,000 mg/l SO_4^{2-} (Iron Mountain, CA; Nordstrom and Alpers, 1990).

The reaction that oxidizes pyrite and generates hydrogen ion and sulfate is (SRK, 1989):

$$FeS_2 + 7/2O_2 + H_2O = Fe^{2+} + 2SO_4^{2-} + 2H^+ \qquad (1)$$

Under sufficiently oxidizing conditions (dependent on both Eh and pH), ferrous iron, Fe (II), will oxidize to ferric ion, Fe(III):

$$Fe^{2+} + 1/4O_2 + H^+ = Fe^{3+} + 1/2H_2O \qquad (2)$$

This reaction consumes hydrogen ion, acting as a buffer at around pH 2.0, and may explain why acid mine waters rarely attain pH levels below

about 2.0 (Nordstrom, 1985). The kinetics of this reaction are relatively slow, about 10^{-6} millimoles/hour (Singer and Stumm, 1970). At pH values above 2.3 to 3.5, the solution will be in the iron hydroxide stability field, and Fe(III) may precipitate as $Fe(OH)_3$, again generating hydrogen ions (SRK, 1989):

$$Fe^{3+} + 3H_2O = Fe(OH)_{3(s)} + 3H^+ \qquad (3)$$

This series of reactions generates 5 hydrogen ions and consumes 1, for a net of 4 hydrogen ions generated per mole of pyrite oxidized. The overall process can be represented as:

$$FeS_2 + 15/4O_2 + 7/2H_2O = Fe(OH)_{3(s)} + 2SO_4^{2-} + 4H^+ \qquad (4)$$

At very low pH, pyrite can be oxidized by ferric iron in the *absence* of oxygen, via (Nordstrom, 1977):

$$FeS_2 + 14Fe^{3+} + 8H_2O = 15Fe^{2+} + 2SO_4^{2-} + 16H^+ \qquad (5)$$

The kinetics of this reaction are rapid, on the order of 0.002 milli-moles FeS_2 per hour (Garrels and Thompson, 1960). If reaction 5 were the only means of oxidizing pyrite, reaction 2 could not generate enough ferric iron to sustain reaction 5 at the rate of 0.002 mmols/hr., and acid generation would be limited by the rate of reaction 2 (Singer and Stumm, 1970). Unfortunately, reaction 1 is faster than reaction 2, and a shortage of oxygen or water in most AMD situations is unlikely.

Pyrite oxidation is a self-maintaining mechanism, since the rate increases with lower pH, which oxidizes more pyrite and generates more H^+ (and another oxidizing agent, Fe^{3+}), further lowering the pH, and continuing the cycle (Nordstrom et al, 1979b). AMD from mine pit walls, mine shafts, or waste dumps can theoretically continue until all the sulfide has been oxidized, a process that may take centuries or millennia to run to completion.

According to SRK (1989), the primary chemical factors which determine the rate of acid generation are:

* pH
* Temperature
* Oxygen content of the gas phase, if saturation is < 100%
* Oxygen concentration in the water phase
* Degree of saturation with water (water content)
* Chemical activity of Fe^{3+}
* Surface area of exposed metal sulfide
* Chemical activation energy required to initiate acid generation.

Experiments show that the bacteria Thiobacillus ferrooxidans can enhance the rate of pyrite oxidation (by reaction 2) six orders of magnitude (Lacey and Lawson, 1970). This would produce more than enough ferric iron to sustain reaction 4, and AMD could proceed in the absence of oxygen. The limiting factor in this case will be the growth rate of T. ferrooxidans (Nordstrom, 1985).

Small, "framboidal" pyrite crystals ($<10^{-6}$ m diameter) are the most reactive form of pyrite (Caruccio et al, 1970). The reactivity of this form stems from the fact that framboidal pyrite exhibits the largest surface area per mass of pyrite than any other form of pyrite. However, surface area per mass could be equally as large for a highly fractured sulfide ore body (Nordstrom, 1985).

In unmined ore deposits, insufficient oxygen is available to react with sulfide minerals for AMD to occur at a rate that causes discernible impacts on waters. Reaction (1) shows that 7/2 moles of O_2 generate 2 moles of H^+, but dissolved oxygen in soil waters is generally less than 0.6 mmol O_2 per liter (Drever, 1988). Once mining exposes sulfide minerals to the atmosphere, and if sufficient meteoric or ground water are available, pyrite oxidation and acid generation will ensue.

Acid can be neutralized by calcium carbonate, via the reaction: (SRK, 1989):

$$CaCO_3 + H^+ \rightarrow Ca^{2+} + HCO_3^-$$

Other carbonate minerals provide acid neutralizing capability, but will generally be too scarce in most mine environments to have a significant effect. The exception is dolomite ($CaMg(CO_3)_2$), which can form thick depositional sequences similar to limestone. Sodium carbonate minerals are shown to have greater buffering capability than calcium carbonates (Davison and House, 1988). Neutralization by the sodium salt leads to a final alkalinity greater than that obtained using the calcium salt. Since sodium carbonates are more soluble and have faster dissolution kinetics, a smaller volume of rock should be required to neutralize a given volume of acid water. However, with the exception of evaporitic terrains or in alluvium overlying mineral deposits, sodium carbonates will be greatly subordinate to calcium and magnesium carbonates in the systems of interest in Nevada.

Silicates, and some hydrous iron and aluminum oxides, also consume hydrogen during weathering, but generally have limited buffering capability (SRK, 1989). For example, $Al(OH_3)$ can neutralize acidic solutions by the reaction:

$$Al(OH_3) + 3H^+ \rightarrow Al^{3+} + 3H_2O$$

Although dissolution of carbonates, and other acid neutralizing minerals, will suppress the production of hydrogen ions, the reaction will still increase the levels of TDS in the solution.

Precipitation of amorphous ferric hydroxide can armor buffering minerals (Davis and Runnells, 1987), and "hide" them from acid solutions. This is discussed more thoroughly in other sections.

AMD can be modeled after some difficult variables are defined, such as the mass of sulfide available for oxidation, the kinetics of the oxidation reaction, rate of introduction of water into the system, and the volume of solution into which the dissolution occurs. A model of pyrite oxidation has been developed (Davis and Ritchie, 1986) and

applied in pit water chemical modeling (PTI, 1992).

Prediction of potential AMD has been predicted by laboratory experiments involving sulfide bearing rock from the mine (PTI, 1992; SRK, 1989). A balance of acid generating rock vs. acid neutralizing rock should reveal the potential for AMD to be sustained in the long term. In the absence of testing, chemical modeling can provide a guess, by integrating an estimate of the mass of sulfide that will be dissolved and the mass of buffering minerals as well (PTI, 1992).

Dissolved solids: High concentrations of the major ions will present less threat toxicologically than trace metals, but will contribute to overall water quality degradation by increasing total dissolved solids (TDS). High TDS in mine-derived waters are caused by two major processes (Nordstrom and Ball, 1985): 1) the oxidation of metallic sulfides, such as pyrite, sphalerite, chalcopyrite, galena, and arsenopyrite to produce high concentrations of trace metals and sulfate, and 2) acid dissolution of silicate bedrock (feldspar, micas, clays, etc.) that produce high concentrations of aluminum, silica, calcium, magnesium, sodium, and potassium.

The dissolution of carbonate host rocks will introduce Ca^{2+}, Mg^{2+}, and HCO_3^- into solution. Dissolution of silicate host rocks will add dissolved species of Si, Al (depending on pH), Na, K, Ca, Mg, Fe, and HCO_3^-. If evaporites are present, concentrations of SO_4, Cl, Na, and K could be increased. At near-neutral pH expected in carbonate-hosted pit waters, the concentrations of Ca, Mg, and HCO_3^- should be controlled by carbonate equilibria. With increasing pH, carbonate control will yield to silicate control.

Attenuation of dissolved metals in a drainage basin with distance, or in a lake with time, will occur due to oxidation, precipitation, adsorption, and dilution (Nordstrom and Ball, 1985).

Silica: Dissolved silica generally does not reach extreme

concentrations, due to solubility controls by silicate minerals such as kaolinite or other clays (Drever, 1988). Only above about pH 9 does silica solubility increase beyond approximately 10^{-4} molal (activity of dissolved species) as shown by figure 5-3. In AMD situations, silica concentration can also be influenced by adsorption (Chapman et al, 1983).

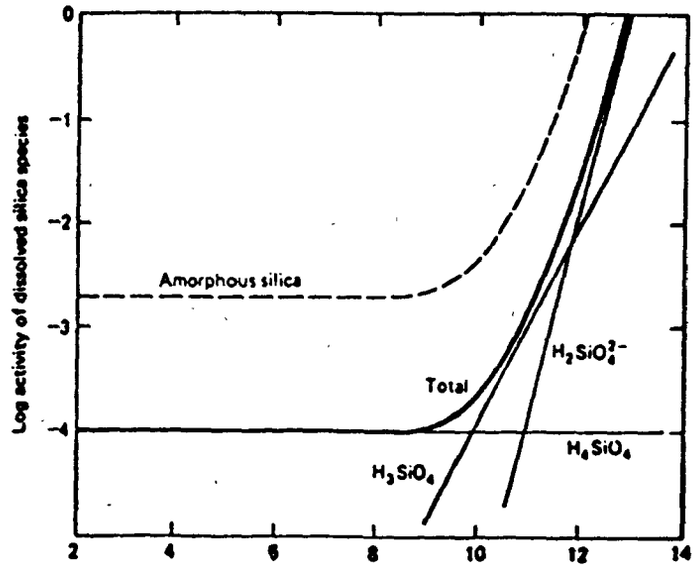

Figure 5-3: Activities of dissolved silica species in equilibrium with at 25°C, as a function of pH (from Drever, 1988).

Sulfate: Sulfate has an EPA standard, so prediction of sulfate concentration and migration is important. Sulfate normally behaves conservatively in mine-derived solutions (Davis and Runnells, 1987), although it may compete for adsorption sites at low pH (Chapman et al, 1983), and may precipitate if subjected to Eh/pH changes (Filipek et al, 1987). Sulfate concentrations will generally increase in solution as sulfides are oxidized, and may not be affected by neutralization.

Nordstrom and Ball (1985), and Davis and Runnells (1987) suggest that sulfate is probably the best conservative tracer during downstream

dilution of acid mine waters, because it usually exists at high concentration at the effluent source, and should be relatively unaffected by precipitation or adsorption processes. This behavior may make sulfate the best indicator among major ions of acid mine drainage in many systems, after trace metals are removed by adsorption and pH is neutralized by dilution.

Trace Elements: Trace elements are defined as those elements that generally appear in waters at concentration of less than 1 mg/l (Drever, 1988). Trace elements are of concern and must be monitored because of their potential toxicity to aquatic and terrestrial life (see review in Macdonald, 1992). Trace metals can reach extremely high concentrations in mine-related waters, as was discussed previously under acid mine drainage.

The behavior of trace metals in pit water will be difficult to model for several reasons. First, the quantity of metals dissolved from the pit wallrock into the water will be difficult to predict, due to the masses of metals contained in the wallrock, the morphology and mineralogy of the metals (disseminated vs. massive, sulfide vs. oxide), the availability of metal to fluids (associated with fractures, armoring, etc.), the nature of the solution (saturation state, pH, Eh), and variable rates of reaction due to all of the above. Second, the mass that remains as dissolved metal in the pit water will depend on several factors, most notably the presence of Fe hydroxides and other solids which can remove trace metals from solution by adsorption, and the pH/Eh of the fluid, which will control the stability of species in solution. In general, trace metal concentrations will be higher at lower pH, decreasing rapidly as the pH approaches neutrality. Third, the thermodynamic data (K_{sp}, $\Delta H_r°$) for some trace metal species are questionable (Nordstrom, 1992, personal communication). If the

thermodynamic data is inaccurate, the model will be inaccurate.

The trace metal analytical data from pit waters should be used with caution, because of potential problems in sample collection, storage, and analyses (Lyons, personal communication). Analytical data for As, Ag, and Cu could be acceptable, but data for Cd, Hg, Pb, and Zn could be cause for concern.

The following paragraphs discuss the trace metals that may be important in pit water chemical modeling.

Aluminum: Aluminum concentrations are generally very low in natural waters, usually less than 1 μg/l, but increase rapidly at low or high pH (Drever, 1988). The minerals believed to control aluminum concentrations, gibbsite and kaolinite, are very insoluble at neutral pH (Nordstrom, 1982) as shown by figure 5-4. Studies indicate that gibbsite controls aluminum solubility for slightly acid to neutral pH (above pH 5.7, Davis and Runnells, 1987; at the Leviathan mine, above pH

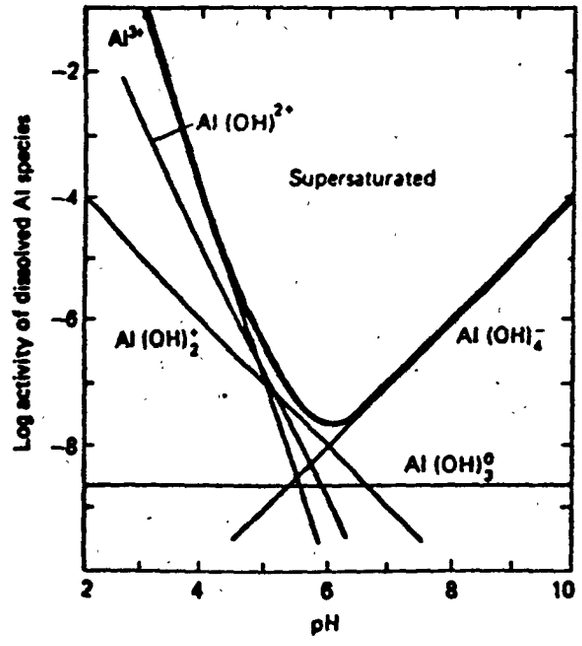

Figure 5-4: Activities of dissolved aluminum species in equilibrium with gibbsite [$Al(OH)_3$] at 25°C, as a function of pH (from Drever, 1988)

4.5, Nordstrom and Ball, 1985). Davis and Runnells (1987) found that $AlOHSO_4$ is the control at lower pH values. Nordstrom and Ball (1985) suggest that the solubility of aluminum at Leviathan below pH 4.5 is controlled by the kinetics of the leaching rate of aluminum from bedrock and soils.

Aluminum can reach high concentrations in acid mine waters. The concentration of dissolved aluminum at a depth of 100m in the Berkeley Pit is 206 mg/l (Davis and Ashenberg, 1989). With rising pH, such as through dilution or neutralization, aluminum minerals should precipitate. Filipek et al (1987) observed that gibbsite and kaolinite became supersaturated at pH 5.25 and above, and suggested that precipitation of a hydrolyzed aluminum mineral will occur above pH about 4.9. In carbonate hosted pit waters, with neutral pH, aluminum concentrations should be too low to warrant concern. However, Al will be a greater concern in acid drainage situations that have potential to pollute freshwater systems. At low pH, the extreme sensitivity of aluminum solubility to pH changes (Figure 5-4) can cause release of significant amounts of Al. Davis et al (1991) showed that a pH drop from 5.2 to 5.1 could release .3 mg/l Al into solution, increasing Al concentration over the chronic toxicity threshold for trout embryo. Poor plant growth in soils located near acid mine drainage sites is also attributed mainly to toxic concentrations of dissolved Al (van Breemen, 1973).

Several possible mechanisms can account for attenuation of dissolved aluminum concentrations. At neutral pH, Al will precipitate as residual weathering products such as clays. Busenberg and Clemency (1976) found that mica and montmorillonite are rapidly precipitated from the ions released by the weathering of feldspars. Aluminum may precipitate as illite clay, aluminum sulfate, or amorphous $Al(OH)_3$ (Davis and Runnells, 1987). Aluminum can also be removed from solution via adsorption onto solids such as hydroxides (Chapman et al, 1983). In

AMD waters, gibbsite, alunite, basaluminute, and jurbanite are the most common precipitates (Florence and Batley, 1980; Nordstrom, 1982; Chapman et al, 1983; Rampe and Runnells, 1989). Al mobility has also been shown to be governed by fluoride activity (Plankey et al, 1986).

Arsenic: Arsenic has multiple valence states and can form over 245 mineral compounds (Lynch, 1988). The kinetics of oxidation and reduction of arsenic species are believed to be slow (Seyler and Martin, 1989), which causes both As(III) and As(V) species to be present in some solutions. Biological activity may be the reason for this behavior (Masscheleyn et al, 1991).

Sources of arsenic in precious metal mines include orpiment (As_2S_3), realgar (AsS), arsenopyrite (FeAsS), arsenic-bearing oxides, and iron sulfides. Arsenic concentrations are dependent on many factors, including redox, pH, adsorption, biological activity, and kinetics (Macdonald, 1992). Arsenic species have a high affinity for adsorption onto hydroxides (Pierce and Moore, 1982). Since most arsenic species are anionic, adsorption increases with decreasing pH, the opposite behavior shown by cations (Balistrieri and Murray, 1983; Dzombak and Morel, 1990; Davis and Leckie, 1980). As(III) compounds are generally more toxic than As(V) compounds, and inorganic As compounds are more toxic than organic As compounds (Bitton and Gerba, 1984). Removal of arsenic from solution can occur through precipitation of scorodite ($FeAsO_4 \cdot 2H_2O$) and by adsorption onto iron hydroxides (Nordstrom and Ball, 1985; Pierce and Moore, 1982). Much information is available on the role of biota in controlling arsenic chemistry (e.g. see review in Macdonald, 1992), but a discussion is beyond the scope of this study.

Under the oxidizing and neutral pH conditions likely found in most sediment-hosted pit waters, As(V) species are more stable (Figure 5-5; see also speciation files, this report), and generally outnumber As(III)

species. With decreasing pH and/or Eh, As(III) species will become more stable, as demonstrated in the Berkeley pit, in which total As(V) exceeded total As(III) by less than one order of magnitude (Davis and Ashenberg, 1989).

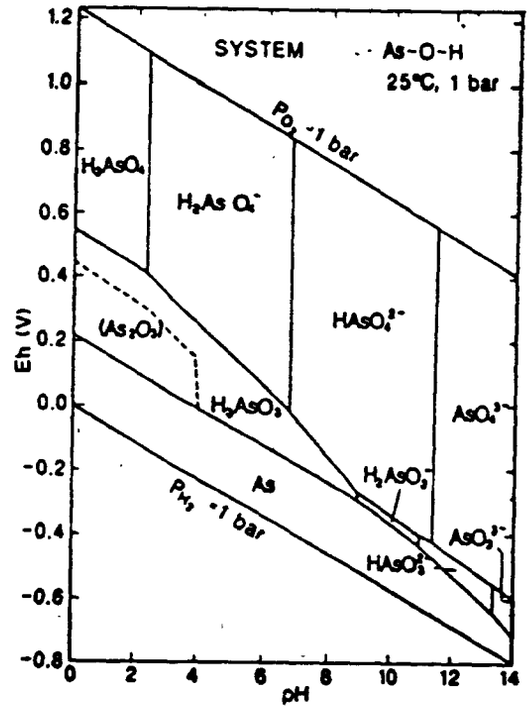

Figure 5-5: Eh-pH diagram for part of the system As-S-O-H. The assumed activities of dissolved species are As = 10^{-6}, S = 10^{-3} (from Brookins, 1988)

Cadmium: Cadmium has been observed to behave conservatively in AMD systems (Davis et al 1991; Chapman et al, 1983). Cadmium has high adsorption affinity for amorphous hydroxides at neutral pH (Davis et al, 1987; McBride, 1980), but is strongly inhibited by competition for adsorption sites from other ions (Balistrieri and Murray, 1982). Cadmium has an EPA standard, so a prediction of mining related impacts is necessary. Under circum-neutral and oxidizing conditions, the dominant (unadsorbed) species are free Cd^{2+} and $CdCO_3$ (Brookins, 1988).

In AMD situations, the dominant species should be free Cd^{2+}.

Copper: Copper has a redox chemistry (Brookins, 1988), so will be sensitive to Eh-pH changes imposed on mine water. Copper has been seen to behave conservatively in AMD conditions (Chapman et al, 1983), even when subject to dilution (Filipek et al, 1987). However, Davis et al (1991) observed non-conservative behavior of copper in the Clear Creek AMD system, where copper concentrations associated with particulate fractions were an order of magnitude higher than in the dissolved fraction. Davis et al (1991) explain that this may be due to the pH_{50} (the pH at which 50% of the metal remains in solution) of Cu vs. Zn (Cu = 4.5, Zn = 5.5). Their experimental data says that >90% of Cu is expected to be adsorbed at pH 6.0. Their MINTEQA2 simulations indicated that Cu^{2+} and $CuSO_4^{\circ}$ are the dominant species at low pH, whereas $Cu(OH)_2^{\circ}$ dominates at neutral pH. All Cu minerals were undersaturated, indicating Cu removal via adsorption. In AMD situations, copper concentrations can be high enough to be controlled by mineral phase solubility. At their Daylight Creek (NSW, Australia) study area, Chapman et al (1983) observed precipitation of a copper mineral they suggested was $Cu_2(OH)_2CO_3$.

Iron: Iron has multiple valence states and is strongly controlled by redox. In most natural (oxygenated) surface waters, iron should generally be in the ferric (Fe^{3+}) state, which is very insoluble. Therefore, iron mobility will be controlled by the precipitation of ferric hydroxides. Under more reducing conditions, such as in groundwater, ferrous iron (Fe^{2+}) may dominate other iron species and Fe^{3+} precipitation will not occur. As the Eh-pH diagram for iron species shows (Figure 5-6), many natural waters, at near neutral pH and slightly oxidizing conditions, may lie near the phase boundary between Fe^{2+} and $Fe(OH)_3$.

Iron concentrations are very sensitive to pH as well as redox.

Davis, et al (1991) discovered that dissolved iron concentrations in a Colorado stream were determined by the solubility of different amorphous

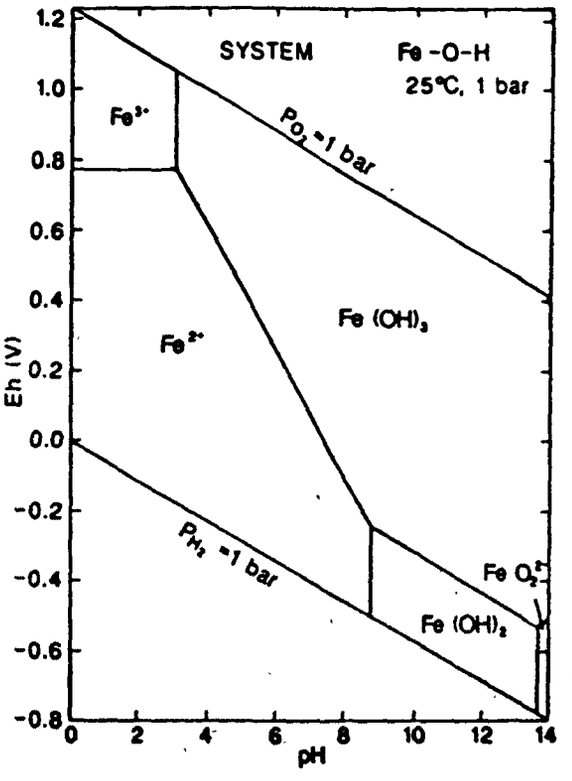

Figure 5-6: Eh-pH diagram for part of the system Fe-O-H assuming $Fe(OH)_3$ as stable Fe(III) phase. Assumed activity of dissolved Fe = 10^{-6}, (from Brookins, 1988)

ferric hydroxide forms present. As pH increased due to dilution by more alkaline tributaries, iron was removed from solution by the reaction:

$$Fe(OH)_2^+ + OH^- \longrightarrow Fe(OH)_3(s).$$

This was verified by calculating the saturation index for ferrihydrite as a function of distance from the source of the AMD (Davis et al, 1991). The extreme sensitivity of iron to pH and pe is seen in Figure 5-7, which shows that a shift in pe or pH can result in a change

in iron concentrations by several orders of magnitude.

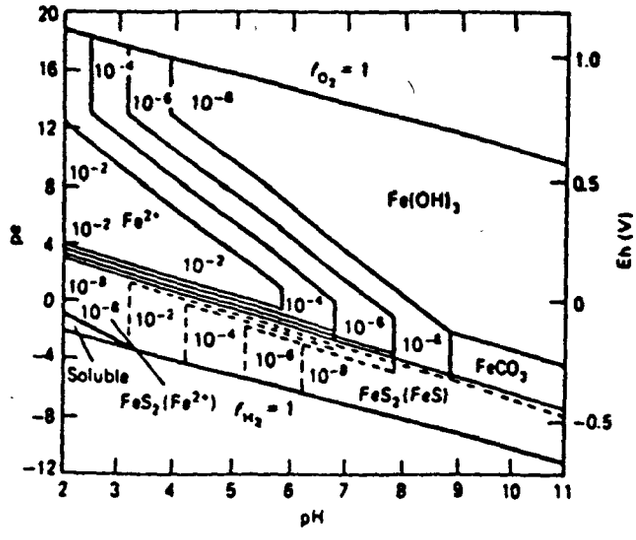

Figure 5-7: Contours of dissolved iron as a function of pe and pH, assuming $pCO_2 = 10^{-2}$, $\Sigma S = 10^{-2}$.

Jarosite will commonly precipitate in AMD waters if the pH is between 1.5-2.5, and sufficient dissolved iron is present (Nordstrom et al, 1979b). In some extremely acidic AMD streams, jarosite precipitation might not occur close to the source, but will appear downstream as the pH rises to the appropriate range. Jarosite precipitation occurs as predicted by chemical modeling at the Berkeley Pit (Davis and Ashenberg, 1989).

Under most conditions, free ferric iron is never more than about 8% of the total iron. Nordstrom et al (1979b) found in four AMD streams that $FeSO_4^\circ$ can constitute up to 50% of the total dissolved ferrous ion. Organic complexing of iron may be important in some waters, but in AMD terrains the organic matter is probably fully protonated and has only a

minor effect on complexing (Nordstrom et al, 1979b).

The solubility data for ferric hydroxide and ferrous sulfide minerals show much variability depending on crystallinity (Ball et al, 1980). For this reason researchers should consider a range of phases in chemical models involving iron (Plummer, et al, 1983). Further complications are introduced by the definition of dissolved vs. particulate iron, the distinction between the two often being defined operationally as the size fraction that passed through the filter used in sampling.

Lead: Lead is very particle reactive, with high affinity for adsorption onto hydroxide precipitates. With sufficient ΣCO_2, the dominant lead species in circum-neutral, oxidizing waters should be $PbCO_3$ (Brookins, 1988). Lead generally appears in very low amounts in most precious-metal deposits (Percival et al, 1988). Low concentrations, combined with high particle reactivity, may preclude lead from being a problem in pit waters.

Manganese: Manganese has been observed to behave conservatively in low pH, oxidizing environments (Rampe and Runnells, 1989; Davis et al, 1991) and even in diluted AMD systems (Filipek et al, 1987). Manganese is expected to precipitate in more oxidizing, alkaline conditions (Davis et al, 1991). Manganese hydroxides are considerably better scavengers of trace metals from solution than iron hydroxides (review by Chao and Theobald, 1976), and therefore could be an important control of trace metals in pit water.

Mercury: Mercury is insoluble and concentrations are generally very low in natural waters (Fitzgerald, 1979). However, mercury is very common in precious metal deposits, and may be present in resultant pit water (see Table 1-4). Mercury exhibits a redox chemistry in natural waters (Brookins, 1988), and has an EPA primary standard.

Zinc: Zinc has no redox chemistry, and has shown to be both conservative (Filipek, et al, 1987; Chapman et al, 1983) and non-

conservative (Bencala et al, 1987) in AMD systems. Zinc has a moderately high adsorption affinity for amorphous ferric hydroxide (Tessier et al, 1985; Karlsson et al, 1988). The dominant Zn species in circum-neutral, oxidizing waters should be either free Zn^{2+} or $ZnCO_3$ (Brookins, 1988), depending on ΣCO_2.

Oxidation/Reduction (Redox): Redox potential will be a critical mechanism controlling dissolved metal concentrations, speciation, and mineral phase stability in pit water. Oxidizing conditions (positive Eh) favor stability of Fe-hydroxides, hence enhancing adsorption of trace metals onto the Fe-hydroxides and removal from solution. Reducing conditions (negative Eh) favor destabilization of Fe-hydroxides and possible dissolution, which will cause desorption of trace metals to solution. Metals released to solution could potentially be transported out of the pit into a downgradient aquifer and contaminate water supplies.

Both natural and pit lakes can become chemically stratified, causing vertical gradients of both dissolved oxygen (O_2) and redox potential, as in the Berkeley Pit (Davis and Ashenberg, 1989). The likelihood of vertical stratification in pit lakes will depend on the factors that determine the extent of mixing in the pit lake (thermal input, wind velocity, etc.). The ability of redox potential to influence lake chemistry through stratification can be modeled by dividing the lake into vertical cells, each with its own redox potential, dissolved oxygen, or relative activities of specified redox couples.

Verification of the existence of a redox change can be shown by the relative concentrations among redox couple speciation between two locations along a hydrologic flow path, such as between groundwater and a pit. As Plummer (1983) demonstrated with sulfide species, if

concentrations go from nondetectable to detectable, then the problem involves redox.

For the most accurate chemical model application, one should analyze for concentrations of each redox couple of interest, such as ferrous and ferric iron, that might be important in the water (Nordstrom et al, 1979b). Nordstrom et al (1979b) outlined some fairly rigorous criteria that must be met before a measured Eh can be related to a specific redox couple. These criteria are generally not met in natural waters, but AMD waters may prove the exception. In 60 samples of AMD waters, Nordstrom et al (1979b) found that measured Eh correlated well with Eh calculated from the ferrous/ferric couple with the Nernst equation. They also discovered that the Eh calculated using the O_2/H_2O couple was higher than the measured value. The redox state of the water is thus determined by the ferrous-ferric ratio, and O_2 is not in equilibrium with the ferrous-ferric couple.

Adsorption/coprecipitation: Adsorption onto mineral surfaces is generally believed to be the dominant controlling mechanism for trace element concentrations in natural waters (Drever, 1988), and could also control concentrations of dissolved metals in pit water. Metals such as Al, As, Cd, Cu, Fe, Hg, Mn, Ni, Pb and Zn can readily adsorb onto particulate matter (Karlsson et al, 1988; Tessier et al, 1985; reviews by Turekian, 1977, and Murray and Brewer, 1977). Important inorganic sorbents include hydroxides of Al, Fe, Mn, and Si. Despite the complexity of natural waters and the many parameters that can control adsorption, the agreement of field data with laboratory experiments and with theory is relatively good (Tessier et al, 1985).

The stability of iron hydroxide solid is strongly dependent on both pH and Eh. The Eh-pH stability diagram for iron (Figure 5-6) shows that $Fe(OH)_3$ is more stable in higher pH, oxidizing waters. A decrease

in Eh (anoxia) or pH will cause the solution to move out of the $Fe(OH)_3$ stability field, into the Fe^{2+} field, which could potentially dissolve the $Fe(OH)_3$ and release any sorbed metals into solution. This is a concern in pit water chemical evolution, if carbonate buffering is absent or becomes inhibited through processes such as armoring. Anoxia may also develop if turnover fails to occur.

Fe and Mn concentrations have been observed to decrease along a flow path that experiences a pH increase (Wicks and Groves, 1993). The pH dependent solubilities of both hydroxides are seen in the reactions:

$$2Fe^{2+} + O_2 + 4H_2O = 2Fe(OH)_3 + 2H^+$$

$$2Mn^{2+} + O_2 + 6H_2O = 2Mn(OH)_3 + 4H^+$$

Wicks and Groves observed that this decrease is accompanied by precipitates of Fe and Mn hydroxides in the stream.

High sensitivity to pH is further seen in a laboratory study by Davis et al (1991), which demonstrated that approximately 90% of Zn was adsorbed at pH of 6.8, and 50% at pH 5.5. They suggest that in the event of blowout (rapid discharge of AMD to surface water body), sediments could potentially desorb significant non-point loads of Zn.

Adsorption reactions can be described in a simplified manner by formation or surface complexation constants similar to solubility product constants. The adsorption of a metal ion, M, onto an oxide surface can be represented by (Benjamin and Leckie, 1981; Balistrieri and Murray, 1983):

$$SOH_x + M \overset{{}^*K_A}{=} SOM + xH^+$$

where SOH_x represents the free surface sites, SOM represents the surface complex, and x is the average number of H^+ ions released per M adsorbed. If ${}^*K_A$ is considered as an "average" equilibrium constant, and expressing the above variables in terms of concentrations, then the

surface complexation constant is:

$$^{*}K_A = \frac{[SOM]\,[H^{+}]}{[SOH_x]\,[M]}$$

As the above equation demonstrates, $^{*}K_A$ is pH dependent. The adsorption behavior of cations generally conforms to the curves shown in Figure 5-8. Adsorption of cations is insignificant at low pH, because hydrogen ions outcompete other cations for adsorption sites. Increasing pH increases adsorption of cations in simple systems and thus should also increase K_A according to the above equation. (Tessier et al, 1985). Cation adsorption is analogous to hydrolysis in that both increase and release protons with higher pH (James and Healy, 1972).

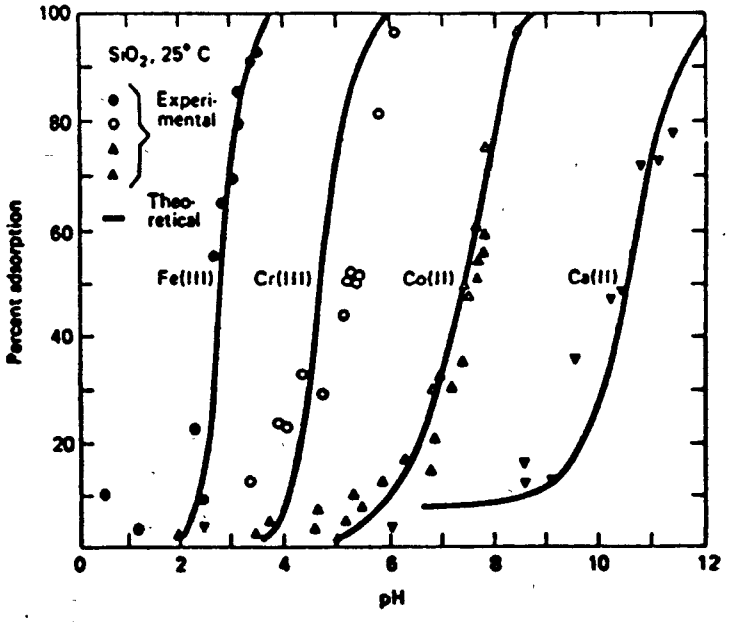

Figure 5-8: Experimental data and computed curves for adsorption of metals on SiO_2 (James and Healy, 1972), from Drever (1988).

Adsorption of trace metals onto iron oxyhydroxides typically increases from near 0% to near 100% as the pH increases through a narrow

critical range of ~2 pH units, referred to as the "adsorption edge" (Tessier, et al, 1985). Without exception, Tessier, et al's experiments for adsorption of Cd, Cu, Pb, Ni, Zn onto oxic lake sediments showed sloping curves with higher adsorption with increasing pH. Lead adsorption with varying pH is shown in figure 5-9A. In these examples, adsorption tails off to zero at about pH 4.0, but approaches 100% at about pH 7.0. Experiments by Davis et al (1991) showed that the affinity of metal ions for pure amorphous ferric oxyhydroxide is Cd < Mn < Zn < Cu.

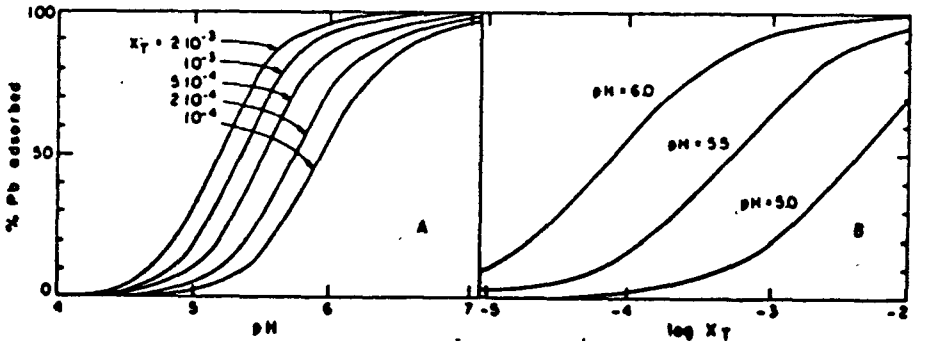

Figure 5-9: Adsorption of lead on alumina (γ-Al_2O_3). A) as a function of pH for different surface site concentrations; B) as a function of surface site concentration at different pH (from Morel and Hering, 1993).

Anion adsorption is a mirror image of cation adsorption, stronger at lower pH, and weaker at high pH (Balistrieri and Murray, 1982). An example is arsenic, which forms primarily anionic species in solution. Figure 5-10 shows the adsorption behavior of an arsenic species.

The extent of adsorption of trace metals onto iron hydroxides is believed to depend strongly upon certain characteristics of the adsorbent surface, such as porosity and specific surface area (Kinniburgh and Jackson, 1981).

Adsorption density (moles of metal adsorbed per mole of adsorbent), Γ, can be written for adsorption onto iron oxyhydroxides:

$$\Gamma = \frac{[SOM]}{Fe_T}$$

where Fe_T is the total concentration of iron present as oxyhydroxides (Tessier, et al, 1985). Adsorption increases with increasing site density, as shown by Figure 5-9B.

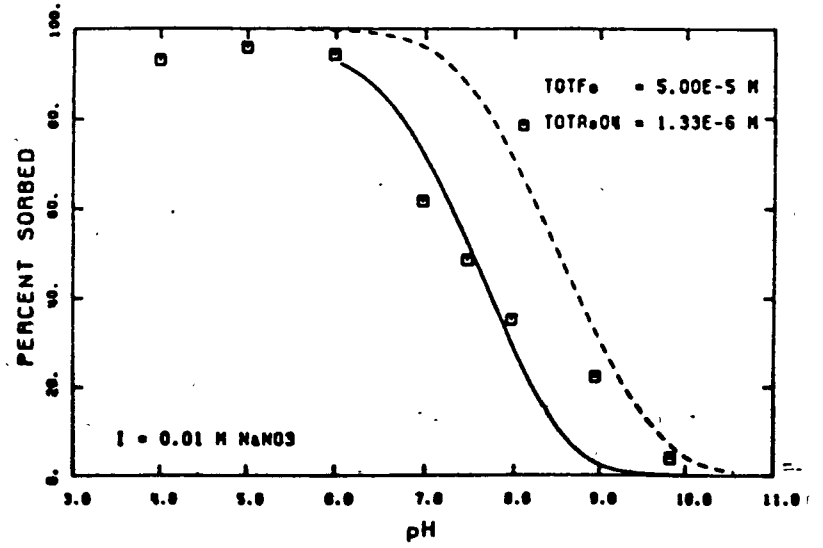

Figure 5-10: Adsorption behavior of an arsenic species (from Dzombak and Morel, 1990).

Kinetics of adsorption can be fast, as demonstrated in Balistrieri and Murray's experiments (1982), which required only 2.5 hours to attain equilibrium. However, longer reaction times could favor an increase in the $^*K_A$ values. Reversibility of the adsorption reaction has been checked in a few occasions and partly verified in short time laboratory adsorption experiments (Tessier et al, 1985).

Ionic strength is not an important control on adsorption in all situations. Balistrieri and Murray (1982) and Swallow et al (1980)

showed that ionic strength does not significantly influence the adsorption of Cu and Pb. The reason may be that adsorption reactions result in no net change in surface charge, and therefore are not susceptible to changes in surface charge caused by ionic strength variations.

Major ions can enhance or inhibit the adsorption of trace metals. Balistrieri and Murray (1982) showed that Mg^{2+} suppresses trace metal adsorption by decreasing the number of available sites, whereas SO_4^{2-} can enhance the adsorption of cations by changing the electrostatic conditions. Benjamin and Leckie (1980) showed that there is competition between metals for sites on surfaces of $\gamma FeOOH$ and γAl_2O_3 even though the available surface sites are far in excess of adsorbing species. Including the adsorption behavior of ions such as Mg^{2+} and SO_4^{2-} in the pit water models would consider the potentially important competitive effects of these ions.

The presence of organic matter can change the adsorption model significantly. Organic matter complexes certain trace metals strongly, particularly Cu (Mantoura, et al 1978), and can adsorb on suspended surfaces (Balistrieri and Murray, 1982), The latter can change the surface characteristics of suspended solids so that they acquire the chemical behavior of organic functional groups such as (-COOH) (Balistrieri and Murray, 1982).

Smith and Jenne (1991) discovered that aging effect the ability of amorphous ferric hydroxides to sorb metals. Older solids exhibited a higher degree of crystallinity making less sites available for adsorption.

Quantifying and modeling adsorption are very difficult, and several theories are currently in use. Although surface complexation constants see wide use, Morel and Hering warn "... no universal equilibrium constant can be simply defined and various adsorption models

differ principally by the manner in which the electrostatic interaction term is calculated," and Dzombak and Morel caution that "equilibrium constants (for adsorption) are not, in fact, constant." Despite the problems, factoring adsorption into pit water chemical models will provide a means of removing metals from the pit water.

The number of input parameters for an adsorption model will depend on the complexity of the model selected. At the minimum, the required parameters are:

* An adsorption constant (K_d)
* Number of adsorption sites available, usually a function of:
  - concentration of adsorbent.
  - type of adsorbent, and its charge in solution.
  - Surface area of adsorbent available to solution.
* Concentration of adsorbate in solution.

MINTEQA2 Adsorption Models

Seven adsorption models are available in MINTEQA2. Surface reactions in MINTEQA2 are written in terms of the neutral surface site SOH, and the equations are written as formation constants.

Non-Electrostatic Adsorption Models: The simplest adsorption models are the activity K_d, Langmuir, and Freundlich models. The activity K_d and Freundlich models make the oversimplifying assumption that an unlimited supply of surface sites is available. This assumption renders competition between different adsorbing species meaningless, and the adsorbing surface cannot become saturated no matter how large the supply of adsorbing ions. The activity K_d model is adequate if the concentrations of the adsorbing metals are low, and the pH and ionic strength are relatively constant (Peterson et al, 1987).

The Langmuir adsorption model requires that the number of available surface sites be specified. This marks an improvement over the activity K_d and Freundlich models, since it eliminates the problem

of unlimited surface sites.

The ion exchange model assumes that the surface site is initially occupied by an exchangeable ion that is released into solution during the exchange process (Allison et al, 1991). The user must supply reaction stoichiometries, exchange constants, and the ions participating in the exchange process.

Electrostatic Adsorption Models: The constant capacitance, diffuse layer, and triple-layer adsorption models include the effects of surface charge and potential on the adsorptive behavior of ions and adsorbents in a system. This influence is incorporated into the mass action equations by including terms that modify the activities of sorbate ions as they approach charged adsorbent surfaces. The activities are modified by accounting for the electrical work necessary to penetrate the zone of electrostatic potential extending away from the surface (Allison et al, 1991). These three models treat trace metal surface reactions as complexation reactions analogous to the formation of complexes in solution. The surface complexation models in MINTEQA2 were developed to describe surface reactions of amorphous metal oxide in aquatic systems, having been successfully applied to them in prior experiments.

In all 3 models, a charge (σ) on the surface is assumed to be balanced by a charge (σ_d) associated with a diffuse layer of counterions, such that $\sigma + \sigma_d = 0$. In the constant capacitance and diffuse-layer models, all specifically adsorbed ions contribute to the surface charge (σ). However, in the triple-layer model, the net charge due to adsorption is the sum of the charges associated with two adsorbing planes rather than one. The innermost of the two planes (the o-plane) specifically adsorbs H^+ and OH^- and is characterized by charge σ_o. The other plane (β-plane) has charge σ_β resulting from adsorption of other ions. The net surface charge is given by $\sigma = \sigma_o + \sigma_\beta$ and is

balanced by the charge in the diffuse layer such that $\sigma + \sigma_d = 0$ (Allison et al, 1991).

The electrostatic potentials associated with the surface charge can influence ion activities in solution. The result is that the activities of background and electrolyte ions near the solid surface are different from the concentration of the same ions in the bulk electrolyte. The activity difference is caused by the electrical work required to move ions across the potential gradient between the charged surface and the bulk solution. The activity change between these regions is a function of the ion charge (z) and the electrical potential (Ψ) near the surface. The relation can be expressed by the Boltzmann equation (Allison et al, 1991):

$$\{X_s^z\} = \{X^z\} \; [e^{-z\Psi/RT}]^z$$

where:

$\{X_s^z\}$ = activity of an ion X of charge z near the surface.
$\{X^z\}$ = corresponding activity of X in bulk solution outside the influence of the charged surface.
$e^{-z\Psi/RT}$ = Boltzmann factor

z = charge of ion
F = Faraday constant
R = ideal gas constant
T = absolute temperature

Surface complexation reactions take a variety of forms, depending on the adsorbing ion and whether the surface is represented as neutral, protonated, or deprotonated. An example of how a reaction is expressed in MINTEQA2 can be illustrated by starting with a basic protonation reaction:

$$SOH + H_s^+ \quad <\!\!\longrightarrow\!\!> \quad SOH_2^+$$

for which the mass action expression is:

$$K = \frac{\{SOH_2^+\}}{\{SOH\} \; \{H_s^+\}}$$

The activity of the surface hydronium ions must be corrected for the work performed in moving them to the charged surface where the reaction occurs. The corrected activity is expressed as:

$$\{H_s^+\} = \{H^+\} \; [e^{-\Psi F/RT}]^z$$

The corrected term is then substituted into the mass action expression to give:

$$K = \frac{\{SOH_2^+\}}{\{SOH\} \; \{H^+\} \; [e^{-\Psi F/RT}]^z}$$

A similar result is seen for the deprotonation reaction (see Allison et al, 1991).

To define a diffuse layer adsorption model in MINTEQA2, the user must provide the following information:

* T_{SOH} = Surface site density (moles of sites/l).
* S_A = Specific surface area of the solid (m^2/g).
* C_s = Concentration of solid in the suspension (g/l).
* Surface reactions in terms of MINTEQA2 components, including the surface complexation (formation) constants, K_{ads}.

Values for T_{SOH}, S_A, and K_{ads} are available from the literature, and C_s can be determined from the concentration of the solid in the system.

The constant capacitance and diffuse-layer models are very similar, differing only in the function relating total surface charge σ_o to surface potential Ψ_o. The constant capacitance model is a special case of the diffuse-layer model for solutions of high ionic strength and surfaces of low potential (Allison et al, 1991).

The constant capacitance and diffuse-layer model specify only one layer in which specifically adsorbed ions define the surface charge σ. That plane is referred to as the o-plane, and its surface charge and potential are designated σ_o and Ψ_o. Hydronium and hydroxyl ions form

the bulk of the surface charge (s_o) on the o-plane. Figure 5-11 shows a schematic model of the diffuse layer model associated with the surface of a solid such as amorphous ferric oxide.

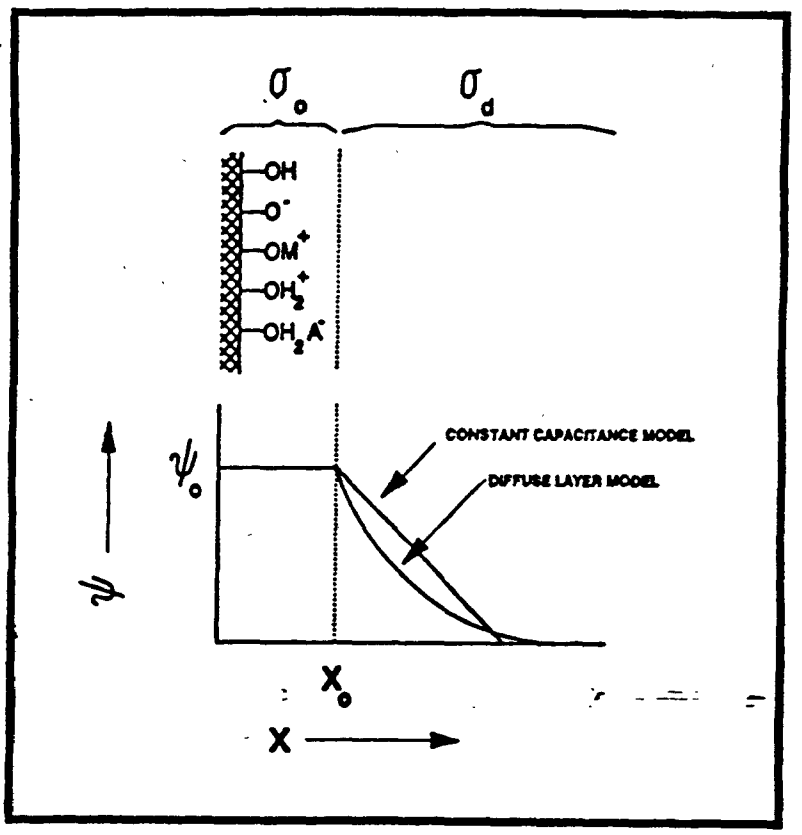

Figure 5-11: Schematic representation of the surface charge/potential relationships used in the constant capacitance and diffuse-layer models (from Allison et al, 1991).

The triple-layer model is slightly more complex than the diffuse layer model, and considers the adsorption layer to be composed of two constant capacitance layers bounded by a diffuse layer of electrolytes (Peterson et al, 1987). A schematic is shown in Figure 5-12. The triple-layer model in MINTEQA2 allows only protonation and deprotonation reactions in the o-plane. Adsorption of other cations and ions occurs

in the β-plane (or inner Helmholtz layer), and non specifically adsorbed ions reside in the diffuse layer or 'd' plane (outer Helmholtz layer).

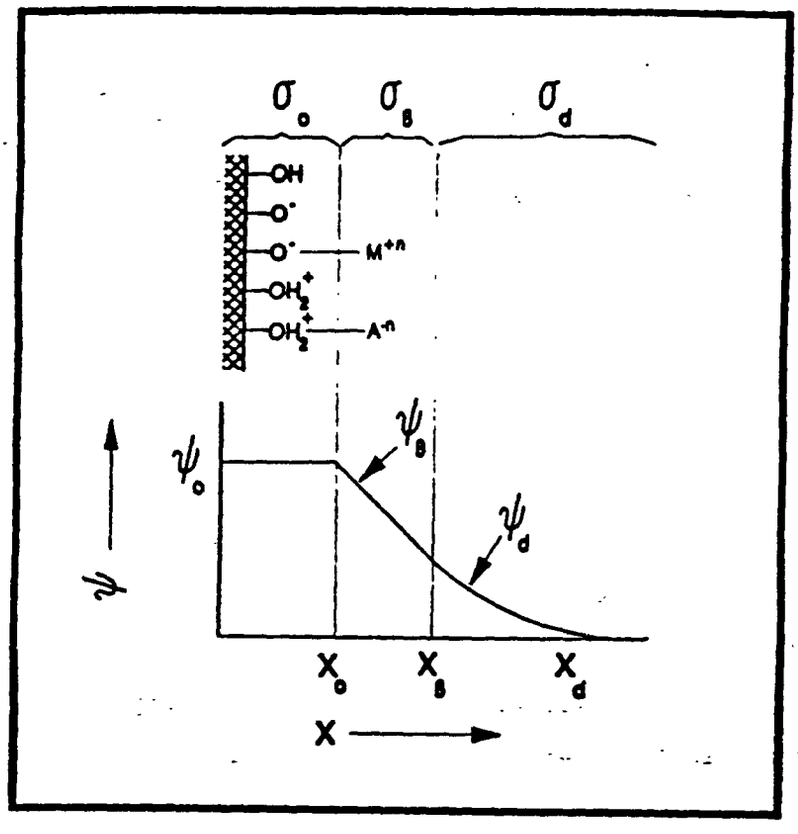

Figure 5-12: Schematic representation of surface species and charge/potential relationships in the triple-layer models (from Allison et al, 1991).

Input parameters for the triple-layer model include two capacitance terms and three electrostatic components. Davis and Runnells (1987) list values for surface site density and capacitance values for adsorption in the triple-layer model.

In the Gold Quarry pit geochemical model, PTI (1992) restricted their adsorption models to the diffuse layer and triple layer models. By fitting the model results to their experimental data for each

specific metal ion of interest (arsenic, cadmium, copper, and lead), they determined which model best described the adsorptive behavior of each ion.

Groundwater/Aquifer Geochemistry: Before applying any hydrogeochemical model to an aquatic system, the modeler needs a high quality, comprehensive chemical analysis for each water to be modeled. Without accurate knowledge of groundwater chemistry, the model will probably be invalid, and may carry erroneous information into water quality prediction, monitoring, and remediation.

In most pit water scenarios, it is reasonable to assume that the aquifer mineralogy near the pit will be the same as or similar to the pit wallrock mineralogy, with the possible exception of ore-related minerals such as trace metals. Water well chemistry in the vicinity of the Universal Gas pit (Geraghty & Miller, 1991) shows major ion concentrations consistent with an aquifer comprised of interbedded carbonate rocks and clastic sedimentary units (i.e., calcium, magnesium, alkalinity, silica). This chemistry may be representative of other upgradient aquifers associated with precious-metal pit waters. The upgradient water may be expected to be in equilibrium with the dominant mineral assemblage.

The equilibrium state of the groundwater (mineral saturation indices) may influence the mineral mass transfer once the water approaches the pit and comes in contact with wallrock minerals. Groundwater in equilibrium with the aquifer may reach equilibrium faster with the pit wallrock, or be less undersaturated with respect to wallrock mineralogy. The result might be less pit wall mineral dissolution, and less mass transfer from the wallrock to the pit water.

Some ore deposits have unusual geologic/geochemical settings that might cause interesting scenarios in local groundwater geochemistry. Ar

example is the Ruth district in Nevada. Ruth is a porphyry copper deposit, with quartz monzonite porphyry the dominant host rock, typical of such systems. However, this intrusive is set within a regional stratigraphic sequence consisting of carbonate rocks. When the Ruth pit water, with low pH and high metals, flows out of the pit and mixes with the carbonate groundwater, the resulting water will likely be significantly different from either of the precursors. The carbonates will probably buffer the groundwater toward neutral pH, causing metals to precipitate from solution.

Reaction Kinetics: Consideration of kinetics in pit water models would greatly improve the validity of the model, but will require more detailed techniques and experiments. Applying experimentally derived kinetic data to complex field situations is difficult.

Many factors influence rates of reaction, the most important perhaps being the surface area of reactant available. This will be constantly changing in field situations during dissolution/precipitation reactions. Without a knowledge of the reactive surface area in contact with a unit volume of water flowing through the pore spaces, kinetic data will remain somewhat empirical and of questionable value from one system to another (Plummer, 1984). Apparent rates of reaction can be derived from inverse modeling if the mass transfer results are combined with estimates of residence times. This procedure has been applied to groundwater systems by Plummer (1984), using isotopic data.

Quantitative interpretation of reaction kinetics in AMD situations is difficult due to the complicated chemical system of buffering (Wicks and Groves, 1993). Rates of $CaCO_3$ dissolution measured in the field are several orders of magnitude slower than rates predicted from the Plummer et al (1978) dissolution rate law (Wicks and Groves, 1993). The experiments of Wicks and Groves revealed that dissolution of Icelandic

Spar $CaCO_3$ in Camp's Gulf Branch was inhibited. They also noted precipitation of hydroxide floc on the calcite crystals, and suggest that the floc inhibited the dissolution by armoring the calcite. Armoring may be a serious problem in pit waters, by preventing dissolution of potential solution buffering minerals. However, armoring may also affect acid generating minerals in a similar manner.

Rates of reaction of pit wallrock minerals might decrease over time, as the saturation state increases and mineral availability decreases. More soluble minerals, or minerals associated with structures or zones of high permeability, might dissolve rapidly during early stages of pit submergence. As these minerals are removed or become armored, dissolution rates may slow.

The kinetics of pyrite oxidation have received great attention. Davis and Ritchie (1987) developed a model for oxidation of pyrite that has been applied in pit water geochemical models (PTI, 1992). The kinetic models generally agree that oxygen availability is the limiting factor in pyrite oxidation. The rate of oxygen diffusion into the pit wall will be a function of the permeability of the wallrock.

None of the codes evaluated in this study explicitly consider kinetics. The rate of reaction may be controlled in PHREEQE and MINTEQA2 by specifying incremental quantities of components participating in reactions for dissolution, precipitation, or other processes. EQ3/6 (Wolery, 1992) incorporates a limited ability to model reaction kinetics.

Equilibrium Thermodynamics: Speciation models of existing pit waters generally show several mineral phases thermodynamically over-saturated. Precipitation of minerals from solution can produce some important changes in pit water chemistry, such as reduction of dissolved solids, removal of metals, and armoring of reactive minerals.

Aluminosilicate thermodynamics (feldspars, pyroxenes, amphiboles, micas, olivines) introduces complications into modeling. Most aluminosilicates weather incongruently, leaving a solid residue behind, such as kaolinite or other clay minerals (Drever, 1988). Many weathering products can be generated, such as mixtures of clays, which could armor other reactive minerals in the system. Modeling results involving aluminosilicate thermodynamics should be interpreted with caution. As stated by Ball and Nordstrom (1991), the use of solubility product constants (K_{sp}) for many silicate minerals (smectites, illites, chlorites, micas, feldspars, amphiboles, pyroxenes, and pyrophyllites) is not recommended because these phases have not demonstrated reversible, equilibrium solubility.

Biological Activity: Biological activity may be important in controlling several aspects of pit water geochemistry, such as redox, reaction kinetics, and chemical speciation. Biological effects were not incorporated into the modeling simulations of this study, but some of the more important aspects deserve mention.

Bacterially mediated oxidation of ferrous iron can enhance pyrite oxidation by up to six orders of magnitude (Lacy and Lawson, 1970). Thiobacillus ferrooxidans is the most common bacteria that oxidize sulfur and iron, but at least 18 others are known (SRK, 1989). Bacteria can also accelerate the oxidation of other sulfides common in mineral deposits (Lundgren and Silver, 1980). SRK (1989) lists the following factors which will determine the bacterial activity, and the associated rate of acid generation:

* Biological activation energy
* Population density of bacteria
* Rate of population growth
* Nitrate concentration
* Ammonia concentration
* Phosphorus concentration
* Carbon dioxide content
* Concentrations of any bacterial inhibitors

Oxidation of organic matter may influence the level of dissolved oxygen in the lake, perhaps accelerating anoxia, which will affect the O_2 available for chemical oxidation. Depletion of O_2 with depth in lakes will commonly be from oxidation of organic matter, but may also be from chemical oxidation (Hutchinson, 1957).

Microbially mediated sulfate reduction, followed by reduced sulfur mineral precipitation, can attenuate the acidity and high concentrations of iron and sulfate in acid mine drainage. Sulfate reduction can partially counteract acidic inputs in freshwater lakes by generating bicarbonate alkalinity via the reaction (Wicks et al, 1991):

$$SO_4^{2-} + 2C_{organic} + 2H_2O \text{ --> } H_2S + 2HCO_3^- \quad (1)$$

This reaction is microbially mediated; the sulfate reduction step requires the presence of organic matter in the sediments to provide a carbon source for the bacteria (Wicks et al, 1991). The sulfide formed in this way must be stored in a reduced form in the sediments to sustain the alkalinity generated (Wicks et al., 1991). At low pH, the sulfide may be released to the atmosphere as hydrogen sulfide gas (Doyle, 1976). If the pH is above 7, HS^- will form rather than H_2S, which will form solid sulfides if any reactive iron is present (Drever, 1988).

Wicks et al (1991) examined sediments of 15 coal strip mine lakes for evidence of sulfate reduction. The end products of reaction (1) were found in the sediments of all 15 lakes, indicating that sulfate reduction occurs followed by authigenic sulfide mineral formation. Both sulfide minerals and organic sulfur were observed in the lake sediments. Organic sulfur phases generally dominate the distribution of end products of sulfate reduction in slightly acidic, sulfate-rich, iron-poor systems (Wicks et al, 1991). Organic sulfur phases also may dominate in AMD lakes, but in iron-rich sediments, sulfate reduction end products are primarily inorganic (Herlihy et al, 1980). If Fe

availability is limiting, an increase in sulfate or organic matter content will not lead to an increase in the FeS or pyrite content of the sediments. In Nevada pit lakes, inorganic reduced sulfur minerals should dominate the authigenic sulfur, since they would be associated with Fe-rich and SO_4-rich sediment.

A variation of reaction (1) is provided by Bell et al (1987):

$$2Fe(OH)_{3(s)} + SO_4^{2-} + CH_3COO^- + H_2 \text{ --> } FeS_{(s)} + Fe^{2+} + 2HCO_3^- + 3H_2O + 3OH^- \qquad (2)$$

which shows that authigenic pyrite formation is controlled by several factors. The extent to which reaction (2) proceeds may be limited by the concentration of any one of the reactants, but organic matter is believed to be the limiting factor in this process (Berner, 1971). Evidence of this in the pit lakes included high correlation between organic matter content and the sulfide minerals, and the low correlation of porewater Fe and porewater sulfate concentrations with any of the S mineral pools (Wicks et al, 1991).

Wicks et al (1991) observed a correlation between age of strip mine lakes and health (water quality). The age of the lakes correlated with the amount of reduced S mineral in the lake sediments. The oldest lake was only 23 years old, yet showed signs of self-remediation through authigenic pyrite formation. The lithologies included limestone, sandstone, and shale, and the pH ranged from 2.6 to 8.0, conditions potentially similar to future Nevada pit lakes. The effects of lake age are: (1) a lessened acidic, sulfate- and Fe-rich load delivered to the sediments as the pyrite weathers from the spoil pile; and (2) amelioration by the alkalinity generating reactions that occur in the sediments. The time schedule (time required for lake to self-remediate: acid neutralization, decreased amount of pyrite oxidation) of any specific lake is determined by the amount of pyrite present in the spoil

that will eventually weather and produce acidity, the thickness of the vadose zone, the precipitation rate in the area, and groundwater flow direction (Wicks et al, 1991).

Photosynthesis can influence the pH of aquatic systems on a cyclic basis (Wetzel, 1983; Drever, 1988). The photosynthesis reaction (Drever, 1988):

$$106CO_2 + 16NO_3^- + HPO_4^{2-} + 122H_2O + 18H^+ + (\text{trace elements, energy}) = C_{106}H_{263}O_{110}N_{16}P_1 + 138O_2$$

utilizes carbon dioxide and hydrogen, thus increasing the pH. Respiration, the reaction in reverse, produces hydrogen which decreases the pH. The variation imposed by photosynthesis can also influence the sorptive behavior of trace metals. Fuller and Davis (1989) observed significant daily fluctuations in trace metal dissolved and sorbed concentrations in their study of Whitewood Creek, South Dakota, which they attributed to uptake/release of trace metals by adsorbents as pH changed due to photosynthesis.

Chemical modeling may reveal biological activity not immediately verifiable or evident in field observations. Nordstrom et al (1979b) noted that jarosite was oversaturated in chemical speciation calculations for some streams, but no obvious yellow iron precipitate was seen in the reaches. Field observations indicated that jarosite precipitation occurred in the micro-environment of bacterial colonies. Nordstrom et al (1979b) conclude that this suggested the existence of a kinetic barrier which hinders jarosite precipitation, but does not hinder ferric hydroxide precipitation, and that this barrier is overcome by the surfaces of bacterial colonies.

Ion Exchange: Ion exchange can be a significant control on the chemistry of water in contact with sediments (Drever, 1988). Ion

exchange may therefore influence cation ratios in pit water, perhaps causing anomalous Na^+/Ca^{2+} or Mg^{2+}/Ca^{2+} ratios. Possible ion exchange reactions are:

$$MgX + Ca^{2+} = CaX + Mg^{2+}$$

$$Na_2X + Ca^{2+} = CaX + 2Na^+$$

where X denotes a clay mineral. In the first reaction, Mg^{2+} in a clay mineral is replaced by a Ca^{2+} ion, and in the second, two Na^+ atoms in a clay are replaced by a Ca^{2+} ion. The first reaction removes one Ca^{2+} ion from solution and adds one Mg^{2+} ion to solution, while the second reaction removes one Ca^{2+} from solution and adds two Na^+ ions to solution.

In experiments involving acidic tailings fluid and calcite-bearing drill core, Davis and Runnells (1987) concluded that ion exchange on montmorillonite clay was responsible for release of Ca^{2+} to solution. Ion exchange can be verified by chemical analysis of ion exchangers (WBL, personal communication).

Physical Factors

Evapoconcentration: Surface water bodies in the arid climate of the Great Basin are subject to high evaporation rates which may exceed the precipitation rates (Figures 5-13 and 5-14; see also Herczeg and Imboden, 1988). For example, in 1984, Big Soda Lake, near Fallon, Nevada experienced 9 cm of precipitation, but 120 cm of evaporation (Kharaka et al, 1984). Evapoconcentration of the pit lake should increase the concentrations of dissolved ions in solution.

Evaporation rates can be estimated by a wide variety of methods (Gray, 1970). Pan rates may overestimate the actual evaporation rate due to higher heat loss than natural water bodies, requiring correction by a conversion factor (Fetter, 1988). Pan rates may also underestimate

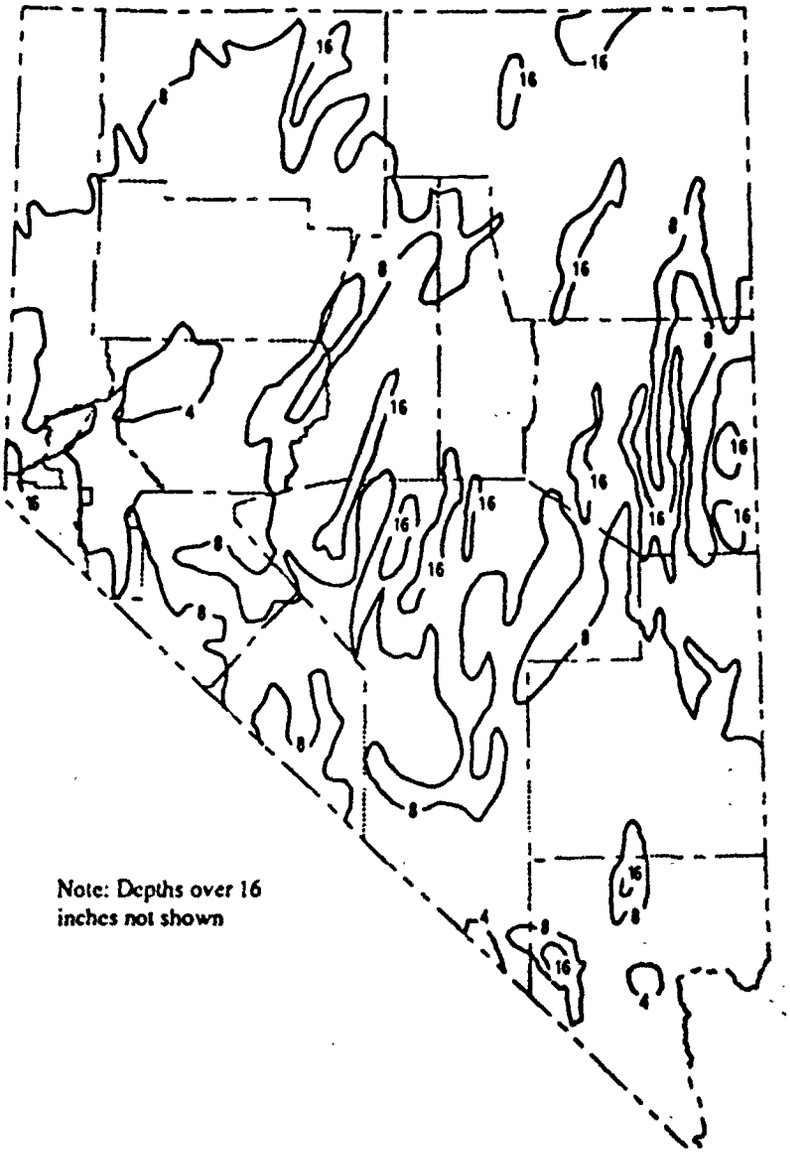

Figure 5-13: Average annual precipitation in Nevada (inches/year); from Nevada Division of Water Planning (1992).

actual rates due to wind speed across the lake and other factors (Gray, 1970).

A geochemical model conducted for Barrick Goldstrike's proposed Betze Pit predicts that evapoconcentration will increase the levels of conservative elements by 2.25 times when steady state is attained, some 200 years after mine closure (BLM, 1991).

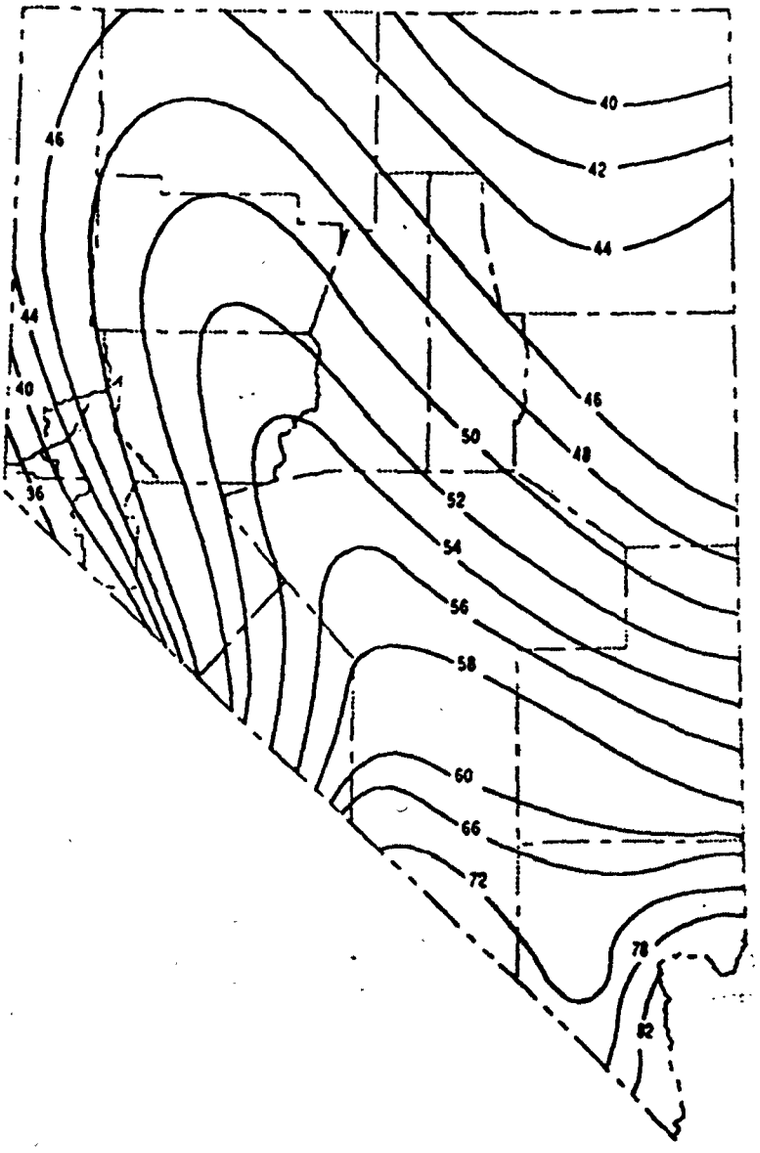

Figure 5-14: Average annual lake surface evaporation in Nevada (inches/year), from Nevada Division of Water Planning (1992).

Limnology: Many physical limnological factors will influence the chemistry of pit lakes, including vertical mixing, temperature, and dissolved gas profiles. The extent to which vertical mixing occurs will determine the likelihood of turnover (Wetzel, 1983). Turnover and mixing will influence several aspects of pit lake chemistry, such as redox, mineral phase and aqueous species stability, and biological activity. Important driving forces determining the occurrence of

turnover include wind energy, chemical density differences, solar radiation, and lake geometry (Wetzel, 1983). Pit lakes could potentially become anoxic at depth, as the O_2 and Eh profiles at the Berkeley Pit illustrate (Figure 5-15). As discussed earlier, anoxic, reducing conditions at the pit bottom, at low to neutral pH, could cause elevated dissolved iron concentrations. Regular turnover and mixing will favor a decrease in iron concentrations and precipitation of ferric hydroxides. A possible drawback of iron hydroxide precipitation is increased turbidity in the water column, which can potentially reduce the heat budget in a pit lake and cause stratification (Parsons, 1977).

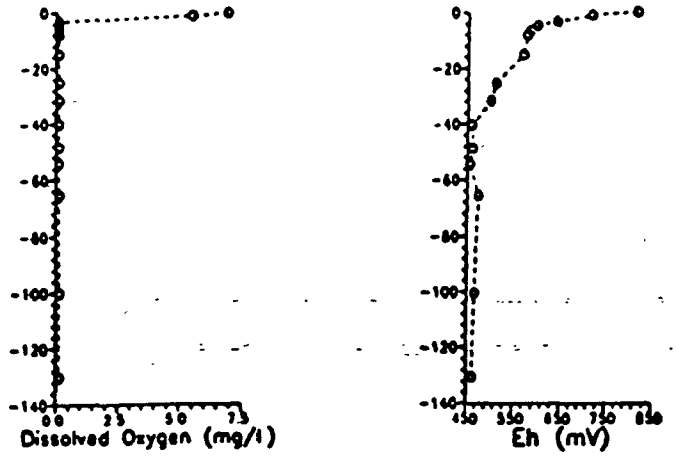

Figure 5-15: Dissolved oxygen and Eh profiles at the Berkeley Pit (from Davis and Ashenberg, 1989)

The temperature of a pit lake will influence its chemistry. Colder water can hold more dissolved gases such as O_2 and CO_2, which will influence many other factors. Seasonal changes in temperature and gas profile of typical lakes are well known (Figure 5-16).

The surface area to depth ratio in pit lakes will be less than most natural lakes, with the closest morphological analog being perhaps Crater Lake, Oregon (Macdonald, 1992; Lyons et al, in press). Such

geometry may decrease the likelihood of wind induced fall and spring turnover, and increase the possibility of perennial anoxia in part of the water column.

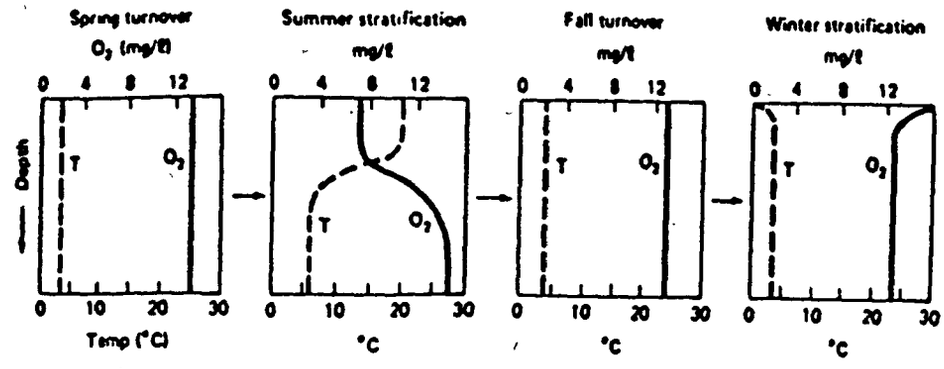

Figure 5-16: Idealized profiles of temperature and dissolved oxygen in oligotrophic (non-productive) lakes (after Wetzel, 1975). The increase in dissolved O_2 with depth is due to the greater solubility of O_2 at lower temperatures (from Drever, 1988).

The location and orientation of some mine site locations may actually enhance the wind speed across the lake. Cortez experiences an apparent funnelling effect, perhaps caused by the orientation of the elongate pit roughly parallel to prevailing wind directions (DAB, personal observation). High freeboard (height of pit wall or shore above water level) of a pit might inhibit the wind velocity across pit lakes.

Limnological models may help development and calibration of pit lake geochemical models. The model CE-QUAL-R1 has been used to model the limnology of the Gold Quarry Pit, using Pyramid Lake as an example (Davis, 1993). Pyramid Lake was deemed the "closest analog" even though the geometries of the two lakes are very different (Lyons et al, in press).

Geothermal input: Due to the anomalously high regional, crustal heat flow in the Great Basin, much of the groundwater is warmer than

average. Much of the geothermal water rises along the young, "Basin and Range," semi-vertical faults that dissect Nevada (NGDC, 1983). Since the ore mineralization at many Cenozoic age mines in Nevada is associated with faults, it follows that some mine sites will be situated in areas of geothermal activity (Macdonald, 1992). Therefore, the potential exists in many post-mine situations for the inflowing groundwater to be significantly warmer than average.

If warm groundwater enters the base of a colder pit lake, density driven vertical mixing may occur, causing turnover on a frequent basis as the warmer, less dense water ascends to the surface. This occurs at Crater Lake, Oregon, a normally very cold mountain lake that experiences deep, geothermal inflow and regular turnover (Williams and Von Herzen, 1983). However, if the warmer water enters high in a cold pit lake, thermal stratification may result, causing a stable situation in which mixing and turnover are unlikely.

Atmospheric Gas Exchange: The ability of the pit lake to take up atmospheric CO_2 and O_2 will influence the redox potential, pH, and the solubility and stability of mineral phases. The pCO_2 will affect pH and carbonate solubility, which in turn influence concentrations of Ca, Mg, and alkalinity. The indirect impacts on pH-dependent metal solubilities could be significant. Plummer et al (1983) found that the calculated mass transfer of pyrite was enhanced 10-fold in their system when closed to CO_2 versus being open to CO_2 input.

The exchange of O_2 will influence redox conditions and the solubilities and concentrations of redox-dependent minerals. As discussed earlier, the impact of Eh dependent metal solubilities could be equally significant, and may make the difference between trace or toxic quantities of metals released into the environment.

The diffusion of O_2 into the pit wallrock could be an important

factor controlling dissolution of trace metals and sulfate into the pit water. Current models of pyrite oxidation assume that the rate limiting step is the rate of O_2 diffusion into the rock (Davis and Ritchie, 1986). The Gold Quarry model applied sensitivity analyses incorporating three different porosities that affected O_2 diffusion into the pit, and hence the mass transfer (PTI, 1992). The three models gave significantly different mass transfer results.

Many lakes with near neutral pH are slightly supersaturated with CO_2 relative to atmospheric pCO_2 (Wetzel, 1983). Soil zone pCO_2 is generally much higher than atmospheric, whereas deep groundwater pCO_2 may be significantly less than atmospheric (Drever, 1988). The pCO_2 of phreatic groundwater in limestone is usually above atmospheric as well (Drever, 1988).

By manipulating the partial pressures of CO_2 and O_2, the model can simulate oxic vs. anoxic, or open vs. closed systems. Fixing the pCO_2 at atmospheric assumes the system is open to the atmosphere. The lake chemical model can be divided into a set of stratified cells, each with a different pCO_2 or pO_2.

Rock/water ratio: The amount of rock exposed to solution (i.e. rock/water ratio between pit wallrock and groundwater + pit water) could exert important control over the mineral mass transfer. The rock/water ratio will be a function of wallrock porosity, permeability, and the water flux into the system. The rate of water flowing into the pit will directly influence the rock/water ratio, which will have an effect on dissolution/precipitation rates. Rapid inflow rate may cause a higher degree of undersaturation in the water, thus enhancing the dissolution of wallrock minerals.

Fractures can greatly increase the permeability, and hence, the groundwater flow rate, through an aquifer. This could have a variety of

effects in pit water evolution. First, if ore minerals such as sulfides are associated with fractures and other structures, the sulfides will be exposed to greater volumes of water than other minerals, causing higher masses of metals dissolved into the water. However, if ore minerals are not associated with structures, or if secondary fracture permeability has been introduced by blasting, the water flowing through fractures could interact with relatively unaltered rock, in which case the dissolution of metals may be suppressed.

More than one aquifer may intersect the pit, such as an alluvial (phreatic) aquifer, underlain by a series of confined or semi-confined aquifers. There may be a much deeper, fracture-controlled, aquifer, perhaps in carbonates, similar to that being encountered in the Carlin trend mines of Eureka, Co., NV (HCI, 1992).

Slope stability in submerged pits could be a complicating factor introducing variation into mine water quality modeling. Wall failure in submerged pits may introduce large errors into the rock surface area predictions of chemical models. Slope stability of the pit wall has the potential to increase the rock/water ratio rapidly and dramatically. Sloughing has decreased the depth of the Berkeley Pit by 38 meters (Davis and Ashenberg, 1989), and the Ruth pit by 37 meters (Woodward-Clyde Consultants, 1992).

The most detailed model of pit water chemical evolution will involve an estimate of the amount of water passing over minerals in the pore spaces of the wallrock, perhaps in concert with kinetic data for dissolution rates of each mineral. These data could be combined with an estimate of pit lake volume and the masses of total metal to be dissolved into it. The pit inflow rates could be calculated from groundwater flow rate as determined from well data. The rock/water ratio would require an estimate of pit wall porosity, which would be complicated by the complexity of structures commonly seen in

hydrothermal ore deposits. A consideration of rock water ratio should incorporate a finely discretized grid, due to the probable variation in the porosity and mineral percentages from site to site in the deposit. An estimate of pit lake volume could be obtained from mine plans, as could the volume or surface area of pit wall available for fluid interaction. By combining these data, one can estimate a flux (and a rock/water ratio) through a given parcel of rock. Ideally, this information can be integrated into chemical models to determine the volume of water that reacts with a specific volume of rock over a specific time interval.

Modeling the rate of inflowing groundwater substantially elevates the level of sophistication of the overall pit water modeling exercise, and was beyond the scope of this study.

Number of Inputs/Outputs in System: The simplest modeling scenario will be one in which the water balance can be expressed as:

$$\Sigma\ (P_i) = \Sigma\ (P_o) + E$$

where:

P_i = sources of water to the pit (groundwater + precipitation)

P_o = sinks of water from the pit (pit outflow to groundwater)

E = evaporation

In other words, the pit has filled to ultimate depth, the system has reached steady state, and no significant inputs or outputs other than those stated above exist.

The contribution to the pit lake from sources other than groundwater, such as surface runoff and precipitation, will complicate the model. The largest contribution of metals into the Berkeley Pit comes not from groundwater, but from surface water draining mine tailings (Huang and Tahija, 1990). The mass of metals from this source

may be impossible to quantify and model, and would require a detailed water/solids budget to the pit.

The rate of local precipitation may be a positive factor in helping to dilute the pit water in some regions. In the arid west, however, the site of most of North America's precious metal pits, precipitation will likely be far outweighed by evaporation (Figures 5-13, 5-14). The rate of precipitation in the Ely, Nevada area (location of Ruth mines, and general location of the Cortez Mine) is 14 inches per year, whereas the evaporation rate from the Ruth pit lake is 45 inches/year (NDEP files). Net evaporation will probably be ubiquitous across Nevada and the entire Great Basin, and evapoconcentration will contribute to higher dissolved solid concentrations in pit waters. Evapoconcentration can be modeled by manual subtraction in MINTEQA2, but is more easily accomplished in PHREEQE.

In most situations, the pit water will likely flow out of the pit and into the adjacent aquifer, under the influence of the local hydraulic gradient. However, if the pit lies on a steep slope, the water could potentially flow over the rim on the downslope side of the pit. This could introduce contaminants into a surface watershed much more rapidly, and over a larger area, than would transport via groundwater.

Time Scale: The pit water chemistry will probably change over time, depending on all of the factors that have been discussed in this section. As stated earlier, evapoconcentration will likely cause a progressive increase in dissolved solid concentrations over time. Pit lakes in the Great Basin, in areas of net discharge, could ultimately become brackish or saline with trace metal concentrations typical of closed basin lakes (see Herczeg and Imboden, 1988).

The time scale of the model will be critical if the pit water is

in contact with different lithologic/mineralogic suites at different stages as the pit fills. A common sedimentary sequence appearing in precious metal deposits is interlayered carbonates and siltstones or shales, as exists at Gold Quarry (PTI, 1992). Two potentially significant scenarios could arise. The first is of greatest concern, that is if a non-buffering lithology is overlain by a buffering lithology which may not be in contact with the rising pit water until well into the future. A more innocuous scenario would be one in which the shale overlies the carbonate, so that the rising pit water is always in contact with carbonates and some buffering capacity is always available as the pit fills.

A pit water will probably reach equilibrium with some of the host mineralogical suites in the wallrock (results shown in later chapter), but the attainment of equilibrium may be many years in the future.

Modeling the pit only at ultimate depth can be risky. Ignoring all the intervening years may neglect decades of contamination, with dangerous consequences to local water quality. An example is the Berkeley Pit, which is projected to top out (without human intervention) in the year 2009, 27 years after dewatering ceased (Davis and Ashenberg, 1989). Conditions at the Berkeley pit today are such that immediate attention is necessary (Duaime, 1992), and local officials are rapidly trying to solve the problem before the pit water reaches the rim (Baum and Knox, 1992).

Hydraulic Gradient: The direction and gradient of groundwater flow may be an important influence on pit wall dissolution, as illustrated by Wicks et al (1991). If sulfide minerals appear on the hydraulically upgradient side of the pit, chances are that mineral dissolution will be enhanced more so than the situation in which the metals exist on the downgradient side. The downgradient side might be

more prone to armoring by mineral precipitation, and perhaps subject to less dissolution than the upgradient side.

High groundwater flow rates may lead to development of a seepage face on the upgradient side of the pit, which may act to destabilize that section of the pit wall and initiate pit wall failure.

Anthropogenic Disturbance: Post-closure anthropogenic disturbances can have positive or negative impacts on water quality, but the complications introduced by such disturbances might make modeling efforts impossible.

Pumping water from the pit lake may induce destabilizing conditions, such as mixing or aerating and moving anoxic-stable species into oxic portions of the pit lake.

At Ruth, Nevada, alkaline gold mill tailings were discharged into the Ruth Pit for several years until August 1987. This resulted in a pH rise to near neutral levels, and a rise in cyanide levels to 5-7 mg/l by fall of 1989 (Dames & Moore, 1990).

Additionally H_2SO_4 was used to leach gold from nearby tailings, some of which ran into one of the pits. Chemical analyses for the Ruth Pit from 1984-86 show pH values in the range of 3-5, whereas 1987 samples show pH up to 6.7 (NDEP files). In 1990, pH of both the Ruth and Kimbley pits were in the neutral range, whereas the pH of the Liberty pit was in the 2-3 range.

Because of the significant anthropogenic disturbances in the Ruth District and Berkeley pits, they were not included in the modeling exercises.

Other Factors

Database limitations: The largest source of discrepancy in chemical models is in the thermodynamic database used by each model

(Nordstrom et al, 1979a). The major species in dilute solutions are relatively unaffected, but the discrepancies increase with higher ionic strength and/or decreasing constituent concentration. The problem becomes more pronounced for trace metal speciation, which can show large variation from small changes in equilibrium constants, pH, redox potential, or temperature.

Downgradient impacts: The water in pit lakes should flow under the driving force of a regional groundwater hydraulic gradient. Unless the water flux out of the pit (evaporation + flow) exceeds the inflow (which should result in a dry pit), the water should flow out of the pit and enter an aquifer or watershed downgradient, taking dissolved solids with it. Contaminants, if contained in pit lakes, probably pose little threat to ecosystems or human water sources. However, if allowed to migrate into an aquifer or watershed that might be a source of water for human consumption, the contaminants in pit water at some mining sites could become a serious concern. Downgradient impacts could be the most important aspect of mine water quality, in the context of environmental contamination, perhaps deserving equal attention in the overall mine water quality modeling exercise.

Once the pit water enters the aquifer and becomes groundwater, the system may become closed to atmospheric gas exchange. Reducing conditions may ensue, which will effect mineral solubilities and aqueous speciation. Sulfides of iron and other metals might precipitate. However, if Eh/pH conditions are similar between the pit and the aquifer, the metals might remain mobile, be transported sufficient distances, and threaten contamination of municipal water supplies. The presence of buffering minerals, such as carbonates, will maintain the pH in the neutral range. The Ruth district is surrounded by carbonate rocks, which could have dramatic effects on the acidic and metal-laden

water that flows from the pits.

The pit lake could conceivably act as a net discharge area depending on its location in the regional hydraulic flow regime, and the combined fluxes of evaporation, pit outflow, and groundwater inflow. In such cases, contaminants will be contained in the pit, with no migration downgradient.

Although most groundwater flow rates are typically slow, on the order of a few meters per year, large pits have the potential to transport tremendous volumes of water and dissolved solids. As an example, the flow rate into the Berkeley Pit is estimated to be 7.6 million gallons per day (Davis and Ashenberg, 1989), while evaporation is estimated at 0.08 millions gallons per day (Camp Dresser and McKee, 1988). Under eventual steady conditions, the balance is 7.52 million gallons per day that could potentially flow out of the pit into the downgradient aquifer. Using iron as an example, if the dissolved concentration at 100 meters depth (1040 mg/l) is considered an average, and assuming that all dissolved iron is carried out, then over 29 metric tons of iron could be transported out of the pit each day into the aquifer downslope:

$$\text{Tons Fe per day} = \frac{(1040\ \text{mg})}{(1\ \text{liter})} \times \frac{(1\ \text{kg})}{(10^6\ \text{mg})} \times \frac{(1\ \text{ton})}{(1000\ \text{kg})} \times \frac{(3.7854\ \text{l})}{(1\ \text{gal})} \times 7.52\ \text{MGD}$$

$$= 29.6 \text{ metric tons of Fe per day.}$$

Similar calculations reveal potential daily transport of 14.1 metric tons of Zn, 6.2 metric tons of Cu, 5.9 metric tons of Al, 0.05 metric tons of Cd, and 201 metric tons of SO_4^{2-}.

6. PIT WATER MODELING APPROACHES

The development of the conceptual and numerical models for this study proceeded in the following stages. First, the Cortez pit was selected as an example location for the simulations. An inverse model was developed and used to determine mass transfer between the pit wall and an upgradient, initial water to generate the final pit water. The inverse model results were used as input to the forward model in an attempt to duplicate the real world condition. Some of the questions posed during conceptualization of both the inverse and forward models include:

* Is the quality of the available chemical analyses for the sites acceptable? Are enough data available for a valid model?
* What minerals might reach equilibrium in the system, such as the major host lithology (e.g. calcite, dolomite, gypsum, silicates)? These will be defined as reversible reactions in the numerical model.
* What minerals are participating in irreversible (dissolution) reactions, and what are their mass transfers?
* What are the relative rates of dissolution of pit wall minerals, and how can they be incorporated into the model?
* What is the extent of gas exchange in the system, and how does it influence pit water chemistry.
* How does adsorption vs. mineral precipitation influence mineral partitioning between the aqueous and solid phase?

This study addresses two possible approaches for modeling pit water chemical evolution. The first is referred to as the rate-independent dissolution approach, and the second as the rate-dependent dissolution approach.

Rate-independent dissolution: The rate-independent dissolution approach assumes uniform dissolution of pit wall minerals independent of reaction kinetics or mineral solubilities. The model assumes that a fixed thickness of pit wall (e.g. 1 foot) dissolves around the interior

submerged surface of the pit, with resultant mass transfer of all constituent elements into solution. A schematic representation is shown in figure 6-1. The method ignores the differential weathering that could result from different mineral solubilities and/or different dissolution kinetic rates.

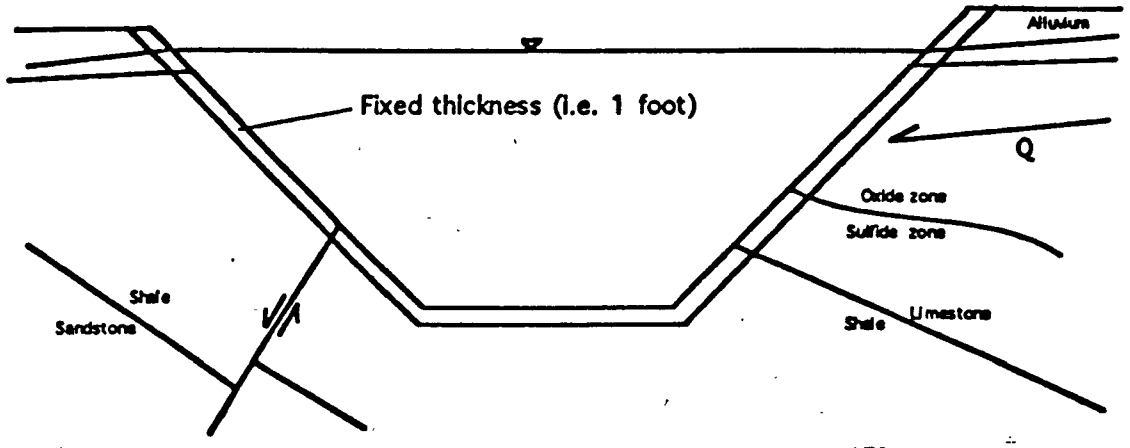

Figure 6-1: Schematic cross-section of rate-independent pit wall dissolution model.

The rate-independent approach greatly simplifies the system such that it can be easily modeled. In the absence of definitive or reliable data on mineral proportions or dissolution rates, this may be the only approach for dissolving elements into the pit water. The information required to perform this simulation includes:

1) Inflowing groundwater chemistry.
2) Local precipitation and evaporation rates.
3) Masses of all minerals in pit wall rock.
4) Volume of pit lake (ultimate or incremental depth).
5) Aqueous speciation and equilibrium model, and adsorption model if desired.

The approach simply dissolves the minerals into the pit lake, giving a bulk concentration of solid per volume of solution in the pit lake, from which the concentration can be easily calculated. An equilibrium model such as MINTEQA2 can be applied to simulate changes in aqueous concentration after mineral precipitation, and an adsorption model can be used to simulate further removal of selected dissolved constituents.

The risks of the rate-independent dissolution approach are obvious. Pit wall dissolution is likely not congruent, since more soluble minerals such as sulfides and carbonates should dissolve faster and in greater quantities than silicates, clays, or oxides/hydroxides. Also, minerals associated with structures and less competent rock such as alluvium will probably dissolve in greater mass.

The improbability of the rate-independent dissolution model is demonstrated by table 6-1, which shows the mineral masses for the Cortez pit wallrock and the Cortez pit water, plus mole ratios for both. Table 6-1 reveals that iron is the least abundant element (on a mole basis) of those tabled for the pit wallrock. With the exception of aluminum, iron

Table 6-1: Moles of element per kilogram of rock in Cortez pit wallrock, and concentrations (mmol/l) of dissolved solids in pit water.

	wallrock *	mole ratio (vs. Fe)	pit water (mmol/l) **	mole ratio (vs. Fe)
C	10.3	1030	4.63	1928
Ca	5.7	570	1.13	472
Mg	4.7	467	0.74	310
Si	4.6	465	0.57	70
K	0.2	16	0.30	125
S	0.02	2	0.94	239
Al	0.5	49	0.0	0
Fe	0.01	1	0.0024	1

Source: * Wells and Mullens (1973); Wells et al (1969).
** See Table 1-4.

is also the least abundant in the water. However, sulfur goes from a

mole ratio (S:Fe) of 2:1 in the wallrock to a ratio of 239:1 in the water. The likely source of sulfate to the pit water is dissolution of sulfides (shown by models in next chapter), which should introduce iron and sulfate into the pit water in a 1:2 ratio. Since sulfate can be assumed to act conservatively in the water (not precipitating or adsorbing), the S:Fe ratio of 239:1 indicates that a significant mass of iron is removed from solution, either by precipitation, adsorption, or other mechanism. In actuality, the iron is removed via precipitation of ferric-hydroxide, as demonstrated by models in next chapter.

The inescapable conclusion is that a rate-independent dissolution model that dumps iron and sulfur into the pit water in the proportions that they exist in the pit wallrock will ignore the processes that control the partitioning of iron between the aqueous and solid phases. This method will grossly underestimate the amount of iron that dissolves into the pit water, by approximately 2 orders of magnitude. A "bulk" chemistry (concentration before precipitation and adsorption processes are modeled) two orders of magnitude higher than the ultimate concentration in solution is precisely the amount predicted by the forward models in the next chapter.

Additional discrepancies between the wallrock and the pit water are seen in aluminum and silica. Dissolution of aluminosilicates is expected to introduce silica to the pit water, but at neutral pH aluminum will remain behind as clay or other weathering residue. This makes the behavior of silica difficult to predict, but assuming congruent dissolution of silicate minerals will likely overestimate the amount of silica in solution, and may overestimate the buffering that occurs from dissolution of silicates.

Rate-dependent dissolution: The rate-dependent dissolution model acknowledges the probability that different minerals dissolve at

different rates, and incorporates this into the mass transfer calculations. The rate dependent dissolution approach is a case of a reaction path modeling exercise.

In addition to the five parameters required for the rate-independent dissolution model, the rate-dependent model requires information on relative rates of reaction of pit wall minerals. This information may be available from experimental data in the literature, but is best acquired from site-specific laboratory experiments such as batch or column tests, to determine relative rates of reaction of pit wall minerals.

A schematic of the rate-dependent dissolution model is shown in figure 6-2, in which minerals associated with structures, ore zones, or less competent rock units experience greater dissolution.

This study has tried to duplicate a rate-dependent approach by determining the mass transfer that has occurred in the system and applying that information to forward models. Although no information has been incorporated regarding pit wall mineral masses or mineral dissolution rates, the mass transfer obtained from the inverse model has been successfully applied in the forward model to duplicate the actual field situation. This exercise is analogous to the approach referenced in Plummer (1984) in which kinetic information (apparent rates of reaction) is obtained indirectly through inverse modeling.

Coupled: The coupled, or reaction transport, approach attempts to combine aqueous geochemical reactions with the equations of hydrologic advective transport. Very few coupled codes are available (Engesgaard and Kipp, 1992; Nienhuis, 1991; Yeh and Tripathi, 1989), as this is a new sub-discipline of geochemical modeling and few studies applying these codes have been performed. Although consideration of the coupled approach is beyond the scope of this thesis, coupled models have the

potential to become important tools in future modeling studies.

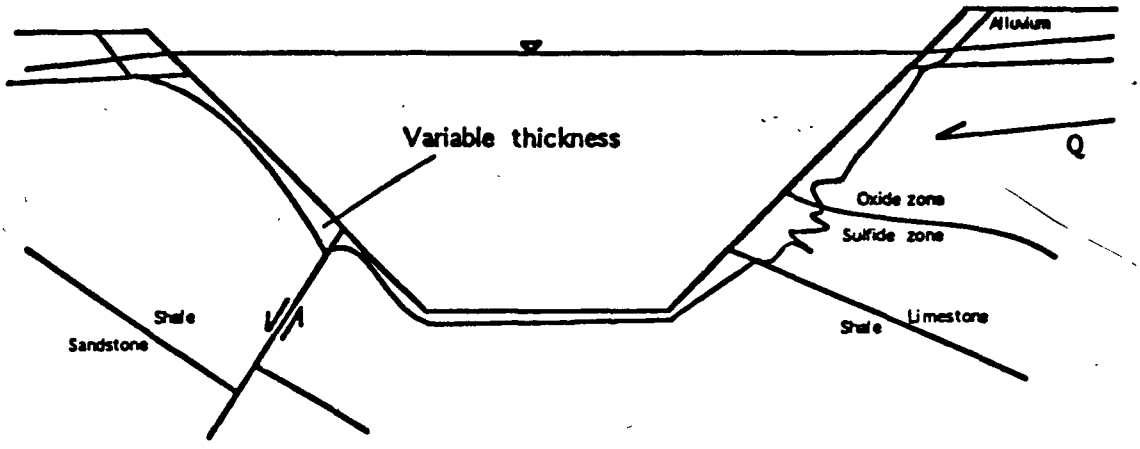

Figure 6-2: Schematic cross-section of rate-dependent pit wall dissolution model.

7. MODELING RESULTS

The Cortez pit in Lander County, Nevada was selected as the example site for the exercise that matched the forward and inverse chemical models. The Cortez Mine was an open pit precious metal mine that was active up until the mid 1970's (Eric Vokt, Cortez Gold Mines, personal communication).

Speciation models were also performed for the Universal Gas pit in Eureka County, Nevada, which has been inactive since about 1983 (Denver Knight Piesold, 1991). These mines are classified as sediment-hosted, disseminated, precious-metal deposits. The primary host lithology for mineralization at both sites is the Silurian Roberts Mountain Formation (Srm). The Srm is primarily carbonate rocks (limestone and dolomite) with minor siliceous interbeds (siltstone). The Universal Gas pit is located one kilometer northwest of the Carlin Gold Mine. The locations of the Cortez and Carlin mine sites are shown in figure 7-1.

Mining activity stopped at the Cortez and Universal Gas sites several years ago, and the water in the pits has apparently reached static conditions. These pits were chosen for several reasons: 1) they may be representative of lakes that will fill many pits left behind by precious metal operations; 2) they are mostly undisturbed by anthropogenic inputs; 3) they have relatively simple water balance situations, i.e. inflow is primarily from groundwater, plus periodic storm event surface runoff; 4) the necessary hydrogeochemical and lithochemical data are available, and of apparently acceptable quality (determined by visual inspection and calculation of ionic balance).

Speciation/Equilibrium Models

Speciation/equilibrium simulations were performed using pit water data from the Cortez pit and the Universal Gas pit. For comparison

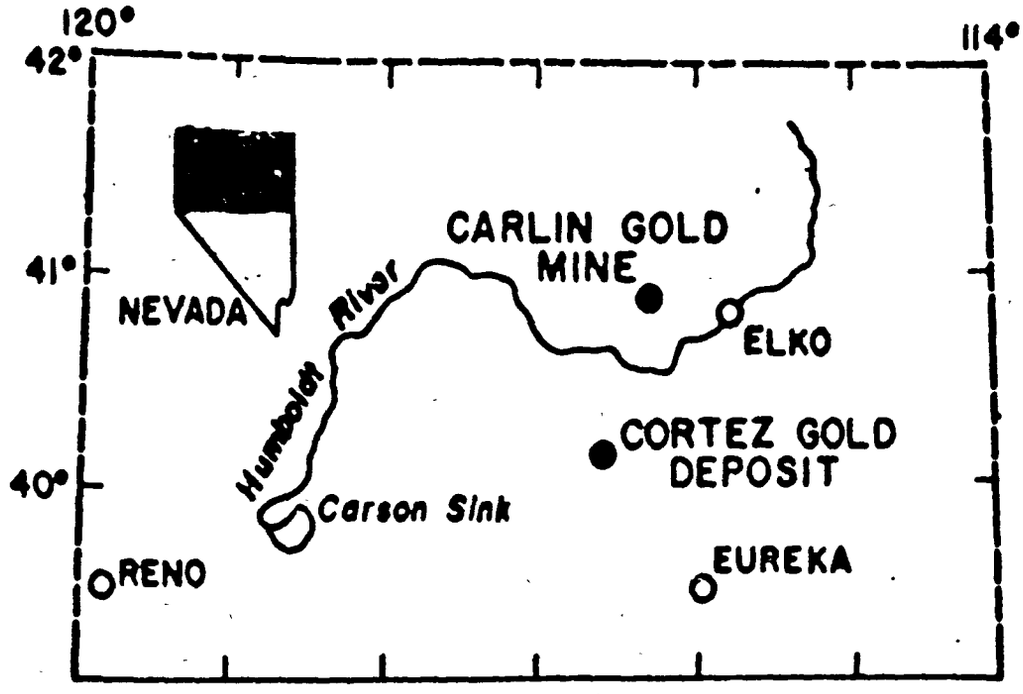

Figure 7-1: Location map for Cortez and Carlin Mines (from Wells et al, 1969).

purposes, pit water analyses were run through WATEQF, WATEQ4F, MINTEQA2, and PHREEQE. The simulations served three purposes: 1) to gain an understanding of the general state of the water, such as chemical speciation and saturation indices of mineral phases; 2) to compare the capabilities of the different programs; 3) to check the validity of the data for application to the inverse simulations (BALANCE), and for subsequent reaction path simulations (PHREEQE, MINTEQA2).

Cortez pit: The original analytical data obtained from Cortez Gold Mines (Table 7-1) exhibited an ionic balance error of approximately 18% (data disk file CZSP01W4.OUT, speciation model of the average of the three analyses). The analyses also lacked data for dissolved silica. The 1993 sampling effort was designed to fill the gaps in the existing data set, and to improve upon the ionic balance.

TABLE 7-1: Cortez pit water chemistry. Source: Cortez Gold Mines (sampled June 1992), values in ppm, NA = not available.

	East end	Middle	West end	Average	
Ca	44.2	43.1	43.1	43.5	
K	11.3	11.4	11.1	11.3	
Na	72.8	72.4	71.4	72.2	
Mg	18.0	17.7	17.7	17.8	
HCO3	225	228	225	226	
SO4	86.5	85.6	81.9	64.67	
Cl	24.8	27.9	26.9	26.53	
F	1.78	1.76	1.76	1.77	
SiO_2	NA	NA	NA	NA	
Ba	0.061	0.060	0.060	0.0603	+
Fe	0.145	0.257	<0.050	0.134	+
Mn	0.005	<0.003	<0.003	0.0017	+
As	0.038	0.037	0.040	0.0383	+
Pb	<0.005	0.006	0.007	0.0043	+
Hg	<0.0005	<0.0005	0.00138	0.00046	+
Zn	<0.005	<0.005	0.006	0.002	+
pH	8.02	8.07	8.13	8.073	

+ Used as model input.

The new data (Table 7-2; CZSP02W4.OUT) show a much better ionic balance (≈4%), and also reveal that the original ionic imbalance was likely caused by an erroneous value for HCO_3^-. The other major ions

TABLE 7-2: Cortez pit water chemistry. Source: UNR/Cortez Gold Mines joint sampling effort (1993). Values in mg/l.

	Surface (0 ft.)	Mid (20 ft.)	Bottom (40 ft.)	Average	
Ca	44.8	45.5	45.9	45.4	+
K	11.7	11.8	11.6	11.7	+
Na	68.3	69.3	68.3	68.63	+
Mg	17.9	18.2	18.2	18.1	+
HCO3	283	282	282	282.3	+
SO4	87.3	96.9	86.4	90.2	+
Cl	24.5	24.5	24.2	24.4	+
NO3	0.13	0.40	0.09	0.2067	+
F	2.4	2.4	2.4	2.4	+
As	0.034	0.030	0.024	0.0293	+
SiO2	34.9	34.4	34.0	34.43	+
pH	7.97	8.14	8.09	8.07	+ *
Eh (mV)	136	149	75	120	+ *
EC (µmho)	680	682	684	682	*
Temp (°C)	21.0	20.2	20.2	20.5	+ *

* Measured in the field.
\+ Used as model input.

show reasonably good agreement between data sets. The 1992 data set included a complete trace metal suite, so the 1993 sampling effort did not include trace metals. For model input, the major element suite from the April 1993 collection was used due to the better major element ionic

balance. These data were used in conjunction with the trace element data collected by Cortez Gold Mines in 1992. The mixing of these data sets is not expected to introduce any significant error to the model. The combined data sets used as model input are shown in Table 7-3.

TABLE 7-3: Input concentrations for Cortez pit water chemical modeling simulations. Source: * UNR/Cortez Gold Mines joint effort (1993); ** Cortez Gold Mines sample (1992).

	(ppm)	
Alkalinity, bicarbonate	282.3	*
Chloride	24.4	*
Fluoride	2.4	*
Nitrate Nitrogen	0.0467	*
Solids, Dissolved (TDS)	432.3	**
Sulfate	90.2	*
Arsenic	0.0383	**
Barium	0.0603	**
Calcium	45.4	*
Iron	0.134	**
Mercury	0.0004	**
Potassium	11.7	*
Magnesium	18.1	*
Manganese	0.0017	**
Sodium	68.63	**
Lead	0.0043	**
Silica	34.43	*
Zinc	0.002	**
pH	8.067	*

Universal Gas Pit: Table 7-4 shows the chemical analytical data from the Universal Gas pit which were used as input for the models. The 1991 analyses were used for all components with the exception of nitrate and ammonia. The activity ratios for the nitrogen species were used to calculate the pe/Eh of the water.

The chemical analyses for the Universal Gas pit water shows some similarities to the Cortez pit water, but also some key differences, such as chloride, aluminum, sulfate, alkalinity, calcium, and a few trace metals. The input and output for all speciation simulations for the Cortez and Universal Gas pits, and for well SC-5B, are on datadisk 1. The names and contents of the files are listed in Table 7-5.

The speciation simulations for the Cortez pit water show some predictable results. A portion of the actual output file (CZSP01W4.OUT) is shown in Table 7-6. In all output sets, both pit waters and the well

TABLE 7-4: Water chemistry, Universal Gas pit. Source: Geraghty & Miller (values in ppm).

	Sample date 4/23/91 *	3/12/90 **
Alkalinity, bicarbonate	77.5	118.3
Alkalinity, total	85.5	97
Chloride, titrimetric	342	NA
Chloride	NA	198
Conductivity, in µmhos/cm.	NA	903
Cyanide, total	NA	0.06
Cyanide, weak acid diss.	NA	< 0.02
Fluoride	0.394	0.2
Ammonia	NA	0.13
Nitrate Nitrogen	0.111	1.3
Nitrate	NA	5.7
Solids, Dissolved (TDS)	691	550
Sulfate	30.7	23
Silver	< 0.02	< 0.01
Aluminum	0.174	< 0.2
Arsenic	< 0.180	< 0.01
Boron	0.185	0.12
Barium	0.12	0.388
Cadmium	< 0.007	< 0.005
Calcium	145	94
Cobalt	0.02	< 0.05
Chromium	< 0.01	< 0.01
Copper	< 0.007	< 0.025
Iron	0.134	< 0.1
Mercury	< 0.5	< 0.0002
Potassium	3.74	8
Magnesium	38	21.1
Sodium	50	38
Nickel	< 0.015	< 0.04
Lead	< 0.05	< 0.003
Selenium	< 0.13	< 0.005
Silicon	9.11	53.7
Tin	< 1.3	NA
Strontium	0.514	NA
Tellurium	< 0.075	NA
Titanium	< 0.001	NA
Thallium	< 0.15	NA
Tungsten	0.051	NA
Vanadium	< 0.007	NA
Zinc	< 0.005	< 0.02
pH	8.67	7.74

Source: * Westmont Gold (NDEP files)
** Geraghty & Miller, Inc.

are near equilibrium with respect to the carbonate minerals aragonite, calcite, dolomite, magnesite, and siderite. The pit waters are slightly oversaturated, whereas the well is slightly undersaturated. This is expected, since both pits are situated in carbonate host rocks, and well SC-5B is emplaced in the carbonate Srm formation.

The pit waters are also near equilibrium with respect to several silica and iron oxide phases. The silica phases are no surprise, since siltstones are interbedded with the carbonates in all three settings.

The speciation of the Universal Gas pit water shows a slightly more saline composition (ionic strength = 0.017, or $10^{-1.77}$) than the

Table 7-5: File names and contents of speciation model output files.

Cortez pit water speciation simulations

CZSP01WF.IN	WATEQF input file	CZSP01MT.IN	MINTEQA2 input file
CZSP01WF.OUT	WATEQF output file	CZSP01MT.OUT	MINTEQA2 output file
CZSP01W4.DAT	WATEQ4F input file	CZSP01PH.IN	PHREEQE input file
CZSP01W4.OUT	WATEQF output file	CZSP01PH.OUT	PHREEQE output file
CZSP02W4.DAT	WATEQ4F input file *	CZSP02W4.OUT	WATEQ4F output file *

Universal Gas pit water speciation simulations

UGSP01WF.IN	WATEQF input file	UGSP01MT.IN	MINTEQA2 input file
UGSP01WF.OUT	WATEQF output file	UGSP01MT.OUT	MINTEQA2 output file
UGSP01W4.DAT	WATEQ4F input file	UGSP01PH.IN	PHREEQE input file
UGSP01W4.OUT	WATEQ4F output file	UGSP01PH.OUT	PHREEQE output file

Well SC-5B speciation simulations

SC5B01W4.DAT	WATEQF input file	SC5B02MT.IN	MINTEQA2 input file
SC5B01W4.OUT	WATEQF output file	SC5B02MT.OUT	MINTEQA2 output file
SC5B01MT.IN	MINTEQA2 input file *	SC5B01PH.IN	PHREEQE input file
SC5B01MT.OUT	MINTEQA2 output file *	SC5B01PH.OUT	PHREEQE output file

* Second Cortez pit water speciation, using 92-93 composite.

** This simulation executed to determine Eh using specified redox couple for the actual speciation in next simulation.

Table 7-6: Cortez pit water speciation, portion of output file CZSP02W4.OUT showing saturation indices.

Phase	Log IAP/KT	Log IAP	Log KT
Aragonite	.449	-7.860	-8.309
Barite	.168	-9.876	-10.044
Calcite	.596	-7.860	-8.456
Cerrusite	-1.778	-14.962	-13.185
Chalcedony	.357	-3.248	-3.604
Chrysotile	-.878	31.888	32.766
Cristobalite	.401	-3.248	-3.649
Diopside	-.983	19.274	20.257
Dolomite (d)	.516	-15.900	-16.415
Dolomite (c)	1.084	-15.900	-16.984
Fe3(OH)8	3.266	23.488	20.222
FeOH)2.7Cl.3	6.487	3.447	-3.040
Ferrihydrite	1.939	6.830	4.891
Fluorite	-.423	-11.077	-10.654
Goethite	7.830	6.830	-1.000
Greenalite	2.182	22.992	20.810
Gypsum	-1.846	-6.427	-4.581
Hematite	17.321	13.659	-3.662
Maghemite	7.273	13.659	6.386
Magnesite	-.080	-8.040	-7.960
Magnetite	19.185	23.489	4.304
Quartz	.800	-3.248	-4.048
Sepiolite(c)	-.034	15.846	15.880
Siderite (d)	-.555	-11.005	-10.450
Siderite (c)	-.143	-11.005	-10.862
Silica gel	-.180	-3.248	-3.068
SiO2 (a)	-.498	-3.248	-2.749
Talc	3.473	25.393	21.920
Tremolite	6.279	63.941	57.662
ZnSiO3	1.286	4.421	3.135

Cortez pit water (ionic strength = 0.00845 or $10^{-2.07}$). A portion of the output file from speciation model UGSP01W4.OUT is shown in Table 7-7. The pH in the pit (8.67) is higher than the groundwater (7.06), suggesting that the buffering effect of carbonates is enhanced by the system being open to CO_2.

Discussion: The advantages of each code become apparent when the output files are compared for the speciation models of the Cortez pit water (Table 7-8) and the Universal Gas pit water (Table 7-9).

WATEQF: As the tables show, WATEQF contains no database for several trace elements present in the Cortez pit water, and that may be important in other pit waters derived from precious metal hydrothermal deposits (As, Hg, Pb, Zn). This deficiency limits the effectiveness of WATEQF in pit water modeling applications, and its use is not recommended.

WATEQ4F: WATEQ4F can manage all of the aforementioned elements except mercury. In addition, WATEQ4F can handle other potentially important mine-derived trace metals, including Ag, Cd, Cs, Cu, Ni, Rb, Se, and U. WATEQ4F also maintains a very flexible and comprehensive approach to redox conditions. WATEQ4F should serve adequately in speciation/equilibrium of all pit waters, except those for which mercury speciation modeling is desired, and should be included within the overall pit water modeling exercise.

MINTEQA2: The size of the databases in MINTEQA2 and WATEQ4F are similar. The number of minerals in the MINTEQA2 model is slightly higher for each sample than in the WATEQ4F model, whereas the number of aqueous species is slightly higher in WATEQ4F. Both of these codes are relatively easy to use, and generate the same basic information in the speciation model output files. MINTEQA2 offers more flexibility than WATEQ4F in some aspects (e.g. calculation of activity coefficients, adjusting partial pressures of gases), but the advantages

Table 7-7: Universal Gas pit water speciation, portion of output file UGSP01W4.OUT showing saturation indices.

Phase	Log IAP/KT	Log IAP	Log KT
Adularia	.691	-19.882	-20.573
Albite	-.522	-18.524	-18.002
Allophane(a)	-.971	7.895	8.866
Allophane(P)	.116	7.895	7.778
Annite	34.496	-51.149	-85.645
Anorthite	-.495	-20.209	-19.714
Aragonite	.946	-7.391	-8.336
Ba3(AsO4)2	11.779	-38.331	-50.110
Barite	-.193	-10.163	-9.970
Beidellite	2.299	-42.973	-45.272
Boehmite	.164	8.748	8.584
Calcite	1.089	-7.391	-8.480
Chalcedony	.032	-3.520	-3.551
Chlorite 14A	10.082	78.462	68.380
Chlorite 7A	6.710	78.462	71.752
Chrysotile	3.676	35.876	32.200
Clinoenstite	-.556	10.786	11.342
Cristobalite	.067	-3.520	-3.587
Diaspore	1.869	8.748	6.879
Diopside	2.036	21.930	19.894
Dolomite (d)	1.400	-15.140	-16.540
Dolomite (c)	1.950	-15.140	-17.090
Fe3(OH)8	.224	20.446	20.222
FeOH)2.7Cl.3	6.581	3.541	-3.040
Ferrihydrite	1.873	6.764	4.891
Fluorite	-1.622	-12.222	-10.600
Gibbsite (c)	.637	8.747	8.110
Goethite	7.764	6.764	-1.000
Hematite	17.537	13.529	-4.008
Huntite	-.670	-30.638	-29.968
Illite	2.272	-37.995	-40.267
Kaolinite	3.021	10.456	7.435
Kmica	7.574	20.277	12.703
Laumontite	3.712	-27.248	-30.960
Leonhardite	15.259	-54.497	-69.756
Maghemite	7.143	13.529	6.386
Magnesite	.280	-7.749	-8.029
Magnetite	16.709	20.446	3.737
Manganite	-1.549	23.791	25.340
Montmoril BF	5.244	-29.669	-34.913
Montmoril AB	4.970	-24.718	-29.688
Montmoril Ca	2.099	-42.928	-45.027
Phillipsite	.671	-19.203	-19.874
Prehnite	2.630	-9.065	-11.695
Pyrophyllite	6.402	-41.912	-48.314
Quartz	.461	-3.520	-3.980
Rhodochrs(d)	-.740	-11.130	-10.390
Rhodochrs(c)	-.000	-11.130	-11.130
Sepiolite(d)	-.609	18.051	18.660
Sepiolite(c)	2.291	18.051	15.760
Silica gel	-.502	-3.520	-3.018
SiO2 (a)	-.808	-3.520	-2.712
Strontianite	-.904	-10.175	-9.271
Talc	7.438	28.837	21.399
Tremolite	16.122	72.696	56.574
Wairakite	-.540	-27.248	-26.708

for simple speciation models are relatively insignificant. The biggest advantages of MINTEQA2 are seen in the implementation of forward models, which are performed later.

Table 7-8: Comparison of portions of output files for Cortez pit water speciation simulations.

	WATEQF	WATEQ4F	MINTEQA2	PHREEQE
Ionic strength	.0093	.0093	.0116	.0093
Total aqueous species	59	128	127	57
Total minerals	59	130	143	106
Number of iron species	14	26	20	8
Number of arsenic species	0	9	9	3
Number of mercury species	0	0	13	3
Number of lead species	0	20	20	3
Number of zinc species	0	15	16	7
log pCO_2	-2.67	-2.67	-2.37	-2.67
Oversaturated minerals	6	20	24	16

PHREEQE: The unrevised PHREEQE (as obtained from the USGS) contains no thermodynamic data for the trace elements As, Hg, Pb, and Zn. PHREEQE was customized in this study, specifically for the Cortez pit water simulations, by adding the following eight elements to the permanent database:

Arsenic	Mercury
Cadmium	Silver
Copper	Thallium
Lead	Zinc

Additionally, 113 aqueous species and 130 minerals composed of these elements were permanently added to the PHREEQE thermodynamic database. This expanded version of PHREEQE can now model a limited number of minerals and aqueous species for all ions of interest in the Cortez pit water, including Hg (Table 7-8). The ability to modify or expand the database represents the biggest advantage of PHREEQE over WATEQF or WATEQ4F.

Table 7-9: Comparison of portions of output files for Universal Gas pit water speciation simulations.

	WATEQF	WATEQ4F	MINTEQA2	PHREEQE
Ionic strength	.0170	.0170	.0175	.0170
Total aqueous species	81	119	96	45
Total minerals	89	109	118	77
Number of iron species	14	26	20	5
Number of arsenic species	0	9	9	2
log pCO_2	-3.91	-3.91	-3.59	-3.92
Oversaturated minerals	30	40	45	27

The principal disadvantage of PHREEQE is that it is the most difficult of these codes to learn. This drawback, plus the smaller off-the-shelf database, make PHREEQE less desirable for simple speciation models than either WATEQ4F or MINTEQA2. Learning to apply PHREEQE to even simple tasks, such as ordinary speciation simulations, is a chore which researchers may find impractical. MINTEQA2 or WATEQ4F can be learned in less time, and have a larger trace metal database than even the expanded PHREEQE.

The time necessary to expand the PHREEQE database with the necessary elements, species and minerals can be immense (several weeks for this study), but after its done once, the code can be used for a variety of simulations. The ability to move easily between speciation and reaction path models provided significant flexibility in the pit water models, and represents the biggest advantage of PHREEQE. The output files for the Cortez and Universal Gas pits illustrate the relative sizes of the thermodynamic databases of each code, and the usefulness of each to the application of speciation modeling. Clearly, the databases of WATEQ4F and MINTEQA2 exceed the others, and provide the most comprehensive speciation models. The only advantage WATEQ4F has

over MINTEQA2 for speciation modeling is in speciating a redox problem for which no pe/Eh is available, but for which data are available for a specific redox couple. WATEQ4F can speciate in only one iteration, whereas MINTEQA2 requires two.

Inverse Model

The inverse model attempts to determine the chemical mass transfer that has occurred along a hydrologic flow path. The USGS computer code BALANCE (Parkhurst et al, 1980) was used to determine the mass transfer that occurred between the upgradient groundwater and the Cortez pit water. In the case of pit water modeling, the mass transfer occurs during rock/water interaction between the upgradient groundwater and pit wall minerals + atmospheric gases.

Input: The input required for an inverse model includes chemical analyses for two waters (initial and final) along a hydrologic flow path, and a set of mineral phases (including gases) believed to be responsible to produce the second water from the first through dissolution and precipitation of the mineral phases.

Water chemistry: The final water (i.e. the "final well") for the pit water inverse simulation is obvious, namely the pit water chemical analysis. As the analytical data in Table 7-2 illustrate, there is no significant chemical stratification evident in the Cortez pit water, so an average of the three depths was deemed satisfactory. Furthermore, the water has possibly experienced mixing anyway due to active pumping from the lake.

Selection of an initial water for the Cortez pit water model presents a small problem. According to mine personnel, there is no well located upgradient of the Cortez pit that can be used as representative input water to the pit, so an exact initial water chemistry is not available. Monitoring wells located downgradient or lateral to the pit

show anomalously high levels of some trace metals (NDEP, 1992), and have probably been influenced by ore mineralogy, or contaminated by anthropogenic activity. Whatever the source of the metals, these waters would not be representative of groundwater immediately upgradient of the Cortez Pit. Consequently, chemical analytical data for these wells were not used in the simulations.

However, the host rock formation at both the Cortez and the Universal Gas sites is the Silurian Roberts Mountain Limestone (Srm). The water chemistry from a well (Well SC-5B) approximately 200 meters northeast of the Universal Gas pit and hydraulically upgradient (Denver Knight Piesold, 1991) may reasonably represent the groundwater upgradient of the Cortez pit. Monitoring well SC-5B was, therefore, selected as the initial water for the Cortez pit water models.

Well SC-5B is approximately 115 feet deep, and taps a deep alluvial aquifer at the alluvium/bedrock contact. The water chemistry in Well SC-5B (Table 7-10) is consistent with that of the Universal Gas pit, indicating that this aquifer is the likely source of the Universal Gas pit water (Knight Piesold, 1992).

Unfortunately, the use of an initial water not along the hydrologic flow path makes the inverse model invalid. However, the framework of the model remains valid, and only the actual input numbers are different. Once the correct data become available, they can be easily incorporated into the model to generate valid, site-specific results. The scope of this study only permitted the use of available data and resources. Funding was not available to drill new monitoring wells.

Some general predictions of possible mass transfer are possible through brief examination of the two water chemistry samples. For ions which show higher concentrations in the pit water than in the well (e.g. alkalinity, sulfate, magnesium, sodium) we may predict that one or more mineral phases containing these components must be dissolving along flow

path. For ions which show lower concentrations in the pit water (e.g., calcium, iron, zinc) some type of removal mechanism is at work, such as mineral precipitation or adsorption.

TABLE 7-10: Chemical analyses for Well SC-5B, Universal Gas site, Nevada (sampled 3/12/90, source: Geraghty & Miller).

	ppm
Alkalinity, bicarbonate	112.2
carbon	22.1
Chloride, titrimetric	86
Fluoride	0.5
Solids, Dissolved (TDS)	322
Ammonia	0.07
Nitrate Nitrogen	0.7
Nitrate	3.1
Boron	0.11
Sulfate	37
Sulfur	12
Barium	< 0.2
Calcium	51
Iron	0.34
Lithium	NA
Potassium	5
Magnesium	13.8
Manganese	0.079
Sodium	31
Silica (SiO_2)	83.22
Silicon	38.90
Aluminum	< 0.2
Arsenic	0.01
Copper	< 0.025
Lead	< 0.003
Mercury	0.0002
Zinc	0.022
pH	7.06

Phases: An inverse model requires a set of potential mineral phases, including gases, that may react with the initial water to result in the final water chemistry. Selection of potential mineral phases was based on publications and reports for the geology of the Cortez mine site, the Roberts Mountain formation, and the aquifer geochemistry (Denver Knight Piesold, 1991; Radtke et al, 1987; Wells and Mullens, 1973; Wells et al, 1969).

The primary host lithology at both the Cortez and Universal Gas sites is the Silurian Roberts Mountain Formation (Srm), which is believed to be up to 470 meters thick (Denver Knight Piesold, 1991). The Srm consists of dolomite and limestone with siliceous (chert), silty, and argillaceous interbeds. A minor host at the Universal Gas

mine is the Ordovician Vinini Formation (Ov), consisting of shales, siltstones, and chert with minor quartzite and limestone. The phases selected for the inverse model are shown in Table 7-11.

Table 7-11: Mineral and gas phases selected for Cortez Pit water inverse model.

Calcite	K-Mica	Magnesite	NaCl
Ca/Na EX	Galena	Sphalerite	MnO_2
Illite	CO_2 gas	Rhodochrosite	Gibbsite
Dolomite	Fluorite	Arsenopyrite	Barite
Goethite	Pyrite	Cinnabar	K-Feldspar
Gypsum	SiO_2	Sphalerite	Kaolinite
Ca-Montmo	K-Montmo	Plagioclase	Mg/Na EX
Na-Montmo	=SOH:Zn	"CH2O" (organic matter)	

Results: BALANCE found 1716 possible combinations of phases that could account for the water evolution, but only 2 that satisfied the constraints specified. The calculated mass transfer of the selected model is shown in Table 7-12. A positive number indicates addition to

Table 7-12: Mass transfer model calculated by BALANCE, first iteration (concentrations in μmol/kg.):

Plagioclase	+	F	106.9250
Fluorite	+	F	50.0130
=SOH:Zn		F	- .3059
Galena	+	F	.0208
Cinnabar	+	F	.0013
Arsenopy	+	F	.3772
NaCl	+	F	1583.3785
Barite	+	F	.4391
Calcite		F	2787.7720
MnO_2		F	-1.4091
Gypsum			-3031.0075
Pyrite	+		1238.1746
K-Montmo			-767.3370
Illite			707.6120
SiO_2			-740.1979
Goethite			-1242.1746

solution via mineral dissolution or in-gassing, and a negative number indicates removal from solution by mineral precipitation or out-gassing.

The phase ≡SOH:Zn was arbitrarily chosen as a removal mechanism for zinc, and the negative number indicates removal from solution via adsorption. The earlier predictions of dissolution of mineral phases of carbonate (calcite), sodium (NaCl), magnesium (illite), and sulfate (pyrite) have held true, as have predictions of precipitation of mineral phases of calcium (gypsum), and iron (goethite). To help interpret whether these are believable, we can refer to the output from the WATEQ4F calculations.

The WATEQF output for the Cortez pit water data shows several minerals near equilibrium or oversaturated, including carbonates, iron oxide minerals, and silica phases. These minerals may actually be precipitating at some point along the hydrologic flow path (e.g. in the pit water), so the models that predict precipitation of these phases may be plausible.

An important contrast in the chemical analyses for the initial and final waters pertains to dissolved zinc. Most trace element concentrations are higher in the final (pit) water than in the initial (well), with the exception of zinc. This prompted the definition of a generic sink for zinc in the final water. The phase ≡SOH:Zn, possible adsorption onto a solid phase, was arbitrarily chosen to represent a removal mechanism for zinc.

A few comments are warranted regarding the BALANCE model results. This model may only remotely resemble the actual mass transfer that has occurred along the flow path from Well SC-5B to the Cortez pit water. Potential effects of evapoconcentration or other processes (i,e, increases in concentration of "conservative" ions) were not considered in the model. Hence, BALANCE had to devise sources for some ions (chosen from the phases provided by the modeler), such as halite (NaCl) and pyrite (FeS_2), which showed an increase between the initial and final waters. The mass transfers of these ions determined by the model

may significantly exceed that which actually occurred in the system, if the mass transfer occurred at all.

To account for the desired final concentration of S, the model had to increase pyrite dissolution, which also increased Fe in the proportion equal to the stoichiometric ratio of pyrite (1:2). However, the final Fe concentration (Cortez pit water analysis) is less than the initial (Well SC-5B), so BALANCE removed the excess Fe by precipitating goethite (FeOOH).

Calcite dissolution accounted for the mass transfer of bicarbonate alkalinity from the well to the pit water, but resulted in an excess of calcium, which was removed via precipitation of gypsum ($CaSO_4 \cdot 2H_2O$).

Chloride in the initial water is higher (86 ppm) than in the final (24.4 ppm), and perhaps reflects artifacts of anthropogenic influence. Constraining the model by including chloride would have forced BALANCE to devise a means of removing chloride from the final water via precipitation. The only chloride phases in the BALANCE database are evaporites (e.g. halite, NaCl and sylvite, KCl), but the Cortez pit water is far too dilute to favor precipitation of evaporite minerals. For this reason, chloride was not constrained in the BALANCE models.

Sodium was accounted for through dissolution of plagioclase (selected stoichiometric ratio $Al_{1.5}Ca_{0.5}Na_{0.5}Si_{2.5}$), and halite (NaCl). The existence of halite in the Cortez pit system is hypothetical, but other potential sodium sources are also difficult to determine. The use of plagioclase to account for all of the sodium would have increased the mass transfer of Al, Ca, and Si proportionally and may have caused the model to fail.

The effect of interacting variables is once again demonstrated in the modeling effort, as well as the "balancing" act that the code must perform to obtain a fit to the mass transfer model. Some of the model results shown in Table 7-12 can be rightly questioned, such as the

precipitation of gypsum and dissolution of halite. The modeler must use good geochemical "common sense" to interpret the validity of the possible models generated by the code.

The limitations of the model, and the inability to account for all of the processes at work in the chemical evolution of the Cortez pit water, prevent the formulation of a model that matches the real world exactly. However inaccurate the results may be, they represent the best mass transfer model obtainable for the Cortez pit water at this point. Hence, with the mass transfer calculated, the inverse results can now be applied to the forward model.

Forward Models

The forward model determines the chemistry of the final water, in this case pitwater, which results from reactions between the upgradient groundwater and the pit wallrock, and subsequent precipitation and adsorption reactions in the pit water. The results from the BALANCE model (Table 7-12) were run through PHREEQE to model the addition of dissolved species to the pit water via mass transfer from the pit wall. The minerals that were chosen to introduce specific major elements and trace metal into the pit in the required concentrations are shown in Table 7-13.

Mass Transfer: An assumption that may be incorporated into pit water chemical models is that the water will eventually come to equilibrium with some of the primary host mineralogies. Speciation simulations for existing pit waters (Cortez, Table 7-6, CZSP02W4.OUT; Universal Gas, Table 7-7, UGSP01W4.OUT) show equilibrium with respect to several carbonate and silica phases (e.g. calcite, dolomite, amorphous silica, quartz) which may be primary minerals in the carbonate and siltstone lithologic units. Another example is the Liberty pit water, for which the speciation model (LISP01PH.OUT) shows equilibrium

with several silica minerals (amorphous silica, chalcedony, quartz) that might comprise the quartz monzonite host rock. However, aluminosilicate phases that may also comprise the host (albite, microcline, muscovite, kaolinite, and gibbsite) are significantly undersaturated. As later models demonstrate (sensitivity analyses), a solution in equilibrium with these aluminosilicate phases will likely be buffered in the range of pH 5-6. Since this pH is significantly greater than that seen in the majority of igneous hosted pit waters, the assumption of equilibrium with aluminosilicate minerals is probably not valid. Data for the Berkeley pit are lacking in silica concentrations (saturation insufficient), so no comparison is available.

Table 7-13: Minerals used in mass transfer reaction models.

Ion	Source Mineral
Calcium	Calcite ($CaCO_3$)
	Dolomite ($CaMg(CO_3)_2$
Carbon (alkalinity)	Calcite ($CaCO_3$)
	Dolomite ($CaMg(CO_3)_2$
Chloride	Halite (NaCl)
Magnesium	Dolomite ($CaMg(CO_3)_2$
Potassium	K-Feldspar ($KAlSi_3O_8$)
	K-Mica ($KAl_3Si_3O_{10}(OH)_2$
Sodium	Halite (NaCl)
	Plagioclase ($Ca_{0.5}Na_{0.5}Al_{1.5}Si_{2.5}O_8$)
Silica	K-Feldspar ($KAlSi_3O_8$)
	K-Mica ($KAl_3Si_3O_{10}(OH)_2$
	Plagioclase ($Ca_{0.5}Na_{0.5}Al_{1.5}Si_{2.5}O_8$)
Sulfate	Sulfides listed below.
Arsenic	Arsenopyrite (FeAsS)
Barium	Barite ($BaSO_4$)
Fluoride	Fluorite (CaF_2)
Iron	Pyrite (FeS_2)
Lead	Galena (PbS)
Manganese	Rhodochrosite ($MnCO_3$)
Mercury	Cinnabar (HgS)
Zinc	Sphalerite (ZnS)

Since calcite and dolomite constitute a large fraction of the host rocks at the Cortez deposit, they were specified as reversible reactions in PHREEQE (allowed to attain equilibrium). The pH, Eh, and partial

pressures of O_2 and CO_2 were taken from the earlier pit water speciation models of the Cortez and Universal Gas pit waters, which indicated that the pCO_2 is generally in the range of $10^{-2.67}$, slighter higher than atmospheric.

A portion of the PHREEQE output file CZRX01PH.OUT showing the final concentration of the pit water is shown in Table 7-14.

Table 7-14: Concentration of pit water after PHREEQE mass transfer model (CZRX01PH.OUT).

ELEMENT	MOLALITY	LOG MOLALITY	MG/L
Ca	1.917060D-03	-2.7174	76.8
Mg	1.631618D-03	-2.7874	39.7
Na	2.985860D-03	-2.5249	68.6
K	1.279370D-04	-3.8930	5.0
Fe	1.244668D-03	-2.9049	69.5
Mn	1.438594D-06	-5.8421	0.079
Al	1.603950D-04	-3.7948	4.3
Ba	4.391000D-07	-6.3574	0.0603
Si	1.652966D-03	-2.7817	99.3
Cl	4.010174D-03	-2.3968	142.2
bicarb. alk.			132.6
S	2.862955D-03	-2.5432	275.8
N	5.001722D-05	-4.3009	0.7
B	1.018007D-05	-4.9922	0.11
F	1.263552D-04	-3.8984	2.4
As	5.107694D-07	-6.2918	0.038
Zn	3.366368D-07	-6.4728	0.022
Pb	2.080000D-08	-7.6819	0.0043
Hg	1.127481D-08	-7.9479	0.0023
pH		7.6893	
pe		2.4745	
IONIC STRENGTH		.0168	
TEMPERATURE		20.5000	
ELECTRICAL BALANCE		1.1064D-04	

Examination of this output file reveals some discrepancies with the actual Cortez pit water, and even some unrealistic numbers. Most notable, the aluminum concentration is much higher than the actual Cortez pit water, and even much higher than is possible at neutral pH. The calcium, magnesium, iron, and sulfate concentrations are also higher than actual.

The reason for the discrepancies is that PHREEQE cannot remove ions from solution via mineral precipitation unless the minerals are specified in reversible reactions. The BALANCE model found several phases that would be expected to precipitate in the Cortez pit water

mass transfer model, but PHREEQE cannot simulate the reactions.

Precipitation: To account for precipitation reactions, the next step is to run the PHREEQE output through MINTEQA2, and model the changes that occur to the solution after minerals are removed by precipitation. Table 7-15 is a portion of the output file for the precipitation model (CZPR01MT.OUT).

Table 7-15: Results of Cortez pit water precipitation simulation in MINTEQA2 (CZPR01MT.OUT).

NAME	DISSOLVED MOL/KG	DISSOLVED PERCENT	SORBED MOL/KG	SORBED PERCENT	PRECIPITATED MOL/KG	PRECIPITATED PERCENT	MG/L
NO2-1	1.950E-18	100.0	0.000E-01	0.0	0.000E-01	0.0	<<
CO3-2	2.232E-03	51.4	0.000E-01	0.0	2.113E-03	48.6	134
Hg2+2	5.760E-09	100.0	0.000E-01	0.0	0.000E-01	0.0	.0023
Pb+2	2.077E-08	100.0	0.000E-01	0.0	0.000E-01	0.0	.0043
H3AsO4	2.151E-07	42.3	0.000E-01	0.0	2.928E-07	57.7	.0161
Na+1	2.987E-03	100.0	0.000E-01	0.0	0.000E-01	0.0	68.7
K+1	1.280E-04	100.0	0.000E-01	0.0	0.000E-01	0.0	5.0
Zn+2	3.369E-07	100.0	0.000E-01	0.0	0.000E-01	0.0	.022
Mn+2	1.439E-06	100.0	0.000E-01	0.0	0.000E-01	0.0	.079
F-1	1.265E-04	100.0	0.000E-01	0.0	0.000E-01	0.0	2.4
SO4-2	2.874E-03	100.0	0.000E-01	0.0	0.000E-01	0.0	276
H3BO3	1.019E-05	100.0	0.000E-01	0.0	0.000E-01	0.0	.11
Cl-1	4.015E-03	100.0	0.000E-01	0.0	0.000E-01	0.0	142.3
H3AsO3	5.039E-16	100.0	0.000E-01	0.0	0.000E-01	0.0	<<
Al+3	7.304E-09	0.0	0.000E-01	0.0	1.595E-04	100.0	1.97E-04
Ba+2	2.655E-10	0.1	0.000E-01	0.0	4.392E-07	99.9	3.65E-05
Fe+2	7.955E-16	100.0	0.000E-01	0.0	0.000E-01	0.0	4.44E-14
NO3-1	2.055E-26	100.0	0.000E-01	0.0	0.000E-01	0.0	<<
NH4+1	1.130E-05	100.0	0.000E-01	0.0	0.000E-01	0.0	.2
Hg(OH)2	1.653E-16	100.0	0.000E-01	0.0	0.000E-01	0.0	3.88E-11
Mn+3	3.338E-29	100.0	0.000E-01	0.0	0.000E-01	0.0	1.83E-24
Fe+3	1.153E-15	0.0	0.000E-01	0.0	1.246E-03	100.0	6.44E-11
H4SiO4	1.252E-06	0.1	0.000E-01	0.0	1.650E-03	99.9	.0752
Mg+2	6.665E-04	40.8	0.000E-01	0.0	9.680E-04	59.2	16.2
Ca+2	6.978E-04	36.4	0.000E-01	0.0	1.220E-03	63.6	27.97

Sum of CATIONS = 5.344E-03 Sum of ANIONS 1.160E-02
PERCENT DIFFERENCE = 36.91 (ANIONS - CATIONS)/(ANIONS + CATIONS)

NON-CARBONATE ALKALINITY = 9.621E-07
EQUILIBRIUM IONIC STRENGTH (m) = .01222
EQUILIBRIUM pH = 8.067
EQUILIBRIUM pe = 2.474 or Eh = 144.17 mv

Table 7-15 depicts a more realistic scenario, and is starting to approach the measured Cortez pit water chemistry. The dissolved concentrations of several species have been reduced by the precipitation of various mineral phases.

The dissolved aluminum concentration is back down to an acceptable level for neutral pH waters ($\approx 10^{-8}$ mol/kg.), due to the precipitation of aluminum phases. Calcium and magnesium concentrations are approaching

the measured concentrations as well, having been slightly reduced through precipitation of carbonate phases.

However, the MINTEQA2 model has precipitated other minerals that have reduced the levels of several important components well below their measured concentrations in the pit water. The ions most affected are iron, silica, barium, and arsenic. Iron has been almost entirely removed from solution by the precipitation of hematite. Barium and arsenic have been reduced through precipitation of $Ba(AsO_4)_2$, and dissolved silica has been reduced through precipitation of Ca-nontronite. Furthermore, sulfate is about three times higher than the actual concentration, and chloride is almost an order of magnitude higher.

The model clearly needs refining. Before proceeding with the adsorption model, the possible solubility controls for these components need to be evaluated. This marks the beginning of the calibration loop for the modeling exercise.

Calibration: Referring back to Table 7-6, the Cortez pit water speciation model (CZSP02W4.OUT) showed oversaturation with several mineral phases, including carbonates, silicates, and iron oxides (shown again in Table 7-16). If the water analysis is run through MINTEQA2,

Table 7-16: Cortez pit water speciation, output file CZSP01W4.OUT

Phase	Log IAP/KT	Phase	Log IAP/KT
Aragonite	.449	Barite	.168
Calcite	.596	Chalcedony	.357
Cristobalite	.401	Dolomite (d)	.516
Dolomite (c)	1.084	Fe3(OH)8	3.266
FeOH)2.7Cl.3	6.487	Ferrihydrite	1.939
Goethite	7.830	Greenalite	2.182
Hematite	17.321	Maghemite	7.273
Magnetite	19.185	Quartz	.800
Talc	3.473	Tremolite	6.279
ZnSiO3	1.286		

allowing precipitation to remove the components of oversaturated

minerals, the concentrations of some ions in the simulated final solution drop several orders of magnitude below actual concentrations. Due to kinetics and other factors (incongruent dissolution/precipitation behavior, ambiguous K_{sp} data), the possibility of all of these mineralsactually precipitating in the pit water is remote. This leads to the conclusion that the most oversaturated phases are not likely controlling the solubilities and concentrations of the ions. For trace metals, the most likely control is adsorption.

At this point in model interpretation, the modeler must once again draw on geochemical common sense. An understanding of geological and geochemical processes under earth's surface conditions helps eliminate implausible results and isolate the more probable scenario(s). Some of the phases shown in Table 7-16 can be eliminated from the model because they do not exhibit reversible dissolution/precipitation behavior under low temperature conditions. Examples are cristobalite, hematite, magnetite, talc, quartz, and tremolite.

To account for the solubility and adsorption controls throughout the inverse and forward model exercise, the model must be calibrated by working backwards from the final condition. By systematically excluding the oversaturated phases in MINTEQA2 precipitation models, the minerals most likely controlling the concentrations of dissolved iron, silica, arsenic, and barium in solution can be determined. This exercise will also determine the iron partitioning that occurs between the solid and aqueous phases for later adsorption models. Once the precipitation calibration loops are complete, then the partitioning of trace metals believed controlled by adsorption can be calibrated (As, Hg, Pg, Zn).

File CZPR10MT.OUT is the output file for the calibration run used to determine the iron partitioning. The file shows the mass of iron precipitated and the resulting iron in solution. The mass of amorphous ferric hydroxide precipitated (as FeOOH), to result in a dissolved iron

in Table 7-18. The first adsorption iteration has removed significant percentages of As, Hg, Pb, and Zn, as well as minor amounts of Ba, Ca, and sulfate. As expected, the final concentrations of the trace metals have been reduced below their actual concentrations in the pit water, necessitating a calibration loop similar to that used for precipitation.

Table 7-18: Output file showing equilibrium distribution of Cortez pit water after adsorption model (CZAD01MT.OUT).

IDX	NAME	DISSOLVED MOL/KG	DISSOLVED PERCENT	SORBED MOL/KG	SORBED PERCENT	PRECIPITATED MOL/KG	PRECIPITATED PERCENT
732	SO4-2	2.862E-03	100.0	2.870E-07	0.0	3.520E-07	0.0
500	Na+1	2.986E-03	100.0	0.000E-01	0.0	0.000E-01	0.0
950	Zn+2	3.544E-08	10.5	3.012E-07	89.5	0.000E-01	0.0
180	Cl-1	4.010E-03	100.0	0.000E-01	0.0	0.000E-01	0.0
270	F-1	1.264E-04	100.0	0.000E-01	0.0	0.000E-01	0.0
280	Fe+2	5.863E-07	0.0	0.000E-01	0.0	1.243E-03	100.0
60	H3AsO3	6.648E-18	16.4	3.400E-17	83.6	0.000E-01	0.0
360	Hg2+2	5.635E-09	100.0	0.000E-01	0.0	0.000E-01	0.0
410	K+1	1.279E-04	100.0	0.000E-01	0.0	0.000E-01	0.0
600	Pb+2	3.304E-11	0.2	2.077E-08	99.8	0.000E-01	0.0
470	Mn+2	1.439E-06	100.0	0.000E-01	0.0	0.000E-01	0.0
150	Ca+2	7.235E-04	37.7	1.738E-06	0.1	1.192E-03	62.2
2	H2O	3.952E-06	113.6	-4.725E-07	-13.6	0.000E-01	0.0
61	H3AsO4	3.362E-09	0.7	5.074E-07	99.3	0.000E-01	0.0
330	H+1	2.194E-03	100.1	-3.166E-06	-0.1	0.000E-01	0.0
281	Fe+3	9.277E-07	100.0	0.000E-01	0.0	0.000E-01	0.0
1	E-1	1.127E-08	100.0	0.000E-01	0.0	0.000E-01	0.0
471	Mn+3	3.947E-29	100.0	0.000E-01	0.0	0.000E-01	0.0
361	Hg(OH)2	1.835E-16	60.0	1.225E-16	40.0	0.000E-01	0.0
460	Mg+2	1.173E-03	71.9	0.000E-01	0.0	4.593E-04	28.1
770	H4SiO4	8.912E-05	5.4	0.000E-01	0.0	1.564E-03	94.6
100	Ba+2	8.686E-08	19.8	2.542E-10	0.1	3.520E-07	80.2
140	CO3-2	2.189E-03	68.5	0.000E-01	0.0	1.008E-03	31.5

Charge Balance: SPECIATED

Sum of CATIONS = 6.253E-03 Sum of ANIONS 1.138E-02
PERCENT DIFFERENCE = 2.909E+01 (ANIONS - CATIONS)/(ANIONS + CATIONS)
EQUILIBRIUM IONIC STRENGTH (m) = 1.294E-02
EQUILIBRIUM pH = 8.067
EQUILIBRIUM pe = 2.520 or Eh = 146.67 mv

******* DIFFUSE LAYER ADSORPTION MODEL ********

**** Parameters For Adsorbent Number 1 ****

Electrostatic Variables: psi0 = 0.003137 sig0 = 0.000831
psib = 0.000000 sigb = 0.000000
psid = 0.000000 sigd = 0.000000
Adsorbent Concentration (g/l): 0.074
Specific Surface Area (sq. meters/g): 600.00

Calibration of trace metal adsorption is slightly less time consuming than precipitation calibration. To achieve the correct trace metal partitioning, the bulk concentrations are simply increased until the final dissolved concentration is obtained. The results of the adsorption calibrations are shown in file CZAD02MT.OUT, and are

summarized in Table 7-19. Table 7-19 reveals that the final concentrations of each trace metal ion is reduced by approximately 1-2

Table 7-19: Adsorption Calibrations (MINTEQA2)

	Bulk log mol	Final log mol	mg/l
As	-5.22	-5.81	0.116
Hg	-7.77	-8.07	0.0017
Hg(OH)2		-15.58	5.27E-11
Hg2+2		-8.07	0.0009
Pb	-5.79	-7.74	0.0038
Zn	-6.47	-7.55	0.0018

orders of magnitude from the initial bulk concentration. It must also be noted in the results of CZAD02MT.OUT that mercury cannot be calibrated by this procedure, because the only Hg species for which the MINTEQA2 diffuse layer adsorption model has complexation constants is $Hg(OH)_2$. The most common mercury species in the pit water, according to the MINTEQA2 speciation model (CZSP01MT.OUT), is $Hg_{(aq)}$ by several orders of magnitude. Therefore, the most abundant mercury species will not even be considered by the adsorption model.

All the information needed to run a complete forward model for pit water chemical evolution is now available.

Second iteration: The first model iteration demonstrates that, for modeling purposes, the existing Cortez pit water chemistry is not necessarily the "final water." Thermodynamic constraints and partitioning from solubility and adsorptive controls necessitate an iterative calibration process to fine tune the mass transfer results. To continue the calibration, results from CZAD02MT.OUT (Table 7-19) must be entered again into BALANCE to determine the mass transfer in the context of the newly determined solubility and adsorption controls.

In the second iteration, BALANCE found 1820 possible combinations

concentration in solution of 0.134 mg/l, is 5.201E-04 mol/kg Fe, or 0.0735 g/l FeOOH. This mass of precipitated iron was used as input to the adsorption models to define the amount of sorbent available in solution.

Accordingly, file CZPR18MT.OUT is the output file for the calibration of silica partitioning. The barium partitioning was determined simply by excluding the solid $Ba(AsO_4)_2$, and allowing solubility control by barite. Consequently, arsenic control was also removed by the exclusion of $Ba(AsO_4)_2$.

Table 7-17 shows the results of the precipitation calibrations. To end up with 0.134 mg/l ($10^{-5.62}$ mols/kg) dissolved Fe in solution, a mass of $10^{-3.28}$ mols/kg Fe must be dissolved from the pit wall into solution, combined with solubility control as specified by the exclusion option. For a final concentration of 34.43 mg/l SiO_2 ($10^{-3.24}$ mol/kg.), a mass of $10^{-2.32}$ mol/kg must dissolve. For a final Ba concentration of 0.0603 mg/l ($10^{-6.36}$ mol/kg), a mass transfer of $10^{-4.47}$ mol/kg is required.

Calibration of the Cortez pit water model indicates that the bulk concentration of dissolved iron is approximately 2 orders of magnitude higher ($10^{-3.28}$ mols/kg) than the final concentration of $10^{-5.62}$ mols/kg. Eleven iron minerals were excluded in the MINTEQA2 model to determine this aspect of iron solubility control (CZPR10MT.OUT). Exclusion of six silica phases revealed that the silica bulk concentration is approximately one order of magnitude higher than the final concentration of $10^{-3.24}$ mols/kg.

Calibration of the only phase controlling the modeled zinc concentration ($ZnSiO_3$) resulted in a bulk concentration of over 200 mg/l to result in 0.002 mg/l in final pit water, over 5 orders of magnitude difference. This result suggests that zinc concentration is less likely controlled by mineral solubility than adsorption onto solids.

As a time saving measure, most of the calibration runs were

performed independently of the other components. In some cases, the

Table 7-17: Precipitation Calibrations (MINTEQA2)

	Bulk log mol	Final log mol	mg/l	Excluded
Fe	-3.28	-5.62	0.135	Hematite FeOH)2.7Cl.3 Magnetite Goethite Lepidocrocite Mag-ferrite Maghemite Ferrihydrite Fe3(OH)8 Jarosite K Siderite
SiO_2	-2.32	-3.23	34.78	Quartz Cristobalite Chalcedony SiO2 (a,gl) SiO2 (a,pt) ZnSiO3
H_4SiO_4	-2.32	-3.23	55.63	
Ba	-4.47	-6.36	0.0603	Ba(AsO4)2

final run gave slightly different results when included with all other dependent components. For example the iron precipitation calibration, which determined that 5.201E-04 mol/kg Fe mass transfer resulted in 0.0735 g/l FeOOH precipitated and 0.134 mg/l dissolved Fe in the final solution, gave slightly different results when all precipitation and adsorption models were included (see CZAD01MT.OUT). To completely calibrate the model, an iterative loop would be necessary similar to those used for each individual component.

Adsorption: The next step is to determine the trace metal partitioning as a result of adsorption onto mineral solids. The only solid considered as an adsorbent was amorphous ferric hydroxide, for which an abundance of adsorption data and constants are available. The input parameters for amorphous ferric hydroxide in the diffuse layer adsorption model are (Dzombak and Morel, 1990):

Concentration of adsorbent in solid (g/l):	0.074 g/l
Specific surface area (m^2/g):	600
Site concentration (m/l or m/g):	8.953E-05 (site 1) 3.581E-03 (site 2)
Surface potential (volts):	Defined by MINTEQA2 diffuse layer adsorption model

The first adsorption model, before any calibration adjustments, is shown

of phases that could account for the water evolution, and 18 that satisfied the constraints specified. The model selected is marked by an (*) in Appendix B, and is shown in Table 7-20.

Table 7-20: Results of BALANCE model in second iteration.

Plagioclase	+	F	3057.6800
Fluorite	+	F	50.0130
≡SOH:Zn		F	- .0154
Galena	+	F	1.6337
Cinnabar	+	F	.0070
Arsenopy	+	F	5.9564
CO_2 gas		F	3609.4638
NaCl	+	F	108.0000
Pyrite	+	F	512.0656
Barite	+	F	33.6800
K-Feldsp	+	F	171.3500
Calcite		F	-1593.7647
Gypsum			-511.5883
Kaolinite	-		-2378.9350
Rhodochr			-1.4091
Dolomite	+		386.7400

These results were again run through PHREEQE in the second iteration, to produce the bulk water chemistry before precipitation and adsorption controls were modeled. These results are shown in Table 7-21 (file CZRX02PH.OUT).

Note once again some minor discrepancies involving ions predicted to precipitate as mineral phases, such as calcium, magnesium, silica, and sulfate. These can be calibrated further in PHREEQE and MINTEQA2 to more closely approximate the bulk concentrations arrived at in the prior MINTEQA2 iteration.

The results of the second PHREEQE model are run through MINTEQA2, resulting in the output file (CZAD02MT.OUT), a portion of which is shown in Table 7-22. A comparison of the model results and the actual Cortez pit water chemistry is shown in Table 7-23. Examination of these numbers shows that the measured Cortez pit water chemistry still has not been achieved. Of special interest is arsenic, for which the model

predicts to exceed the actual concentration by a factor of about three (and in violation of federal primary drinking water standards). A final calibration iteration was performed to bring arsenic in line with the actual concentration in the Cortez pit water (CZAD03MT.OUT). Reduction of the bulk arsenic concentration (from 6.09E-06 molal) to 3.3E-06 molal

Table 7-21: Concentration of pit water after PHREEQE mass transfer model; second iteration (CZRX02PH.OUT).

ELEMENT	MOLALITY	LOG MOLALITY	MG/L
Ca	2.170879D-03	-2.6634	87.0
Mg	1.836022D-03	-2.7361	45.3
Na	2.985845D-03	-2.5249	68.6
K	1.279370D-04	-3.8930	5.0
Fe	5.241170D-04	-3.2806	29.27
Mn	1.438594D-06	-5.8421	.0079
Al	4.586550D-03	-2.3385	123.8
Ba	3.368000D-05	-4.4726	4.6
Si	9.029891D-03	-2.0443	542.6
Cl	2.534774D-03	-2.5961	89.9
C	1.918798D-03	-2.7170	
bicarbonate alkalinity			117.1
S	1.456713D-03	-2.8366	139.8
N	5.001722D-05	-4.3009	3.1
B	1.018007D-05	-4.9922	.11
F	1.263552D-04	-3.8984	2.4
As	6.089929D-06	-5.2154	.4563
Zn	3.366368D-07	-6.4728	.022
Pb	1.634000D-06	-5.7867	.3386
Hg	1.697481D-08	-7.7702	.0034

PH = 7.6458
PE = 2.5180
IONIC STRENGTH = .0164
TEMPERATURE = 20.5000
ELECTRICAL BALANCE = 1.1064D-04

brought the dissolved arsenic concentration in the final pit water down to 0.0154 mg/l. The effect on other ions in solution was minimal, and only noticeable for those metal cations which compete with arsenic for adsorption sites.

Tables 7-23 and 7-24 show that most other ions are within their actual concentrations by a factor of two or three. This may be considered acceptable margin of error for major ions. These concentrations could be fine-tuned through continued calibration, a process that may continue for several iterations until the correct mass

transfer values, solubility controls, and adsorption controls are identified. The third iteration is as far as this study was taken. The output files for all of the forward simulations that are on datadisk are listed in Table 7-24.

Table 7-22: Portion of output file showing equilibrium distribution of Cortez pit water after adsorption model, second iteration (CZAD02MT.OUT).

NAME	DISSOLVED MOL/KG	DISSOLVED PERCENT	SORBED MOL/KG	SORBED PERCENT	PRECIPITATED MOL/KG	PRECIPITATED PERCENT
SO4-2	1.423E-03	97.7	1.131E-08	0.0	3.354E-05	2.3
Zn+2	2.798E-08	8.3	3.086E-07	91.7	0.000E-01	0.0
Mn+2	1.439E-06	100.0	0.000E-01	0.0	0.000E-01	0.0
Cl-1	2.535E-03	100.0	0.000E-01	0.0	0.000E-01	0.0
F-1	1.264E-04	100.0	0.000E-01	0.0	0.000E-01	0.0
Fe+2	7.601E-08	0.0	0.000E-01	0.0	5.239E-04	100.0
H3AsO3	3.377E-15	23.1	1.126E-14	76.9	0.000E-01	0.0
Hg2+2	8.485E-09	100.0	0.000E-01	0.0	0.000E-01	0.0
K+1	1.279E-04	100.0	0.000E-01	0.0	0.000E-01	0.0
Pb+2	1.800E-08	1.1	1.616E-06	98.9	0.000E-01	0.0
Ca+2	6.238E-04	28.7	2.689E-06	0.1	1.543E-03	71.1
Na+1	2.384E-03	79.8	0.000E-01	0.0	6.018E-04	20.2
H3AsO4	1.550E-06	25.5	4.540E-06	74.5	0.000E-01	0.0
Fe+3	1.364E-07	100.0	0.000E-01	0.0	0.000E-01	0.0
Hg(OH)2	2.661E-16	88.3	3.524E-17	11.7	0.000E-01	0.0
Mn+3	3.842E-29	100.0	0.000E-01	0.0	0.000E-01	0.0
Ba+2	1.355E-07	0.4	1.659E-10	0.0	3.354E-05	99.6
Mg+2	1.063E-05	0.6	0.000E-01	0.0	1.825E-03	99.4
H4SiO4	1.547E-03	17.1	0.000E-01	0.0	7.482E-03	82.9
CO3-2	2.118E-03	72.3	0.000E-01	0.0	8.133E-04	27.7

Charge Balance: SPECIATED

Sum of CATIONS = 3.622E-03 Sum of ANIONS 7.473E-03
PERCENT DIFFERENCE = 3.470E+01 (ANIONS - CATIONS)/(ANIONS + CATIONS)
EQUILIBRIUM IONIC STRENGTH (m) = 7.442E-03
EQUILIBRIUM pH = 8.067
EQUILIBRIUM pe = 2.520 or Eh = 146.67 mv

******* DIFFUSE LAYER ADSORPTION MODEL ********

**** Parameters For Adsorbent Number 1 ****
Electrostatic Variables: psi0 = -.027403 sig0 = -.005778
psib = 0.000000 sigb = 0.000000
psid = 0.000000 sigd = 0.000000
Adsorbent Concentration (g/l): 0.074
Specific Surface Area (sq. meters/g): 600.00

This exercise has hopefully demonstrated that the calibration procedure can help the model converge to the desired result, but may take some time.

Table 7-23: Comparison of adsorption model (second iteration) and actual Cortez pit water chemistry.

	Model	Actual
SO4-2	136.7	90.2
Zn+2	0.0018	0.002
Total Mn	0.079	0.0017
Cl-1	89.9	24.4
F-1	2.4	2.4
Total Fe	0.012	0.134
Total As	0.116	0.0383
Total Hg	0.0017	0.0004
K+1	5.0	11.7
Pb+2	0.0037	0.0043
Ca+2	25.0	45.4
Na+1	54.8	68.63
Ba+2	0.019	0.0603
Mg+2	0.26	18.1
SiO2	92.9	34.43
bicarb. alk.	129.2	282.3
pH	8.07	8.07

Summary

The overall pit water modeling exercise as performed in this study can be outlined as follows:

1) Compile data for pit and groundwater geochemistry.

2) First iteration; determine mass transfer with BALANCE.

3) Apply BALANCE mass transfer results in PHREEQE to generate a bulk chemistry of pit water.

4) Apply PHREEQE results to MINTEQA2 to determine changes in solution chemistry from mineral precipitation.

5) Evaluate discrepancies.

6) Calibrate the mass transfer model with MINTEQA2 to determine solubility control of oversaturated phases, and the mass of amorphous ferric hydroxide precipitated for adsorption model.

7) Calibrate mass transfer to determine adsorption partitioning and control.

6) Second iteration; apply results after precipitation/adsorption models in BALANCE to determine mass transfer. New "final water" is the bulk chemistry of first iteration.

7) Apply BALANCE results in PHREEQE.

8) Apply PHREEQE results in MINTEQA2, for final determination of precipitation/adsorption model.

Table 7-24: File names and contents of forward model output files.

Cortez pit water precipitation simulations

CZPR01PH.IN	PHREEQE input file	CZPR18PH.IN	PHREEQE input file
CZPR01PH.OUT	PHREEQE output file	CZPR18PH.OUT	PHREEQE output file
CZPR01PH.IN	PHREEQE input file		
CZPR01PH.OUT	PHREEQE output file		

Cortez pit water adsorption simulations

CZAD01MT.IN	MINTEQA2 input file	CZAD03MT.IN	MINTEQA2 input file
CZAD01MT.OUT	MINTEQA2 output file	CZAD03MT.OUT	MINTEQA2 output file
CZAD02MT.IN	PHREEQE input file		
CZAD02MT.OUT	PHREEQE output file		

Sensitivity Analyses

A set of sensitivity analyses was performed on two subsets of the pit wall dissolution models. The first simulation modeled the effects of variable pyrite dissolution from the pit wall in the presence of different host lithologies. The second simulation modeled the progression of anoxia in the pit water.

Pyrite dissolution: The mass of pyrite dissolved from the pit wall, and hence the mass of iron and sulfate dissolved into the pit water, was varied in three different simulations depicting different host lithologies. The mass of pyrite dissolved into the pit water was increased incrementally in ten steps from 0.0 to 0.1 moles/kilogram, as shown in Table 7-25. In each model, pCO_2 and pO_2 were held constant at the levels determined in the earlier pit water speciation models.

In the "carbonate" scenario, calcite and dolomite were defined as reversible reactions, a situation already proven as likely in prior discussions. In the "granite" scenario, reversible reactions were specified for albite, anorthite, microcline, and amorphous silica, four phases that might appear in a variety of igneous rocks, including granite. In the "shale" scenario, only amorphous silica was specified

as reversible. The results are shown in Table 7-25, and Figure 7-2, and the output files are:

PIT-CO3.OUT	Carbonate lithology
PIT-SIL.OUT	Granite lithology
PIT-SH.OUT	Shale lithology

Figure 7-2 shows that the carbonate system remains buffered at neutral pH throughout the modeled range of pyrite dissolution. The granite system shows a drop at $10^{-3.0}$ moles pyrite dissolved, but the rate of decline decreases and the system remains generally buffered at a pH around 5.0. The shale system, with no buffering capacity available, shows a dramatic pH drop at $10^{-3.0}$ moles pyrite dissolved, and continues to decline to a pH less than 2.0, a scenario seen in some serious acid mine drainage environments.

Table 7-25: Evolution of pH as a function of pyrite dissolved and host rock (Reversible reactions defined for each host: Shale; quartz. Carbonate; calcite, dolomite. Granite; microcline, albite, anorthite, quartz).

Pyrite dissolved (log mol)	Shale host	Carbonate host	Granite host
none	7.67	7.67	7.67
-5.0	7.67	7.75	7.66
-4.5	7.66	7.75	7.65
-4.0	7.61	7.75	7.61
-3.5	7.46	7.73	7.46
-3.0	3.90	7.70	5.82
-2.5	2.51	7.63	5.35
-2.0	2.00	7.53	5.25
-1.5	1.59	7.41	5.18
-1.0	1.22	7.25	5.09

The "granite" scenario is unrealistic because of the low probability of the pit water reaching equilibrium with any aluminosilicate phases. Speciation of the Liberty pit water shows equilibrium with a few silica phases, but no aluminosilicates. The result is insufficient buffering capacity, and development of acidic

waters with high concentrations of metals.

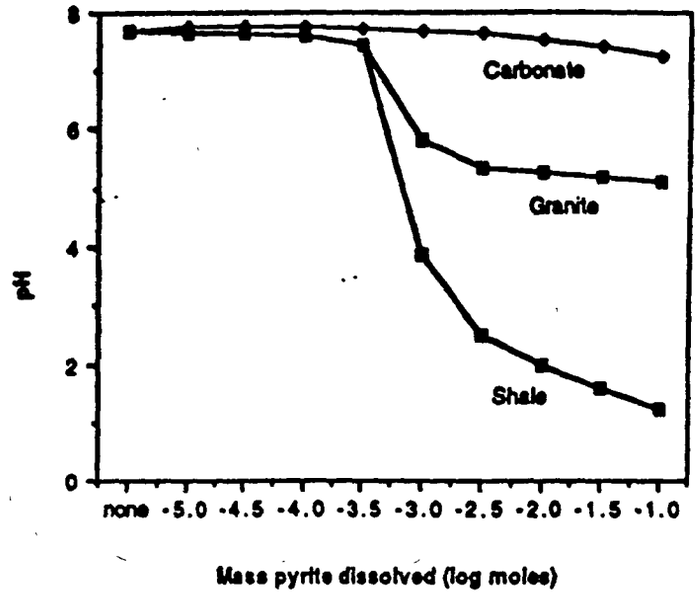

Figure 7-2: Evolution of pH as a function of pyrite dissolved and host rock (Reversible reactions defined for each host: Carbonate - calcite, dolomite; Granite - microcline, albite, anorthite, quartz; Shale - quartz).

From Figure 7-2, one can infer some interesting implications regarding possible scenarios for future pit waters in Nevada. Carbonate hosted deposits, and even those with a minor siliceous component such as Cortez, may remain buffered throughout their evolution. However, pit waters in more siliceous host lithologies may develop acidic conditions similar to those depicted in Figure 7-2. Since the granite scenario depicted here represents the best possible case (i.e. equilibrium with aluminosilicate minerals), a more likely outcome might be the development of pH somewhere between the "granite" and "shale" scenarios.

As stated earlier, over one-fourth of Nevada's precious metal deposits (approximately 30) are hosted in igneous rocks. Of the three that are currently known to be water-filled, two (Ruth and Liberty) are acid mine drainage situations. The potential for the remaining 27

igneous-hosted deposits, as well as sediment-hosted deposits with no significant carbonate component, to develop similar conditions might be a subject where future research should be emphasized.

Anoxia progression: In the second sensitivity analysis, anoxia was simulated by removing oxygen from the system through incremental reduction of pO_2 (partial pressure of oxygen) in the water. The results are shown in Table 7-26, and can be found on datadisk 2 (CZRX03PH.OUT).

Table 7-26 shows that if the system goes anoxic to the point at which pe = -5.53, approximately 2.553E-04 moles of solid $Fe(OH)_3$ (0.0273 g/l) will dissolve, thus increasing the dissolved Fe concentration to 3.708E-04 moles/kg. (21 mg/l). The value of 2.553E-04 moles of solid $Fe(OH)_3$ dissolved represents approximately one-third of the total amorphous ferric hydroxide that was precipitated in the MINTEQA2 model. If that much $Fe(OH)_3$ actually dissolves, up to one-third of the species that were adsorbed on the $Fe(OH)_3$ surface (i.e., trace metals) could be released back into solution, resulting in a "blowout" of trace metals to the environment.

Table 7-26: Simulated anoxia in Cortez pit lake. Datadisk 2 file CZRX03PH.OUT.

pO_2	pe	pH	Dissolved Fe (total)	$Fe(OH)_3$ Mass transfer
-45	1.87	8.07	3.082E-08	-1.8128E-07
-50	0.62	8.07	3.293E-07	2.985E-07
-55	-0.673	8.11	4.698E-06	4.369E-06
-60	-2.153	8.34	3.165E-05	2.695E-05
-65	-3.80	8.74	1.155E-04	8.388E-05
-70	-5.53	9.22	3.708E-04	2.553E-04

This scenario is highly improbable however, because a decline in pe to a level as low as -5.53 is unlikely without other redox processes intervening. As anoxia progresses, sulfate reduction should begin at about pe = -3, causing precipitation of sulfides and generation of

alkalinity (Drever, 1988), which would preclude dissolution of iron hydroxides and release of trace metals. Only in the absence of organic matter (an unlikely scenario) would the pe drop unimpeded to levels as low as -5.53. A more plausible scenario, and the situation which presents the greatest concern in pit water chemistry at neutral pH, involves the situation in which the pe drops to the range 0 to -3.0. This would cause the system to move from the stability field of ferric iron to that of ferrous iron (Figure 5-7), with possible destabilization of ferric hydroxides and a subsequent increase in total dissolved iron concentration.

8. CONCLUSIONS

* Pit water chemical modeling is difficult and influenced by many interrelated variables.

* A good understanding of system geology is required for each step in the model, from speciation through to inverse and forward models. This information should be obtained from a combination of chemical, XRD, and petrographic analyses of drill core and pit wallrock.

* A good understanding of geochemical and geologic process is necessary for successful interpretation of models and elimination of the implausible. There is no substitute for geochemical "common sense."

* Precipitation and adsorption will be important process removing ions from solution, depending on system Eh and pH.

* The partitioning from solubility and adsorptive controls must be considered in mass transfer models.

* Rate-independent dissolution models will generate unrealistic mass transfer calculations. The likely result will be an underestimation of dissolution of important minerals such as pyrite.

* Rate-dependent dissolution models will produce the most realistic mass transfer results. Site-specific experimental data on reaction kinetics are required for model input.

* Speciation modeling is a vital part of the overall pit water modeling process (MINTEQA2, WATEQ4F), by helping to guide interpretation of inverse and forward modeling results.

* This study has answered the question posed at the beginning of the thesis, by proving that a combination of inverse and forward modeling methods using BALANCE, PHREEQE (expanded), and MINTEQA2 is able to duplicate real world conditions within reasonable error.

* This model can be easily applied to future pit waters after the incorporation of experimental kinetic data.

9. RECOMMENDATIONS

This study has shown that the aqueous geochemistry of an existing pit lake can be reasonably duplicated through a combination of inverse and forward modeling methods. However, predicting the future water chemistry for a pit that does not even exist will not have the luxury of an inverse model for the particular site. The results of an inverse model from an existing site, such as the Cortez pit, may not be applicable to other locations because many critical variables will differ greatly among mines. Many factors might be similar, such as host lithology, mineralogy, and local evaporation, but not likely identical.

The question remains, can the model developed in this study be applied to future pit water modeling situations? I believe the answer to this is yes, but proof of that lies in further study, such as laboratory experiments involving site-specific pit wallrock. If the mass transfer predicted by the model can be duplicated in laboratory experiments that determine the dissolution of minerals from the actual site wallrock, then the model should be applicable to other sites using the results for similar experiments on the local wall rock.

The forward modeling techniques used in this study perform reasonably well for the Cortez pit water simulations, and the incorporation of site-specific mass transfer data, obtained from laboratory experiments, should give equally valid results for any site.

None of the computer codes applied in this study are specifically designed for the task of modeling pit water chemistry. MINTEQA2 comes the closest with its large trace metal database and adsorption modeling capability. Unfortunately, MINTEQA2 cannot model a system reaction path as PHREEQE can, so the two codes are best applied in tandem in the pit water simulation.

To produce the most accurate and valid model possible, the

following procedure is recommended:

1) Obtain a high quality water analysis for the upgradient groundwater, and run through speciation model to ascertain the speciation and saturation state of the water.

2) Determine amounts and proportions of all minerals in the pit wallrock. Location and geometry of ultimate pit should be available from mine plans. The best source for this data will be chemical analyses and/or XRD work performed on drill core samples.

3) Conduct laboratory experiments to determine mass transfer that occurs from interaction between the upgradient groundwater and the pit wall, under a variety of conditions (anoxic vs. oxic, closed vs. open).

4) Determine bulk chemistry of pit water by applying the mass transfer results obtained in the laboratory study (PHREEQE). A mass transfer of solid, from a known volume of water passed through a known mass of wallrock can be extrapolated to the entire pit lake system.

5) Determine the final pit lake chemistry by applying the precipitation and adsorption model (MINTEQA2).

Recommendations for Further Study

There are many components of the overall pit water modeling problem that are only partially understood, and for which existing models or data may be suspect. Until more is known about these aspects of the problem, pit water modeling will be at best a collection of educated guesses incorporating many assumptions. Each of these aspects is broad enough to be evaluated in a separate study, and better information regarding each would greatly improve future pit water models:

* Behavior of iron hydroxide (Eh/pH stability and control) and its ability to scavenge metals in pit lakes.

* Behavior of trace metals such as arsenic, cadmium, mercury, and zinc in pit lake environments. Are there any equilibrium solubility controls or is control entirely by adsorption?

* Thermodynamic data for aluminosilicates and potential solubility control in pit lakes.

* Reaction kinetics of sulfides and host rock minerals.

* Effect of armoring on acid generating vs. acid neutralizing minerals.

* Limnology; will pit lakes turnover or not?
* Role of organic matter and associated rates of microbial oxidation.

10. REFERENCES

ALLISON J.D., BROWN D.S., and NOVO-GRADAC K.J. (1991) MINTEQA2/PRODEFA2, A Geochemical Assessment Model for Environmental Systems: Version 3.0 User's Manual. U.S. Environmental Protection Agency, Environmental Research Laboratory, Athens, GA.

BACK, W. (1966) Hydrochemical Facies and Ground-Water Flow Patterns in Northern Part of Atlantic Coastal Plain. U.S. Geological Survey Professional Paper 498-A.

BACK, W. (1961) Techniques for mapping of hydrochemical facies. U.S. Geological Survey Professional Paper 424-D: 380-382.

BALISTRIERI L.S. and MURRAY J.W. (1982) The adsorption of Cu, Pb, Zn, and Cd on goethite from major ion seawater. *Geochimica et Cosmochimica Acta* 46, 1253-1265.

BALISTRIERI L.S. and MURRAY J.W. (1983) Metal-solid interactions in the marine environment: estimating apparent equilibrium binding constants. *Geochimica et Cosmochimica Acta* 47, 1091-1098.

BALL J.W., JENNE E.A., and NORDSTROM D.K. (1979) WATEQ2 - A COMPUTERIZED CHEMICAL MODEL FOR TRACE AND MAJOR ELEMENT SPECIATION AND MINERAL EQUILIBRIA OF NATURAL WATERS. In *Chemical Modeling in aqueous systems. Speciation, Sorption, Solubility, and Kinetics* (ed. E.A. Jenne). *ACS Symposium Series* 93, American Chemical Society, Washington D.C., p. 815-835.

BALL J.W., NORDSTROM D.K., JENNE E.A. (1980) ADDITIONAL AND REVISED THERMOCHEMICAL DATA AND COMPUTER CODE FOR WATEQ2 -- A COMPUTERIZED CHEMICAL MODEL FOR TRACE AND MAJOR ELEMENT SPECIATION AND MINERAL EQUILIBRIA OF NATURAL WATERS. U.S. Geological Survey Water Resources Investigations WRI 78-116.

BALL J.W., JENNE E.A., and CANTRELL M.W. (1981) WATEQ3 - A GEOCHEMICAL MODEL WITH URANIUM ADDED: U.S. Geological Survey Open-File Report 81-1183, 81 p.

BALL J.W., and NORDSTROM D.K. (1991) USER'S MANUAL FOR WATEQ4F, WITH REVISED THERMODYNAMIC DATA BASE AND TEST CASES FOR CALCULATING SPECIATION OF MAJOR, TRACE, AND REDOX ELEMENTS IN NATURAL WATERS. U.S. Geological Survey Open-File Report 91-183.

BAUM D., and KNOX M.L. (1992) In Butte, Montana, A is for Arsenic, Z is for Zinc. *Smithsonian* 23, no. 8, 46-56.

BELL P.E., MILLS A.L. and HERMAN J.S. (1987) Biogeochemical conditions favoring magnetite formation during anaerobic iron reduction. *Applied Environmental Microbiology* 53, 2610-2616.

BENCALA K.E., McKNIGHT D.M., and ZELLWEGER G.W. (1987) Evaluation of natural tracers in an acidic and metal-rich stream. *Water Resources Research* 23, 827-836.

BENJAMIN M.M. and LECKIE J.O. (1980) Adsorption of metals at oxide interfaces: Effects of the concentrations of adsorbate and competing metals. In *Contaminants and Sediments*, 2, R.A. Baker ed., 305-322, Ann Arbor Sci. Pub. Ann Arbor, Michigan.

BENJAMIN M.M. and LECKIE J.O. (1981) Multiple-site adsorption of Cd, Cu, Zn, and Pb on amorphous iron oxyhydroxide. *J. Colloid Interface Science* 83, 410-419

BERNER R.A. (1971) *Principles of Chemical Sedimentology*, McGraw-Hill, 240 pp.

BITTON G. and GERBA C.P. (1984) Groundwater Pollution Microbiology. Wiley Interscience 377 pp.

BLM (1991) U.S. Bureau of Land Management. Final Environmental Impact Statement, Betze Project.

BLOOMSTEIN E.I., MASSINGILL G.L., PARRATT R.L., and PELTONEN D.R. (1991) Discovery, Geology, and Mineralization of the Rabbit Creek Gold Deposit, Humboldt County, Nevada. In *Geology and Ore Deposits of the Great Basin* (Raines G.L., Lisle R.E., Schafer R.W., and Wilkinson W.H., eds.), Symposium Proceedings, Geological Society of Nevada, April 1-5, 1991, 821-844.

BOCKRIS J.O.M., and REDDY A.K.N., (1970) *Modern Electrochemistry* 1, Plenum Press, New York.

BONHAM H.F., Jr. (1991) Bulk-Mineable Precious Metal Deposits and Prospects in Nevada. Map 91; Second Edition. Nevada Bureau of Mines and Geology, Mackay School of Mines, University of Nevada, Reno.

BROOKINS D.G. (1988) *Eh-pH Diagrams for Geochemistry*. Springer-Verlag. 176 pp.

BUSENBERG E. and CLEMENCY C.V. (1976) The dissolution kinetics of feldspars at 25°C and 1 atm CO_2 partial pressure. *Geochimica et Cosmochimica Acta* 40, 41-49.

CAMP DRESSER and McKEE (1988) Preliminary water balance for the Berkeley Pit and related underground mine workings. EPA Contract 68-01-6939.

CARUCCIO F.T., GEIDELL G. and SEWELL J.M. (1976) The character of drainage as a function of the occurrence of framboidal pyrite and ground water quality in eastern Kentucky. In *6th Symp. Coal Mine Drainage Res.*, Louisville, KY. 1-16.

CHAO T.T. and THEOBALD P.K. Jr. (1976) The significance of secondary iron and manganese oxides in geochemical exploration. *Economic Geology* 71, 1560-1569.

CHAPMAN B.M., JONES D.R. and JUNG R.F. (1983) Processes controlling metal ion attenuation in acid mine drainage streams. *Geochimica et Cosmochimica Acta* 47, 1957-1973.

DAMES & MOORE, Salt Lake City, UT. Phase IIB Report, Hydrogeology Studies, Ruth Mine, Nevada, For Kennecott Nevada Mines Division, Feb. 9, 1990.

DAVIES C.W. (1962) *Ion Association*. Butterworth, Washington D.C. 190 pp.

DAVIS, A. (1992, 93) PTI Environmental Services. Presentation at 1993 Annual Meeting of the Society for Mining, Metallurgy, and Exploration; Reno, Nevada.

DAVIS A. and RUNNELLS D.D. (1987) Geochemical interactions between acidic tailings fluid and bedrock: use of the computer model MINTEQ. *Applied Geochemistry* **2**, 231-241.

DAVIS A. & ASHENBERG D. (1989) The aqueous geochemistry of the Berkeley Pit, Butte, Montana, U.S.A. *Applied Geochemistry* **4**, 23-36.

DAVIS A., OLSEN R.L., and WALKER D.R. (1991) Distribution of metals between water and entrained sediment in streams impacted by acid mine discharge, Clear Creek, Colorado, U.S.A. *Applied Geochemistry* **6**, 333-348.

DAVIS G.B. and RITCHIE A.I.M. (1986) A model of oxidation in pyritic mine wastes: part 1 equations and approximate solution. *Applied Mathematical Modelling*, **10**, 314-322.

DAVIS J.A. and LECKIE J.O. (1980) Surface Ionization and Complexation at the Oxide/Water Interface. 3. Adsorption of Anions. *Journal of Colloid and Interface Science* **74**, No. 1, 32-43.

DAVIS J.A., FULLER C.C., and COOK A.D. (1987) A model for trace metal sorption processes at the calcite surface: Adsorption of Cd^{2+} and subsequent solid solution formation. *Geochimica et Cosmochimica* **51**, 1477-1490.

DAVISON W. and HOUSE W.A. (1988) Neutralizing strategies for acid waters: Sodium and calcium products generate different acid neutralizing capacities. *Water Research* **22**, No. 5, 577-583.

DENVER KNIGHT PIESOLD Environmental Consultants, Inc. (1991) Waste Characterization Plan, Permit No. NEV 90002, Bullion Monarch Project, Eureka County, Nevada, May 1991.

DOYLE W.S. (1976) Recovery of Acid Strip Mine Lakes, In *Strip Mining of Coal: Environmental Solutions, Pollution Technology Review* No. 27, Noyes Data Corp. New Jersey.

DREVER J.I. (1988) *The Geochemistry of Natural Waters*, 2nd edition. Prentice Hall. 437 pp.

DUAIME, T. (1992). Hydrogeologist, Montana Bureau of Mines and Geology. Personal communication.

DZOMBAK, D.A. and MOREL M.M.F. (1990) *Surface Complex Modeling. Hydrous Ferric Oxide*. Wiley-Interscience, John Wiley & Sons. 393 pp.

ENGESGAARD P. and KIPP K.L. (1992) A Geochemical Transport Model for Redox-Controlled Movement of Mineral Fronts in Groundwater Flow Systems: A Case of Nitrate Removal by Oxidation of Pyrite. *Water Resources Research* **28**, no. 10, 2829-2843.

ENSR CONSULTING AND ENGINEERING, and DREVER J.I. (1991) Water Resources Technical Report for the Betze Project Environmental Impact Statement. Prepared for: USDI Bureau of Land Management, Elko District Office, Elko, Nevada.

FELMY A.R., GIRVIN D.C., and JENNE E.A. (1984) MINTEQ: A Computer Program for Calculating Aqueous Geochemical Equilibria. (NTIS PB84-157148) EPA-600/3-84-031, National Technical Information Service, Springfield, Virginia.

FETTER C.W. (1988) *Applied Hydrogeology.* Second Edition. Macmillan Publishing, New York. 592 pp.

FILIPEK L.H., NORDSTROM D.K., and FICKLIN W.H. (1987) Interaction of Acid Mine Drainage with Waters and Sediments of West Squaw Creek in the West Shasta Mining District, California. *Environment Science and Technology* **21**, 388-396.

FITZGERALD W.F. (1979) Distribution of mercury in natural waters. in *The biogeochemistry of mercury in the environment* (Nriagu J.O., ed.). Elsevier. 696 pp.

FLEMING G.W., and PLUMMER G.W. (1983) PHRQINPT-AN INTERACTIVE COMPUTER PROGRAM FOR CONSTRUCTING INPUT DATA SETS TO THE GEOCHEMICAL SIMULATION PROGRAM PHREEQE. U.S. Geological Survey Water-Resources Investigations Report 83-4236.

FLORENCE T.M. and BATLEY G.E. (1980) Chemical speciation in natural waters. In *Critical Reviews in Analytical Chemistry* (eds B. Campbell and L. Meites), 219-296. CRC Press.

FULLER C.C. and DAVIS J.A. (1989) Influence of coupling of sorption and photosynthetic processes on trace element cycles in natural waters. *Nature* **340**, 52-54.

GARRELS R.M., and MACKENZIE F.T. (1967). Origin of the Chemical Compositions of Some Springs and Lakes. Equilibrium Concepts in Natural Water Systems. In *American Chemical Society Advances in Chemistry Series* **67**, 222-242.

GARRELS R.M., and THOMPSON M.E. (1960) Oxidation of pyrite in ferric sulfate solution. *American Journal of Science* **258**, 57-67.

GARRELS R.M., and THOMPSON M.E. (1962) A Chemical Model for Sea Water at 25°C and One Atmosphere Pressure. *American Journal of Science* **260**, 57-66.

GERAGHTY & MILLER, INC., Environmental Services, Reno, NV (1991) Hydrogeologic Investigation for Mill No. 1 Tailings Facility and Downgradient Drainage Area, Carlin, Nevada, NV02202. Prepared for Newmont Gold Company.

GLYNN P.D., PARKHURST D.L., and PLUMMER L.N. (1992) Principles and Applications of Modeling Chemical Reactions in Ground Water. Short Course, International Groundwater Modeling Center; Colorado School of Mines, Golden, CO.

GRAY D.M., ed. (1970) *Handbook on the Principles of Hydrology.* Water Information Center, Inc. Canadian National Committee for the International Hydrological Decade. 676 pp.

GUILBERT J.M., and PARK C.F., Jr. (1986) *The Geology of Ore Deposits.* W.H. Freeman and Company, New York. 985 pp.

HAMER W.J. (1968) Theoretical mean activity coefficients of strong electrolytes in aqueous solutions from 0 to 100°C: *U.S. National Bureau of Standards, National Standard Reference Data Ser.* 24, 271pp.

HARRIS A.M. (1992) Comstock Mining Services. UNR Hydrology/ Hydrogeology Graduate Seminar, Spring 1992.

HARVIE C.E., and WEARE J.H. (1980) The prediction of mineral solubilities in natural waters: the Na-K-Mg-Ca-Cl-SO_4-H_2O system from zero to high concentration at 25°C. *Geochimica et Cosmochimica Acta* 44, 981-997.

HCI (Hydrologic Consultants, Inc.) (1992) Hydrogeologic Investigation for Gold Quarry Mine. HCI-768. Prepared for Newmont Gold Company.

HCI (Hydrologic Consultants, Inc.) (1992a) MINEDW - a finite-element program for three-dimensional simulation of mine dewatering: unpublished report, 79 pp.

HELGESON H.C. (1968) Evaluation of irreversible reactions in geochemical processes involving minerals and aqueous solution - I. Thermodynamic relations. *Geochimica et Cosmochimica Acta* 32, 853-877.

HELGESON H.C., GARRELS R.M. and MACKENZIE F.T. (1969) Evaluation of irreversible reactions in geochemical processes involving minerals and aqueous solution - II. Applications. *Geochimica et Cosmochimica Acta* 33, 455-481.

HELGESON H.C. (1969) Thermodynamics of Hydrothermal Systems at Elevated Temperatures and Pressures. *American J. of Science* 267, 729-804.

HEM J.D. (1985) Study and Interpretation of the Chemical Characteristics of Natural Water. U.S. Geological Survey Water-Supply Paper 2254, 263 pp.

HERCZEG A.L., and IMBODEN D.M. (1988) Tritium hydrologic studies in four closed-basin lakes in the Great Basin, U.S.A. *Limnol. Oceanography*, 33(2), 157-173.

HERLIHY A.T., MILLS A.L. and HERMAN J.S. (1988) Distribution of reduced inorganic sulfur compounds in lake sediments receiving acid mine drainage. *Applied Geochemistry* 3, 333-344.

HUANG H. and TAHIJA K. (1990) Characteristics and treatment problems of surface and underground waters in abandoned mines at Butte, Montana, In *Mining and Mineral Processing Wastes* (Doyle, F.M., ed.), *Proceedings of the Western Regional Symposium on Mining and Mineral Processing Wastes*, Berkeley, California, May 30 - June 1, 1990, 261-270.

HURLBUT C.S. Jr., and KLEIN C. (1977) *Manual of Mineralogy* (after James D. Dana). 19th Edition. John Wiley & Sons, New York, 532 pp.

HUTCHINSON G.E. (1957) *A Treatise on Limnology*, v.1, John Wiley & Sons, New York, 1015 pp.

HYDRO-SEARCH, INC. (1991) Predicted Post Mining Hydrogeochemistry of the Lone Tree Pit, Valmy, Nevada. Hydro-Search, Inc., Reno, NV. Prepared for Santa Fe Pacific Gold.

INTERA Environmental Consultants Inc. (1983) EQ3/EQ6: Geochemical Models Suitable Performance Assessment of Nuclear Waste Storage: Comparison of PHREEQE and EQ3/EQ6. ONWI-473. Prepared for Battelle Memorial Institute, Office of Nuclear Waste Isolation, Columbus, Ohio.

JAMES R.O. and HEALY T.W. (1972) Adsorption of hydrolyzable metal ions at the oxide-water interface. *Journal of Colloid and Interface Science* **40**, (1), 42-81.

KARLSSON S., ALLARD B. and HÅKANSSON K. (1988) Characterization of suspended solids in a stream receiving acid mine effluents, Bersbo, Sweden. *Applied Geochemistry* **3**, 345-356.

KHARAKA Y.K., ROBINSON S.W., LAW L.M., and CAROTHERS, W.W. (1984) Hydrogeochemistry of Big Soda Lake, Nevada: An alkaline meromictic desert lake. *Geochimica et Cosmochimica Acta* 48, 823-835.

KHARAKA T.K., GUNTER W.D., AGGARWAL P.D., PERKINS E.H., and DeBRAAL J.D. (1988) SOLMINEQ.88: A Computer Program for Geochemical Modeling of Water-Rock Interactions. U.S. Geological Survey, Water-Resources Investigations Report 88-4227. 208 p.

KINNIBURG D.G. and JACKSON M.L. (1981) Cation adsorption by hydrous metal oxides and clay. In *Adsorption of Inorganics at Solid-Liquid Interfaces* (Anderson M.A. and Rubin A.J., eds.), 91-160. Ann Arbor Science Publishers, Inc.

KNIGHT PIESOLD (1992) Site Characterization and Closure Plan, Permit No. NEV 90002, Bullion Monarch Project, Eureka County, Nevada, February 14, 1992.

LACY D.T. and LAWSON F. (1970) Kinetics of the liquid-phase oxidation of acid ferrous sulfate by the bacterium Thiobacillus ferrooxidans. *Biotec. Bioeng.* **12**, 29-50.

LINDBERG R.D. and RUNNELLS D.D. (1984) Ground-water redox reactions: An analysis of equilibrium state applied to Eh measurements and geochemical modeling. *Science* **225**, 925-927.

LUNDGREN D.G. and SILVER M. (1980) Ore leaching by bacteria, *Annual Review of Microbiology*, **34**, 263-283.

LYNCH D.C. (1988) A review of the physical chemistry of arsenic as it pertains to primary metals production, In *Arsenic Metallurgy Fundamentals and Applications*, R.G. Reddy, J.L. Hendrix, and P.B. Queneau, eds., AIME Proceedings, 3-33.

LYONS W.B., DOYLE G.A., PETERSEN R.C., and SWANSON E.E. (in press) The limnology of future pit lakes in Nevada: The importance of shape.

MACDONALD M. SAUNDERS (1992) Water Quality in Open Pit Precious Metal Mines. Master's Thesis (Professional Paper), University of Nevada, Reno.

MACINNES D.A. (1919) The activities of the ions of strong electrolytes: *American Chemical Society Journal* **41**, 1086-1092.

MANTOURA R.F.C., DICKSON A. and RILEY J.P. (1978) The complexation of metals with humic materials in natural waters. *Estuar. Coast. Marine Science* **6**, 387-408.

MASSCHELEYN P.H., DELAUNE R.D., and PATRICK W.H., Jr. (1991) Effect of redox potential and pH on arsenic speciation and solubility in a contaminated soil. *Environmental Science and Technology* **25**, 1414-1419.

MAZOR E. (1991) *Applied Chemical and Isotopic Groundwater Hydrology.* Halsted Press, New York.

McBRIDE M.B. (1980) Chemisorption of Cd^{2+} on calcite surfaces. *Soil Sci. Soc. Amer. J.* **44**, 26-28.

McDONALD M.G. and HARBAUGH A.W. (1984) A MODULAR THREE-DIMENSIONAL FINITE-DIFFERENCE GROUND-WATER FLOW MODEL (MODFLOW) U.S. Geological Survey Open-File Report 83-875, 528 pp.

MILLERO F.J. (1975) The physical chemistry of estuaries, in Church, T.M., ed., *Marine Chemistry in the Coastal Environment*: American Chemical Society Symposium Series 18, 25-55.

MILLERO F.J. (1977) Thermodynamics of the carbonate system in seawater: *Geochimica et Cosmochimica Acta* **43**, 1651-1661.

MILLERO F.J., SCHREIBER D.R. (1982) Use of the ion pairing model to estimate activity coefficients of the ionic components of natural waters. *American Journal of Science* **282**, 1508-1540.

MOREL M.M., HERING J.G. (1993) *Principles and Applications of Aquatic Chemistry.* John Wiley & Sons, Inc. Publishers.

MURRAY J.W., and BREWER P.G. (1977) The mechanisms of removal of iron, manganese, and other trace metals from seawater. In *Marine Manganese Deposits* (G.P. Glasby, ed.) Elsevier, Amsterdam, 391-426.

NDEP (1992, 93) NEVADA DIVISION OF ENVIRONMENTAL PROTECTION, Bureau of Mining Regulation and Reclamation. Files.

NEVADA DIVISION OF WATER PLANNING (1992) Nevada Water Facts. State of Nevada, Department of Conservation and Natural Resources.

NGDC (National Geophysical Data Center) (1983) Geothermal Resources of Nevada. National Oceanic and Atmospheric Administration. 1:500,000 scale Map.

NIENHUIS, P., APPELO T., and WILLEMSEN, G. (1991) Adaptation of Phreeqe for use in a Mixing - Cell Flowtube: PHREEQM. User Guide.

NORDSTROM D.K. (1977) Hydrogeochemical and microbiological factors affecting the heavy metal chemistry of an acid mine drainage system, Ph.D. Dissertation, Stanford University, 210 pp.

NORDSTROM D.K., PLUMMER L.N. WIGLEY T.M.L., WOLERY T.J., BALL J.W., JENNE E.A., BASSETT R.L., CRERAR D.A., FLORENCE T.M., FRITZ B., HOFFMAN M., HOLDREN G.R. Jr., LAFON G.M., MATTIGOD S.V., McDUFF R.E., MOREL F., REDDY M.M., SPOSITO G., THRAILKILL J. (1979a) A Comparison of Computerized Chemical Models for Equilibrium Calculations in Aqueous Systems. In *Chemical Modeling in Aqueous Systems* (E.A. Jenne, Ed.) *ACS Symposium Series* 93, *American Chemical Society*, Washington D.C., 857-892.

NORDSTROM D.K., JENNE E.A., and BALL J.W. (1979b) Redox Equilibria of Iron in Acid Mine Waters. In *Chemical Modeling in Aqueous Systems* (E.A. Jenne, Ed.) *ACS Symposium Series* 93, *American Chemical Society*, Washington D.C., 857-892.

NORDSTROM D.K. (1982) The effect of sulfate on aluminum concentrations in natural waters: some stability relations in the system Al_2O_3-SO_3-H_2O at 298K. *Geochimica et Cosmochimica Acta* 46, 681-692.

NORDSTROM D.K., and BALL J.W. (1983) Chemical models, computer programs and metal complexation in natural waters. Unpublished manuscript.

NORDSTROM D.K. (1985) The Formation of Acid Mine Waters: A Review. *Proceedings of Hazardous Materials Management Conference*, HAZMAT WEST '85, p. 453-457.

NORDSTROM D.K., and BALL J.W. (1985) Toxic Element Composition of Acid Mine Waters From Sulfide Ore Deposits. Mine Water, Granada, Spain, International Mine Water Association, 1985.

NORDSTROM D.K. and ALPERS C.N. (1990) Geochemical Evaluation of Acid Mine Waters at Iron Mountain, Shasta, California, 1990. U.S. Geological Survey Administrative Report. 36 pp.

NORDSTROM D.K., PLUMMER L.N. LANGMUIR D., BUSENBERG, MAY H.M., JONES B.F. and PARKHURST D.L. (1990) Revised chemical equilibrium data for major water-mineral reactions and their limitations, In *Chemical modeling of aqueous systems II* (Melchior D.C. and Bassett R.L. eds.), *ACS Symposium Series* 416, *American Chemical Society*, 398-413.

PANKOW J.F. (1991) *Aquatic Chemistry Concepts*. Lewis Publishers. 683 pp.

PARKHURST D.L., THORSTENSON D.C., and PLUMMER L.N. (1980) PHREEQE - A COMPUTER PROGRAM FOR GEOCHEMICAL CALCULATIONS. U.S.G.S. Water-Resources Investigations 80-96. Revised and reprinted 1990.

PARKHURST D.L., PLUMMER L.N., and THORSTENSON D.C., (1982) BALANCE - A COMPUTER PROGRAM FOR CALCULATING MASS TRANSFER FOR GEOCHEMICAL REACTIONS IN GROUND WATER. U.S. Geological Survey Water-Resources Investigations 82-14.

PARSONS J.D. (1977) Effects of acid mine wastes on aquatic ecosystems. *Water, Air and Soil Pollution* 7, no. 3, 333-354.

PERCIVAL T.J., BAGBY W.C., and RADTKE A.S. (1988) Physical and Chemical Features of Precious Metal Deposits hosted by Sedimentary Rocks in the Western United States. In *Bulk Mineable Precious Metal Deposits of the Western United States* (Schafer R.W., Cooper J.J., and Vikre P.G., eds.), Symposium Proceedings, Geological Society of Nevada, April 6-8, 1987, 11-34.

PETERSON S.R., HOSTETLER C.J., DEUTSCH W.J., and COWAN C.E. (1987) *MINTEQ User's Manual*. Pacific Northwest Laboratory.

PIERCE M.L. and MOORE C.B. (1982) Adsorption of arsenite and arsenate on amorphous iron hydroxide. *Water Research* 16, 1247-1253.

PITZER K.S. (1973) Thermodynamics of electrolytes I: Theoretical basis and general equations. *Journal of Physical Chemistry* 77, 268-277

PITZER K.S. (1979) Theory: Ion interaction approach. Activity Coefficients in Electrolyte Solutions, Volume 1, R.M. Pytkowicz, ed., CRC Press, Boca Raton, Fla., 157-208.

PITZER K.S. (1980) Electrolytes. From dilute solutions to fused salts. *Journal of the American Chemical Society* 102, 2902-2906.

PLANKEY B.P. PATTERSON H.H. and CRONAN C.S. (1986) Kinetics of aluminum fluoride complexation in acid waters. *Environmental Science and Technology* 20, 160-165.

PLUMMER L.N. (1984). Geochemical Modeling: A Comparison of Forward and Inverse Methods. From *The First Canadian/American Conference on Hydrogeology, Practical Applications of Ground Water Geochemistry.*

PLUMMER L.N., JONES B.F., and TRUESDELL A.H. (1976) WATEQF - A FORTRAN IV VERSION OF WATEQ, A COMPUTER PROGRAM FOR CALCULATING CHEMICAL EQUILIBRIUM OF NATURAL WATERS. U.S. Geological Survey Water-Resources Investigations 76-13. 70 p.

PLUMMER L.N., WIGLEY T.M.L. and PARKHURST D.L. (1978). The kinetics of calcite dissolution in CO_2-water systems at 5 to 60°C and 0.0 to 1.0 atm CO_2. *Am. J. Sci.*, 278, 179-216.

PLUMMER L.N., PARKHURST D.L., and THORSTENSON D.C. (1983). Development of reaction models for ground-water systems. *Geochimica et Cosmochimica Acta* 47, 665-686.

PLUMMER L.N., JONES B.F., and TRUESDELL A.H. (1984) WATEQF - A FORTRAN IV VERSION OF WATEQ, A COMPUTER PROGRAM FOR CALCULATING CHEMICAL EQUILIBRIUM OF NATURAL WATERS (Revised). U.S. Geological Survey Water-Resources Investigations Report 76-13

PLUMMER L.N., PARKHURST D.L., FLEMING G.W., and DUNKLE S.A. (1988) A COMPUTER PROGRAM INCORPORATING PITZER'S EQUATIONS FOR CALCULATIONS OF GEOCHEMICAL REACTIONS IN BRINES. U.S. Geological Survey Water-Resources Investigations Report 88-4153. Version 0.2.

PLUMMER L.N., BUSBY J.F., LEE R.W., and HANSHAW B.B. (1990). Geochemical Modeling of the Madison Aquifer in Parts of Montana, Wyoming, and South Dakota. *Water Res. Res.* 26, No. 9, 1981-2014.

PLUMMER L.N., PRESTEMON E.C., and PARKHURST D.L. (1991) AN INTERACTIVE CODE (NETPATH) FOR MODELING NET GEOCHEMICAL REACTIONS ALONG A FLOW PATH. U.S.G.S. Water-Resources Investigations Report 91-4078.

POTTER R.W. II and NORDSTROM D.K. (1977) The weathering of sulfide ores in Shasta County, California, U.S.A. *2nd Int. Symp. Water-Rock Interactions*, Strasbourg, France. I-42 - I-46.

PTI Environmental Services (1992) Chemogenesis of the Gold Quarry Pit Lake, Eureka County, Nevada. Prepared for Newmont Gold Company.

RADTKE A.S., FOO A.T., and PERCIVAL T.J. (1987) Geological and Chemical Features of the Cortez Gold Deposit, Lander County Nevada. *Bulk Mineable Precious Metal Deposits of the Western United States;* Guidebook for Field Trips, 319-325.

RAMPE J.J. and RUNNELLS D.D. (1989) Contamination of water and sediment in a desert stream by metals from an abandoned gold mine and mill, Eureka District, Arizona, U.S.A. *Applied Geochemistry* 4, 445-454.

ROBINSON R.A. and STOKES R.H. (1955) *Electrolyte Solutions.* Butterworths Scientific Publications, London. 559 pp.

RUNNELLS D.D. and LINDBERG R.D. (1990) Selenium in aqueous solutions: the impossibility of obtaining a meaningful Eh using a platinum electrode with implications for modeling of natural waters. *Geology* 18, 212-215

RUNNELLS D.D. and SKODA R.E. (1990) Redox modeling of arsenic in the presence of iron: applications to equilibrium computer modeling, in *Proceedings: Environmental research conference on ground water quality and waste disposal.* EPRI Report EN-6749, p. 22-1 to 22-11.

SAWYER C.N., and McCARTY P.L. (1978) *Chemistry for Environmental Engineering.* McGraw-Hill, 532 pp.

SCHECHER W.D. and McAVOY D.C. (1991) MINEQL⁺: A Chemical Equilibrium Program for Personal Computers. User's Manual Version 2.1. Environmental Research Software/Proctor and Gamble Company.

SEYLER P. and MARTIN J.M. (1989) Biogeochemical Processes Affecting Arsenic Species Distribution in a Permanently Stratified Lake. *Environmental Science and Technology* 23, 1258-1263.

SINGER P.C., and STUMM W. (1970) Acidic Mine Drainage: The Rate-Determining Step. *Science* 167, 1121-1123.

SMITH R.W. and JENNE E.A. (1991) Recalculation, Evaluation, and Prediction of Surface Complexation Constants for Metal Adsorption on Iron and Manganese Oxides. *Environ. Sci. Tech.* 25, 525-531.

SRK (STEFFEN ROBERTSON and KIRSTEN, B.C., Inc.) (1989). Draft Acid Rock Drainage Technical Guide, Volume 1. British Columbia Acid Mine Drainage Task Force Report. Prepared in association with Norecol Environmental Consultants, and Gormely Process Engineering.

STUMM W. and MORGAN J.J. (1981) *Aquatic Chemistry.* John Wiley & Sons. 780 pp.

SWALLOW K.C., HUME D.N. and MOREL F.M.M. (1980) Sorption of copper and lead by hydrous ferric oxide. *Environ. Sci. Tech.* 14, 1326-1331.

TESSIER A., RAPIN, F. and CARIGNAN R. (1985) Trace metals in oxic lake sediments: possible adsorption onto iron oxyhydroxides. *Geochimica et Cosmochimica Acta* 49, 183-194.

THORSTENSON D.C. (1984) The Concept of Electron Activity and Its Relation to Redox Potentials in Aqueous Geochemical Systems. U.S. Geological Survey Open File Report.

TRUESDELL A.H. and JONES B.F. (1969) Ion association in natural brines. *Chemical Geology* 4, 51-62

TRUESDELL A.H. and JONES B.F. (1974) WATEQ, A Computer Program for Calculating Chemical Equilibria of Natural Waters: *Journal of Research*, U.S. Geological Survey, v. 2, no. 2.

TUREKIAN K.K. (1977) The fate of metals in the oceans. *Geochimica et Cosmochimica Acta* 41, 1139-1144.

U.C. (UNIVERSITY OF CALIFORNIA) BERKELEY MINING WASTE STUDY TEAM (1988) Mining Waste Study, Final Report, 416 pp.

U.S. ARMY (1986) CE-QUAL-R1: A numerical one-dimensional model of reservoir water quality; User's Manual. U.S. Army Engineers Waterways Experimental Station, Vicksburg, MS. Instruction Report IR E-82-1.

VAN BREEMEN, N. (1973). Calculation of ionic activities in natural waters. *Geochimica et Cosmochimica Acta* 37, 101-107.

VOKT E. (1992) Geological Engineer, Cortez Gold Mines. Personal communication.

WANG H.F. and ANDERSON M.P. (1982) *Introduction to Groundwater Modeling, finite difference and finite element methods*. W.H. Freeman and Company, New York.

WELLS J.D., STOISER L.R. and ELLIOTT J.E. (1969) Geology and Geochemistry of the Cortez Gold Deposit, Nevada. *Economic Geology* 64, 526-537.

WELLS J.D. and MULLENS T.E. (1973) Gold-Bearing Arsenian Pyrite Determined by Microprobe Analysis, Cortez and Carlin Gold Mines, Nevada. *Economic Geology* 68, 187-201.

WETZEL R.G. (1983) *Limnology*, second edition. Saunders College Publishing. 767 pp.

WICKS C.M., HERMAN J.S., and MILLS A.L. (1991) Early diagenesis of sulfur in the sediments of lakes that receive acid mine drainage. *Applied Geochemistry* 6, p. 213-224.

WICKS C.M., and GROVES C.G. (1993) Acidic mine drainage in carbonate terrains: geochemical processes and rates of calcite dissolution. *Journal of Hydrology* 146, 13-27.

WIGLEY T.M.L. (1977) WATSPEC: A computer program for determining equilibrium speciation of aqueous solutions: British Geomorphological Research Group Technical Bulletin no. 20, 48 pp.

WILLIAMS D.I. and VON HERZEN R.P. (1983) On the Terrestrial Heatflow and Physical Limnology of Crater Lake, Oregon. *Journal of Geophysical Research* 88, B2, 1094-1104.

WOLERY T.J. (1992) EQ3/6, A Software Package for Geochemical Modeling of Aqueous Systems: Package Overview and Installation Guide (Version 7.0). Lawrence Livermore National Laboratory.

WOODWARD-CLYDE CONSULTANTS (1992) Screencheck Environmental Assessment, Robinson Project, prepared for Magma Copper Company, Tucson, Arizona, (Draft).

YEH G.T. and TRIPATHI V.S. (1989) HYDROGEOCHEM: A Coupled Model of Hydrologic Transport and Geochemical Equilibria of Reactive Multicomponent Systems. Oak Ridge National Laboratory Report ORNL-6371, Oak Ridge, TN

APPENDIX A

Debye-Hückel á and b parameters

Ion	á	Ion	á
H^+	9.0	S_3^{2-}	8.0
$SrHCO_3^+$	5.4	S_4^{2-}	10.0
$SrOH^+$	5.0	S_5^{2-}	12.0
$SrCO_3^0$	0.0	S_6^{2-}	14.0
$Cu(S_4)_2^{3-}$	23.0	$Ag(S_4)_2^{3-}$	22.0
$CuS_4S_5^{3-}$	25.0	$AgS_4S_5^{3-}$	24.0
S_2^{2-}	6.5	$Ag(HS)S_4^{2-}$	15.0

Ion	á	b	Ion	á	b
Ca^{2+}	5.0	0.165	SO_4^{2-}	5.0	-0.04
Mg^{2+}	5.5	0.20	HCO_3^-	5.4	0.0
Na^+	4.0	0.075	CO_3^{2-}	5.4	0.0
K^+	3.5	0.015	$H_2CO_3^0$	0.0	0.0
Cl^-	3.5	0.015	Sr^{2+}	5.26	0.121

APPENDIX B

Cortez pit water mass transfer models calculated in BALANCE

********** Model # 1 **********

```
 1:  Cortez Pit water mass transfer
 2:  C 4626.570   1838.800
 3:  S 939.0208    385.200
 4:  AS  6.0904       .134
 5:  BA  33.680       .000
 6:  CA1132.740   1272.500
 7:  FE 524.110      6.088
 8:  K  299.250    127.900
 9:  MG 954.540    567.800
10:  MN  .03094      1.440
11:  NA2985.240   1348.400
12:  HG  .00798       .000
13:  ZN  .32112      .3365
14   F  126.326     26.300
15:  AL     .000      .000
16:  SI4785.780   1385.400
17:  PB 1.63369       .000
18:
19:  CALCITE F CA 1.000  C  1.000  RS 4.000
20:  "CH2O"   +C  1.000
21:  DOLOMITE +CA 1.000  MG 1.000  C  2.000  RS 8.000
22:  FLUORITEF+CA 1.000  F  2.000
23:  ArsenopyF+AS 1.000  FE 1.000  S  1.000
24:  BARITE  F+BA 1.000  S  1.000  RS 6.000
25:  GOETHITE -FE 1.000  RS 3.000
26:  PYRITE  F+FE 1.000  S  2.000  RS 0.000
27:  CinnabarF+HG 1.000  S  1.000
28:  K-MICA  F K  1.000  AL 3.000  SI 3.000
29:  MAGNESIT  MG 1.000  C  1.000  RS 4.000
30:  NaCl     F+NA 1.000  CL 1.000
31:  Ca/Na EX  NA 2.000  CA -1.000
32:  Galena  F+PB 1.000  S  1.000
33:  SphaleriF+ZN 1.000  S  1.000
34:  MnO2       MN 1.000  RS 4.000
35:  ILLITE     K  0.600  MG 0.250  AL 2.300  SI 3.500
36:  CO2 GAS F C  1.000  RS 4.000
37:  K-FELDSPF+K  1.000  AL 1.000  SI 3.000
38:  Gypsum     CA 1.000  S  1.000  RS.6.000
39:  SiO2      +SI 1.000
40:  =SOH:Zn F ZN 1.000
41:  KAOLINIT -AL 2.000  SI 2.000
42:  Ca-Mont  -CA 0.167  AL 2.330  SI 3.670
43:  K-Mont     K  0.330  AL 2.330  SI 3.670
44:  PlagioclF+AL 1.500  CA  .500  NA  .500  SI 2.500
45:  Mg/Na EX  NA 2.000  Mg -1.000
46:  Na-Mont  -NA 0.330  AL 2.330  SI 3.670
```

Plagioclase	+	F	3057.6800
Fluorite	+	F	50.0130
≡SOH:Zn		F	- .0154
Galena	+	F	1.6337
Cinnabar	+	F	.0070
Arsenopy	+	F	5.9564
CO2 gas		F	3608.0547
NaCl	+	F	108.0000
Pyrite	+	F	512.0656
Barite	+	F	33.6800
K-Feldsp	+	F	171.3500
Calcite		F	-1207.0247
Gypsum			-511.5883
Kaolinite	-		-2378.9350
Magnesit			386.7400
MnO2			-1.4091

Plagioclase	+	F	3057.6800
Fluorite	+	F	50.0130
≡SOH:Zn		F	- .0154
Galena	+	F	1.6337
Cinnabar	+	F	.0070
Arsenopy	+	F	5.9564
CO2 gas		F	3996.2038
NaCl	+	F	2280.8535
Pyrite	+	F	512.0656
Barite	+	F	33.6800
K-Feldsp	+	F	1850.5982
Calcite		F	-1207.0247
Gypsum			-511.5883
Illite	-		-2798.7471
Rhodochr			-1.4091
Mg/Na EX			-1086.4268

Plagioclase	+	F	1154.5320
Fluorite	+	F	50.0130
≡SOH:Zn		F	- .0154
Galena	+	F	1.6337
Cinnabar	+	F	.0070
Arsenopy	+	F	5.9564
CO2 gas		F	2656.4807
NaCl	+	F	1059.5740
Pyrite	+	F	512.0656
Barite	+	F	33.6800
K-Feldsp	+	F	171.3500
Calcite		F	-255.4507
Gypsum			-511.5883
Gibbsite	-		-1903.1480
Magnesit			386.7400
MnO2			-1.4091

Plagioclase	+	F	3057.6800
Fluorite	+	F	50.0130
≡SOH:Zn		F	- .0154
Galena	+	F	1.6337
Cinnabar	+	F	.0070
Arsenopy	+	F	5.9564
CO2 gas		F	2909.7770
NaCl	+	F	108.0000
Pyrite	+	F	512.0656
Barite	+	F	33.6800
K-Feldsp	+	F	1850.5982
Calcite		F	-2293.4515
Gypsum			-511.5883
Illite	-		-2798.7471
Rhodochr			-1.4091
Dolomite	+		1086.4268

Plagioclase	+	F	3057.6800
Fluorite	+	F	50.0130
≡SOH:Zn		F	- .0154
Galena	+	F	1.6337
Cinnabar	+	F	.0070
Arsenopy	+	F	5.9564
CO2 gas		F	2908.3680
NaCl	+	F	108.0000
Pyrite	+	F	512.0656
Barite	+	F	33.6800
K-Feldsp	+	F	1850.5982
Calcite		F	-1207.0247
Gypsum			-511.5883
Illite	-		-2798.7471
Magnesit			1086.4268
MnO2			-1.4091

Plagioclase	+	F	1154.5320
Fluorite	+	F	50.0130
≡SOH:Zn		F	- .0154
Galena	+	F	1.6337
Cinnabar	+	F	.0070
Arsenopy	+	F	5.9564
CO2 gas		F	3044.6298
NaCl	+	F	1833.0540
Pyrite	+	F	512.0656
Barite	+	F	33.6800
K-Feldsp	+	F	171.3500
Calcite		F	-255.4507
Gypsum			-511.5883
Gibbsite	-		-1903.1480
Rhodochr			-1.4091
Mg/Na Ex			-386.7400

Plagioclase	+	F	3057.6800
Fluorite	+	F	50.0130
≡SOH:Zn		F	- .0154
Galena	+	F	1.6337
Cinnabar	+	F	.0070
Arsenopy	+	F	5.9564
CO2 gas		F	3609.4638
NaCl	+	F	108.0000
Pyrite	+	F	512.0656
Barite	+	F	33.6800
K-Feldsp	+	F	171.3500
Calcite		F	-1207.0247
Gypsum			-511.5883
Kaolinite	-		-2378.9350
Magnesit			386.7400
Rhodochr	+		-1.4091

Plagioclase	+	F	1154.5320
Fluorite	+	F	50.0130
≡SOH:Zn		F	- .0154
Galena	+	F	1.6337
Cinnabar	+	F	.0070
Arsenopy	+	F	5.9564
CO2 gas		F	2657.8898
NaCl	+	F	1059.5740
Pyrite	+	F	512.0656
Barite	+	F	33.6800
K-Feldsp	+	F	171.3500
Calcite		F	-642.1907
Gypsum			-511.5883
Gibbsite	-		-1903.1480
Rhodochr			-1.4091
Dolomite	+		386.7400

Plagioclase	+	F	1154.5320
Fluorite	+	F	50.0130
≡SOH:Zn		F	- .0154
Galena	+	F	1.6337
Cinnabar	+	F	.0070
Arsenopy	+	F	5.9564
CO2 gas		F	2657.8898
NaCl	+	F	1059.5740
Pyrite	+	F	512.0656
Barite	+	F	33.6800
K-Feldsp	+	F	171.3500
Calcite		F	-255.4507
Gypsum			-511.5883
Gibbsite	-		-1903.1480
Magnesit			386.7400
Rhodochr	+		-1.4091

Plagioclase	+	F	3057.6800
Fluorite	+	F	50.0130
≡SOH:Zn		F	- .0154
Galena	+	F	1.6337
Cinnabar	+	F	.0070
Arsenopy	+	F	5.9564
CO2 gas		F	3996.2038
NaCl	+	F	881.4800
Pyrite	+	F	512.0656
Barite	+	F	33.6800
K-Feldsp	+	F	171.3500
Calcite		F	-1207.0247
Gypsum			-511.5883
Kaolinite	-		-2378.9350
Rhodochr			-1.4091
Dolomite	+		386.7400

Plagioclase	+	F	3057.6800
Fluorite	+	F	50.0130
≡SOH:Zn		F	- .0154
Galena	+	F	1.6337
Cinnabar	+	F	.0070
Arsenopy	+	F	5.9564
CO2 gas		F	2909.7770
NaCl	+	F	108.0000
Pyrite	+	F	512.0656
Barite	+	F	33.6800
K-Feldsp	+	F	1850.5982
Calcite		F	-1207.0247
Gypsum			-511.5883
Illite	-		-2798.7471
Magnesit			1086.4268
Rhodochr	+		-1.4091

Plagioclase	+	F	3057.6800
Fluorite	+	F	50.0130
≡SOH:Zn		F	- .0154
Galena	+	F	1.6337
Cinnabar	+	F	.0070
Arsenopy	+	F	5.9564
CO2 gas		F	3609.4638
NaCl	+	F	108.0000
Pyrite	+	F	512.0656
Barite	+	F	33.6800
K-Feldsp	+	F	171.3500
Calcite		F	-1593.7647
Gypsum			-511.5883
Kaolinite	-		-2378.9350
Rhodochr			-1.4091
Dolomite	+		386.7400

Plagioclase	+	F	3057.6800
Fluorite	+	F	50.0130
≡SOH:Zn		F	- .0154
Galena	+	F	1.6337
Cinnabar	+	F	.0070
Arsenopy	+	F	5.9564
CO2 gas		F	3608.0547
NaCl	+	F	108.0000
Pyrite	+	F	512.0656
Barite	+	F	33.6800
K-Feldsp	+	F	171.3500
Calcite		F	-1593.7647
Gypsum			-511.5883
Kaolinite	-		-2378.9350
MnO2			-1.4091
Dolomite	+		386.7400

Plagioclase	+	F	3057.6800
Fluorite	+	F	50.0130
≡SOH:Zn		F	- .0154
Galena	+	F	1.6337
Cinnabar	+	F	.0070
Arsenopy	+	F	5.9564
CO2 gas		F	3994.7947
NaCl	+	F	2280.8535
Pyrite	+	F	512.0656
Barite	+	F	33.6800
K-Feldsp	+	F	1850.5982
Calcite		F	-1207.0247
Gypsum			-511.5883
Illite	-		-2798.7471
MnO2			-1.4091
Mg/Na EX			-1086.42680

Plagioclase	+	F	3057.6800
Fluorite	+	F	50.0130
≡SOH:Zn		F	- .0154
Galena	+	F	1.6337
Cinnabar	+	F	.0070
Arsenopy	+	F	5.9564
CO2 gas		F	3994.7947
NaCl	+	F	881.4800
Pyrite	+	F	512.0656
Barite	+	F	33.6800
K-Feldsp	+	F	171.3500
Calcite		F	-1207.0247
Gypsum			-511.5883
Kaolinite	-		-2378.9350
MnO2			-1.4091
Mg/Na EX			-386.7400

Plagioclase	+	F	3057.6800
Fluorite	+	F	50.0130
≡SOH:Zn		F	- .0154
Galena	+	F	1.6337
Cinnabar	+	F	.0070
Arsenopy	+	F	5.9564
CO2 gas		F	2908.3680
NaCl	+	F	108.0000
Pyrite	+	F	512.0656
Barite	+	F	33.6800
K-Feldsp	+	F	1850.5982
Calcite		F	-2293.4515
Gypsum			-511.5883
Illite	-		-2798.7471
MnO2			-1.4091
Dolomite	+		1086.42680

Plagioclase	+	F	1154.5320
Fluorite	+	F	50.0130
≡SOH:Zn		F	- .0154
Galena	+	F	1.6337
Cinnabar	+	F	.0070
Arsenopy	+	F	5.9564
CO2 gas		F	2656.4807
NaCl	+	F	1059.5740
Pyrite	+	F	512.0656
Barite	+	F	33.6800
K-Feldsp	+	F	171.3500
Calcite		F	-642.1907
Gypsum			-511.5883
Gibbsite	-		-1903.1480
MnO2			-1.4091
Dolomite	+		386.7400

Plagioclase	+	F	1154.5320
Fluorite	+	F	50.0130
≡SOH:Zn		F	- .0154
Galena	+	F	1.6337
Cinnabar	+	F	.0070
Arsenopy	+	F	5.9564
CO2 gas		F	3043.2207
NaCl	+	F	1833.0540
Pyrite	+	F	512.0656
Barite	+	F	33.6800
K-Feldsp	+	F	171.3500
Calcite		F	-255.4507
Gypsum			-511.5883
Gibbsite	-		-1903.1480
MnO2			-1.4091
Mg/Na EX			-386.7400